UNIVERSIDADE FEDERAL DE UBERLÂNDIA
INSTITUTO DE BIOTECNOLOGIA
PÓS-GRADUAÇÃO EM GENÉTICA E BIOQUÍMICA

ANÁLISE DO SECRETOMA DE BACTÉRIAS ISOLADAS DO ALIMENTO DE LARVAS DE ABELHAS BRASILEIRAS SEM FERRÃO EM *DROSOPHILA MELANOGASTER* MODELO PARA DOENÇA DE ALZHEIMER

Aluna: Tamiris Sabrina Rodrigues

Orientadora: Profª. Drª. Ana Maria Bonetti / IBTEC-UFU

Co-Orientador: Prof. Dr. Carlos Ueira-Vieira / IBTEC-UFU

UBERLÂNDIA – MG
2021

UNIVERSIDADE FEDERAL DE UBERLÂNDIA
INSTITUTO DE BIOTECNOLOGIA
PÓS-GRADUAÇÃO EM GENÉTICA E BIOQUÍMICA

ANÁLISE DO SECRETOMA DE BACTÉRIAS ISOLADAS DO ALIMENTO DE LARVAS DE ABELHAS BRASILEIRAS SEM FERRÃO EM *DROSOPHILA MELANOGASTER* MODELO PARA DOENÇA DE ALZHEIMER

Aluna: Tamiris Sabrina Rodrigues

Orientadora: Profª. Drª. Ana Maria Bonetti

Co-Orientador: Prof. Dr. Carlos Ueira-Vieira / IBTEC-UFU

Tese apresentada à Universidade Federal de Uberlândia como parte dos requisitos para obtenção do Título de Doutora em Genética e Bioquímica (Área Genética)

UBERLÂNDIA – MG

2021

Dados Internacionais de Catalogação na Publicação (CIP)
Sistema de Bibliotecas da UFU, MG, Brasil.

R696a
2021

Rodrigues, Tamiris Sabrina, 1992-
Análise do secretoma de bactérias isoladas do alimento de larvas de abelhas brasileiras sem ferrão em *Drosophila Melanogaster* modelo para doença de Alzheimer [recurso eletrônico] / Tamiris Sabrina Rodrigues. - 2021.

Orientadora: Ana Maria Bonetti.
Coorientador: Carlos Ueira-Vieira.
Tese (Doutorado) - Universidade Federal de Uberlândia, Programa de Pós-Graduação em Genética e Bioquímica.
Modo de acesso: Internet.
Disponível em: http://doi.org/10.14393/ufu.te.2021.5514
Inclui bibliografia.
Inclui ilustrações.

1. Genética. I. Bonetti, Ana Maria, 1949-, (Orient.). II. Vieira, Carlos Ueira, 1981-, (Coorient.). III. Universidade Federal de Uberlândia. Programa de Pós-Graduação em Genética e Bioquímica. IV. Título.

CDU:575

Gloria Aparecida
Bibliotecária - CRB-6/2047

UNIVERSIDADE FEDERAL DE UBERLÂNDIA
Coordenação do Programa de Pós-Graduação em Genética e Bioquímica
Av. Pará 1720, Bloco 2E, Sala 244 - Bairro Umuarama, Uberlândia-MG, CEP 38400-902
Telefone: +55 (34) 3225-8438 - www.ppggb.ibtec.ufu.br - ppggb@ufu.br

ATA DE DEFESA - PÓS-GRADUAÇÃO

Programa de Pós-Graduação em:	Genética e Bioquímica				
Defesa de:	Doutorado Acadêmico - Nº 01/2021 PPGGB.				
Data:	Vinte e um de maio de dois mil e vinte e um	Hora de início:	08:30h	Hora de encerramento:	13:00h
Matrícula do Discente:	11723GBI011				
Nome do Discente:	Tamiris Sabrina Rodrigues				
Título do Trabalho:	Análise do secretoma de bactérias isoladas do alimento de larva de abelhas brasileiras sem ferrão em *Drosophila melanogaster* modelo para Doença de Alzheimer.				
Área de concentração:	Genética				
Linha de pesquisa:	Genética, Biologia e Melhoramento de Plantas e Animais.				
Projeto de Pesquisa de vinculação:	RNAseq de cérebro de modelos biológicos de Doença de Alzheimer e sua utilizaçao na validaçao de peptídeo neuromoduladores.				

Aos vinte e um dias do mês de maio de dois mil e vinte e um, às 08:30 horas, reuniu-se via web conferência pela Plataforma Google Meet, em conformidade com a Portaria nº 36, de 19 de março de 2020 da Coordenação de Aperfeiçoamento de Pessoal de Nível Superior – CAPES e Resolução de nº 06/2020 do Conselho de Pesquisa e Pós-graduação pela Universidade Federal de Uberlândia, a Banca Examinadora, designada pelo Colegiado do Programa de Pós-graduação em Genética e Bioquímica, assim composta: Profª. Drª. Fernanda Gobbi Amorim, Profª. Drª. Andréa Queiroz Maranhão, Prof. Dr. Robson José de Oliveira Júnior, Prof. Dr. Murilo Vieira da Silva e Profª. Drª. Ana Maria Bonetti, orientadora da candidata e demais convidados presentes conforme lista de presença. Iniciando os trabalhos a presidente da mesa, Profª. Drª. Ana Maria Bonetti, apresentou a Comissão Examinadora e a candidata, agradeceu a presença do público, e concedeu à Discente a palavra para a exposição do seu trabalho. A duração da apresentação da Discente e o tempo de arguição e resposta foram conforme as normas do Programa de Pós-graduação em Genética e Bioquímica. A seguir a senhora presidente concedeu a palavra, pela ordem sucessivamente, aos examinadores, que passaram a arguir a candidata. Ultimada a arguição, que se desenvolveu dentro dos termos regimentais, a Banca, em sessão secreta, atribuiu os conceitos finais. Em face do resultado obtido, a Banca Examinadora considerou a candidata:

APROVADA.

Esta defesa de Tese de Doutorado é parte dos requisitos necessários à obtenção do título de Doutora. O competente diploma será expedido após cumprimento dos demais requisitos, conforme as normas do Programa, a legislação pertinente e a regulamentação interna da UFU. Nada mais havendo a tratar foram

encerrados os trabalhos. Foi lavrada a presente ata que após lida e achada conforme foi assinada pela Banca Examinadora.

Documento assinado eletronicamente por **Ana Maria Bonetti**, **Presidente**, em 21/05/2021, às 13:08, conforme horário oficial de Brasília, com fundamento no art. 6º, § 1º, do Decreto nº 8.539, de 8 de outubro de 2015.

Documento assinado eletronicamente por **Robson José de Oliveira Junior**, **Membro de Comissão**, em 21/05/2021, às 13:09, conforme horário oficial de Brasília, com fundamento no art. 6º, § 1º, do Decreto nº 8.539, de 8 de outubro de 2015.

Documento assinado eletronicamente por **Murilo Vieira da Silva**, **Médico(a) Veterinário(a)**, em 21/05/2021, às 13:11, conforme horário oficial de Brasília, com fundamento no art. 6º, § 1º, do Decreto nº 8.539, de 8 de outubro de 2015.

Documento assinado eletronicamente por **Fernanda Gobbi Amorim**, **Usuário Externo**, em 21/05/2021, às 13:12, conforme horário oficial de Brasília, com fundamento no art. 6º, § 1º, do Decreto nº 8.539, de 8 de outubro de 2015.

Documento assinado eletronicamente por **Andrea Queiroz Maranhão**, **Usuário Externo**, em 21/05/2021, às 13:12, conforme horário oficial de Brasília, com fundamento no art. 6º, § 1º, do Decreto nº 8.539, de 8 de outubro de 2015.

A autenticidade deste documento pode ser conferida no site https://www.sei.ufu.br/sei/controlador_externo.php?acao=documento_conferir&id_orgao_acesso_externo=0, informando o código verificador **2732936** e o código CRC **0FD66289**.

Referência: Processo nº 23117.027775/2021-53 SEI nº 2732936

UNIVERSIDADE FEDERAL DE UBERLÂNDIA
INSTITUTO DE BIOTECNOLOGIA
PÓS-GRADUAÇÃO EM GENÉTICA E BIOQUÍMICA

ANÁLISE DO SECRETOMA DE BACTÉRIAS ISOLADAS DO ALIMENTO DE LARVAS DE ABELHAS BRASILEIRAS SEM FERRÃO EM *DROSOPHILA MELANOGASTER* MODELO PARA DOENÇA DE ALZHEIMER

Aluna: Tamiris Sabrina Rodrigues

COMISSÃO EXAMINADORA

Presidente/Orientadora: Profª. Drª. Ana Maria Bonetti

Examinadores: Profª. Drª. Fernanda Gobbi Amorim
Profª. Drª. Andréa Queiroz Maranhão
Prof. Dr. Robson José de Oliveira Júnior
Prof. Dr. Murilo Vieira da Silva.

Data da defesa:

As sugestões da Comissão Examinadora e as Normas PPGGB para o formato da Tese foram contempladas.

Profª. Drª. Ana Maria Bonetti

“A minha fé e as minhas crenças não podem ser um obstáculo para a busca de novos conhecimentos, pelo contrário, quanto mais eu busco conhecimento, mais reforço o que eu acredito”

DEDICATÓRIA

Dedico esse trabalho aos meus pais **Farley Cesar Rodrigues** e **Leida Aparecida Rodrigues** e ao meu marido **Hiago Caixeta Cunha,** pelo amor, confiança e apoio! De vocês vêm minha motivação para me tornar uma pessoa melhor!

AGRADECIMENTOS

Primeiramente, agradeço à **Universidade Federal de Uberlândia,** por oferecer infraestrutura para a realização desse trabalho.

Meus profundos agradecimentos à minha **orientadora Profª Drª Ana Maria Bonetti**, que sempre acreditou no meu potencial e dividiu diariamente sua experiência como educadora e pesquisadora. Por muitas vezes, sua confiança guiou meu desenvolvimento profissional e seu carinho e apoio me fez vencer diversos obstáculos. Obrigada por me dar o privilégio de conviver e aprender ao seu lado. Obrigada por sua amizade.

Agradeço ao meu **co-orientador Prof. Dr. Carlos Ueira Vieira,** pelo incentivo e confiança depositados e por estar sempre disponível para esclarecer minhas dúvidas. Por me fazer acreditar que conseguiria alcançar todos os meus objetivos e pelos inúmeros conselhos dados. Obrigada pela parceria profissional e pessoal. Serei eternamente grata.

Às professoras **Drª Débora Oliveira, Drª Larissa Barbosa, Drª Luana Scalia** e **Drª Lúbia Cristina,** pela amizade e apoio. Vocês foram muito importantes nessa caminhada!

A todos os **colegas e funcionários do Instituto de Biotecnologia** da Universidade Federal de Uberlândia (IBTEC/UFU) pelos serviços prestados e apoio. Em especial, às minhas amigas e companheiras de trabalho **Janaína Mota, Tatiana Perini, Natássia Corrêa, Marina Lima e Luciana Machado.** Obrigada pelo companheirismo incondicional.

À **Pós-doutoranda Patrícia Tieme Fushimura** que, apesar de ter seguido novos caminhos, é uma das minhas grandes influências profissionais.

Aos meus amigos do programa de Pós-Graduação em Genética e Bioquímica (PPGGB).

Aos meus amigos de laboratório, **Emília Rezende, Jéssica Brito, Luiza Diniz, Jéssica Regina, Serena Mares, Letícia Leandro, Matheus Henrique,**

Michelle Sales, Luiz Fernando Covizzi, Lays Rocha, Ana Carolina Costa, Natália Carine, Rafael Bernardes. Obrigada pela convivência, pelas risadas, pelo aprendizado e por tornarem o ambiente laboratorial tão enriquecedor e agradável!

Às Agências de Fomento FAPEMIG, CAPES e CNPq, pelo auxílio financeiro na categoria APQ concedido ao Orientador e Co-orientador dessa Pesquisa.

À **todos** que colaboraram conosco e auxiliaram no desenvolvimento desse trabalho!

AGRADECIMENTOS ESPECIAIS

Agradeço à **Deus** pela vida, por sempre iluminar meus caminhos e por me guiar com sabedoria diante dos obstáculos!

Agradeço aos meus pais, **Farley Cesar Rodrigues** e **Leida Aparecida Rodrigues**, Obrigada pela compreensão diante dos momentos de ausência, pelos conselhos e orações. Obrigada pela amizade, apoio e por sempre incentivarem a busca pelos meus sonhos. Vocês são meu exemplo de conduta e determinação. É um orgulho poder chamá-los de pais. A vocês, o meu amor incondicional!

Ao meu marido e amigo, **Hiago Caixeta Cunha**, que acompanhou bem de perto todo o esforço e dedicação durante o desenvolvimento desse trabalho. Obrigada pela compreensão, carinho, apoio e por ser um dos meus maiores incentivadores. Compartilho com você essa vitória! Obrigada pelo companheirismo e por caminhar ao meu lado!

Aos meus irmãos, pela amizade e companheirismo!

Aos meus sogros **Sr. Gilvane Cunha** e **Srª. Maria Anália Caixeta** e cunhados **Anália Caixeta e Wesley Caixeta,** pelo carinho, apoio e conselhos nessa jornada. A presença de vocês é muito importante na minha vida.

À minha família, por contribuir com a minha formação pessoal e sempre me incentivar. Em especial às minhas avós **Gesa Maria** e **Aparecida Rodrigues**, pelas orações, apoio e carinho.

Aos meus grandes amigos **Lucas Vinícius Ferreira e Lara Leão**. Como é bom ter a amizade e o apoio de vocês!

APOIO FINANCEIRO

Este trabalho foi conduzido no Laboratório de Genética e Laboratório de Nanobiotecnologia, do Instituto de Biotecnologia, Laboratório Multiusuário, da Faculdade de Engenharia Química e Laboratório de Patologia Oral, da Faculdade de Odontologia, da Universidade Federal de Uberlândia (Uberlândia - Minas Gerais, Brasil), com o apoio das seguintes Agências de Fomento:

- Coordenação de Aperfeiçoamento de Pessoal do Ensino Superior (CAPES);
- Conselho Nacional de Desenvolvimento Científico e Tecnológico (CNPq);
- Fundação de Amparo à Pesquisa do Estado de Minas Gerais (FAPEMIG);
- Universidade Federal de Uberlândia (UFU).

SUMÁRIO

LISTA DE FIGURAS

LISTA DE ABREVIATURAS

DA	Doença de Alzheimer
Aβ	Beta-amiloide
cDNA	DNA complementar
APP	Proteína precursora de amiloide
C83	Fragmento C-terminal de 83 aminoácidos associado à membrana
AICD	Domínio intracelular de APP
C99	Fragmento C-terminal de 99 aminoácidos associado à membrana
BACE1	β-secretase
ADAM10	α-secretase
Lys	Lisina
Ala	Alanina
Asp	Aspartato
SNC	Sistema nervoso central
m/z	Massa/carga
ESI	Ionização por eletrospray
MALDI	Dessorção a laser assistida por matriz
MSn	Espectrometria de massa sequencial
TOF-TOF	Tempo de voo - tempo de voo
Q-TOF	Quadrupolo - tempo de voo
FTICR	Ressonância ciclotrônica de íons com transformada de Fourier
LTQ	Armadilha de íons - orbitrap
Q	Orbitrap
CE	Eletroforese capilar
NGS	Sequenciamento de nova geração

RESUMO

A Doença de Alzheimer (DA) é uma doença neurodegenerativa progressiva caracterizada pela presença de placas amiloides, emaranhados neurofibrilares, inflamação, dano oxidativo, perda de sinapses e morte seletiva de neurônios. A inibição da expressão de BACE1 tem sido considerada um alvo terapêutico para a prevenção e tratamento da doença de Alzheimer. Este estudo avaliou a atividade inibitória do BACE1 do secretoma de bactérias isoladas de alimento larval de abelhas sem ferrão de espécies nativas brasileiras, *Melipona quadrifasciata* e *Tetragonisca angustula*. Para tanto, foi realizada a triagem de secretomas nas linhagens transgênicas de *Drosophila melanogaster*, seguida de análises *in silico.* Avaliamos a taxa de sobrevivência da mosca transgênica com fenótipo de olho áspero, gerado pela superexpressão de ortólogos humanos APP e BACE1 no sistema nervoso em desenvolvimento do olho. Modificações morfológicas nos olhos de *D. melanogaster* recém-eclodidos foram examinadas. Verificamos redução das alterações morfológicas no olho, apresentando olhos compostos com superfície lisa, diferença na fusão das omatídeos e presença de grande número de cerdas, nos grupos tratados com os secretomas S9 e S27 quando comparados aos grupos controle. Cortes histológicos mostraram concordância com esta melhora, exibindo olhos compostos com morfologia regular e superfície organizada. O modelo anti-DA de *D. melanogaster* foi tratado com vários secretomas bacterianos por 15 dias após a eclosão. As moscas tratadas com o secretoma S1 apresentaram melhora na taxa de escalada quando comparadas aos grupos controle negativo e veículo. Além disso, os grupos tratados com os secretomas S1 e S27 mostraram um declínio nos níveis de beta-amiloide após 15 dias de tratamento. A análise histológica do cérebro revelou diminuição da neurodegeneração nas moscas tratadas com S1 visualizada pela redução das lesões vacuolares, quando comparada aos grupos NC e veículo. Realizamos a análise proteômica dos secretomas mais eficientes nos testes com *D. melanogaste*r. As análises *in silico* selecionou os peptídeos mais potencialmente bioativos para interagir com BACE1 e beta-amiloide, prevendo o *docking* molecular entre eles. Nossa análise encontrou quatro peptídeos que interagem com BACE1 e Aβ42, com potencial ação na redução do processo

neurodegenerativo. Esses peptídeos potencialmente bioativos podem servir de protótipo para novos fármacos para a prevenção ou tratamento da Doença de Alzheimer. O secretoma de bactérias isoladas do alimento larval de abelhas sem ferrão provou ser uma fonte potencial de moléculas terapêuticas direcionadas a distúrbios neurodegenerativos.

Palavras-chave: Doença de Alzheimer; *Drosophila melanogaster*; Aβ42; BACE1; alimento larval de abelhas sem ferrão; peptídeo bioativo; neurodegeneração.

ABSTRACT

Alzheimer's disease (AD) is a progressive neurodegenerative disorder characterized by the presence of amyloid plaques, neurofibrillary tangles, inflammation, oxidative damage, synapse loss, and selective neuron death. Inhibition of BACE1 expression has been considered a therapeutic target for the prevention and treatment of Alzheimer's disease. This study evaluated BACE1 inhibitory activity of secretome of bacteria isolated from stingless bees' larval food of native Brazilian species, *Melipona quadrifasciata* and *Tetragonisca angustula*. For this purpose, the screening of secretomes in the *Drosophila melanogaster* transgenic strains, followed by *in silico* analysis. We assessed the survival rate of transgenic fly with rough eye phenotype, generated by overexpression of human APP and BACE1 orthologs in the developing nervous system of the eye. Morphological modifications in the eyes of newly hatched *D. melanogaster* were examined. We verified reduction of morphological alterations in the eye, presenting compound eyes with smooth surface, difference in the fusion of the omatids and presence of a large number of bristles, in the groups treated with the S9 and S27 secretomes when compared to the control groups. Histological sections showed agreement with this improvement, exhibiting compound eyes with regular morphology and organized surface. The anti-AD model of D. melanogaster was treated with several bacterial secretomes for 15 days after hatching. The flies treated with the S1 secretome showed an improvement in the climbing rate when compared to the negative control and vehicle groups. Additionally, the groups treated with the S1 and S27 secretomes showed a decline in beta-amyloid levels after 15 days of treatment. The histology analysis of the brain revealed a decrease in neurodegeneration in flies treated with S1 visualized through the reduction of vacuolar lesions, when compared to the NC and vehicle groups. We carried out the proteomic analysis of the most efficient secretomes in the tests with D. melanogaster. The *in silico* analysis selected the most potentially bioactive peptides to interact with BACE1 and beta-amyloid, predicting the docking between them. Our analysis found four peptides that interact with BACE1 and β-amyloid plaques, with potential action in reducing the neurodegenerative process. Thus, our investigations resulted in the identification of potentially bioactive peptides that

can serve as a prototype for new drugs for the prevention or treatment of Alzheimer's Disease. The secretome of bacteria isolated of the larval food of stingless bees proved to be a potential source of therapeutic molecules targeting neurodegenerative disorders.

Keywords: Alzheimer's disease; *Drosophila melanogaster*; Aβ42; BACE1; stingless bees' larval food; bioactive peptide; neurodegeneration

APRESENTAÇÃO

A Doença de Alzheimer (DA) é uma doença neurodegenerativa progressiva caracterizada pela presença de placas amiloides, emaranhados neurofibrilares, inflamação, dano oxidativo, perda de sinapses e morte seletiva de neurônios. A inibição da expressão de BACE1 tem sido considerada um alvo terapêutico para sua prevenção e tratamento. Muitos compostos como, homodímeros de organofosfato, losartan e N-propargilpiperidinas com naftaleno-2-carboxamida ou naftaleno-2-sulfonamida, que têm atividade inibitória da colinesterase ou BACE1, foram estudados nos últimos anos para o tratamento da DA, porém nenhum deles foi eficiente para essa aplicação. Isso reforça a necessidade de desenvolver novos estudos que busquem moléculas biologicamente ativas com potencial de prevenir ou tratar a DA.

No Capítulo I dessa pesquisa, descrevemos a Doença de Alzheimer, sua fisiopatologia, as principais hipóteses etiológicas, os tratamentos medicamentosos existentes e os principais alvos terapêuticos. Explicamos o que são peptídeos bioativos e mostramos o potencial de identificá-los no secretoma de bactérias isoladas do alimento de larvas de abelhas brasileiras sem ferrão. Ressaltamos o uso da *Drosophila melanogaster* como organismo modelo para doenças neurodegenerativas e seu uso para triar moléculas biologicamente ativas com potencial biotecnológico. Por fim, destacamos o uso da proteômica e genômica como ferramentas tecnológicas para o desenvolvimento de terapias para doenças humanas.

No Capítulo II, apresentamos dois artigos científicos, já no formato de envio a publicação, que avaliam os efeitos neuroprotetores de diferentes secretomas de bactérias isoladas do alimento de larvas de abelhas brasileiras sem ferrão, das espécies *Melipona quadrifasciata* e *Tetragonisca angustula.* Diferentes linhagens transgênicas de *D. melanogaster* foram utilizadas, bem como análises proteômica, *in silico* e genômica. Nossas investigações resultaram na identificação de peptídeos potencialmente bioativos que podem servir de protótipo para novos fármacos para prevenção ou tratamento da Doença de Alzheimer.

Capítulo 1

Fundamentação Teórica

1 DOENÇA DE ALZHEIMER

1.1 Epidemiologia e fisiopatologia

A Doença de Alzheimer (DA) é a forma mais comum de demência e a quinta causa de morte em idosos (ALZHEIMER ASSOCIATION, 2018). É caracterizada como um distúrbio neurodegenerativo cerebral progressivo, que resulta em perda de memória e funções cognitivas, frequentemente, acompanhado por distúrbios comportamentais (QUERFURTH et al., 2010). O primeiro estágio clínico é geralmente a perda da memória recente. Com o avanço nos estágios da doença há grande prejuízo das funções cognitivas como, dificuldades na fala, distúrbios de atenção, incapacidade de fazer cálculos, perda das habilidades espaciais e da capacidade de usar objetos (LINDEBOOM, et al., 2004). Esses sintomas são acompanhados por distúrbios comportamentais, como irritabilidade, agressividade, alucinações, hiperatividade (RASKIND, 1995). Os sintomas depressivos estão presentes em cerca de 50% dos pacientes. Além disso, é comum que as pessoas com DA apresentem apatia, lentidão da marcha ou discurso, dificuldade de concentração, perda de peso, insônia e agitação (EASTWOOD et al., 1996).

A idade é o maior fator de risco associado à DA, afetando cerca de 6% da população mundial com mais de 65 anos. Estima-se que existam mais de 35 milhões de pessoas com DA no mundo e essa incidência tende a aumentar com o aumento da expectativa de vida da população (REITZ et al., 2011; 2014). Este número praticamente dobrará a cada 20 anos, chegando a 74,7 milhões em 2030 e a 152 milhões em 2050, segundo relatórios da Associação Internacional de Alzheimer (ALZHEIMER'S DISEASE INTERNATIONAL, 2015; 2019). Estima-se que a cada 3,2 segundos, um novo caso de demência é detectado no mundo e a previsão é de que em 2050, haverá um novo caso a cada 1 segundo (ALZHEIMER'S DISEASE INTERNATIONAL, 2015; 2019).

No Brasil, aproximadamente 12% dos idosos com 60 anos ou mais apresentam algum tipo de demência. Dessas, 40-60% são DA, equivalendo a dois milhões de brasileiros (BOFF et al., 2011). A maioria dos estudos confirma que as mulheres são mais propensas a desenvolver DA, principalmente as de idade mais

avançada (NITRINI et al., 2004). Além disso, a redução da capacidade funcional resultará em óbito desses pacientes, cerca de 10 anos após o início dos sintomas (HASSAN KHAN, 2009).

Embora a doença seja multifatorial e complexa, os pacientes apresentam em comum uma perda maciça de neurônios colinérgicos, deposição de emaranhados neurofibrilares (Figura 1A) em decorrência da hiperfosforilação da proteína associada ao microtúbulo (tau) e deposição/agregação do peptídeo beta-amiloide (Aβ) (Figura 1B) dentro do parênquima cerebral (HUANG et al., 2012).

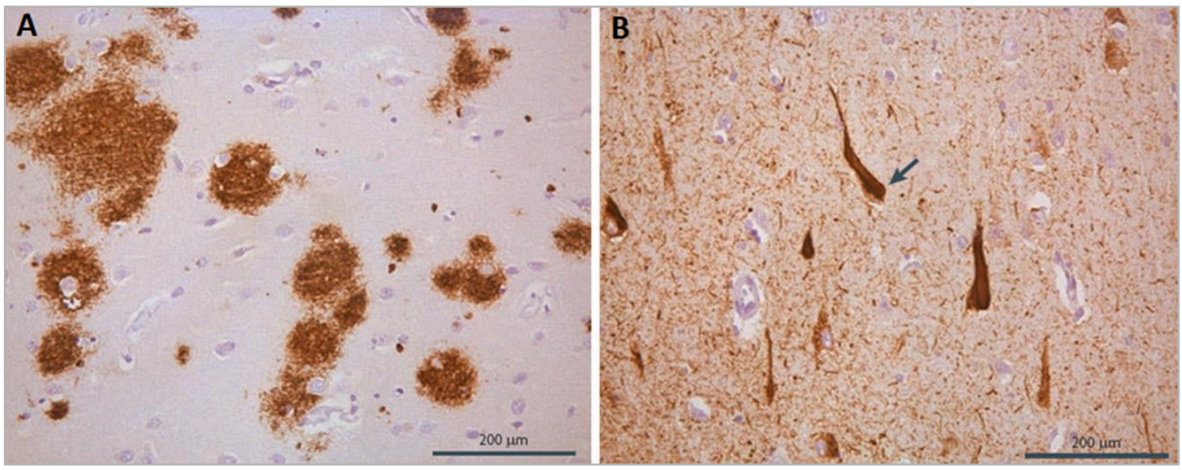

Figura 1. Características da doença de Alzheimer. A. Corte histológico de córtex cerebral humano de paciente afetado pela doença de Alzheimer, corado com anticorpo específfico para β-amiloide (Aβ). Uma das características clássicas da histopatologia da doença de Alzheimer é a aparecimento de lesões extracelulares conhecidas como placas senis ou amilóides, que são compostos pelo peptídeo Aβ. **B**. Corte histológico de córtex cerebral humano de paciente afetado pela doença de Alzheimer, corado com um anticorpo específico para fosforilação da proteína tau. A segunda marca histopatológica da doença de Alzheimer é a presença de lesões intraneuronais conhecidas como emaranhados neurofibrilares (indicados pela seta), que são compostos de filamentos anormais associados à hiperfosforilação da proteína associada à microtúbulos (tau). Fonte: AGUZZI & O'CONNOR (2010). Reproduzido com permissão da *Springer Nature*. Número da Licença de Uso: 5080230234044.

A histopatologia da DA é caracterizada por perda sináptica e morte de neurônios nas regiões responsáveis pela cognição, incluindo o córtex cerebral, o hipocampo, o córtex entorrinal e o estriado ventral (Figura 2) (AGUZZI et al.,

2010). No parênquima cerebral, os pacientes apresentam depósitos de fibras amiloides nas paredes dos vasos sanguíneos, acúmulo de filamentos anormais da proteína tau, perda neuronal e sináptica, ativação da glia e inflamação (SELKOE, 2001). No córtex cerebral é observado excesso da atividade de glutamato e comprometimento do mecanismo de cálcio neuronal, que resulta em apoptose da célula. Além disso, mecanismos como fatores genéticos, epigenéticos e metabólicos, reações inflamatórias, cascatas mitocondriais patogênicas, estresse oxidativo, deficiências de estrogênio e fatores ambientais também estão associados à DA (CAVALCANTI et al., 2012).

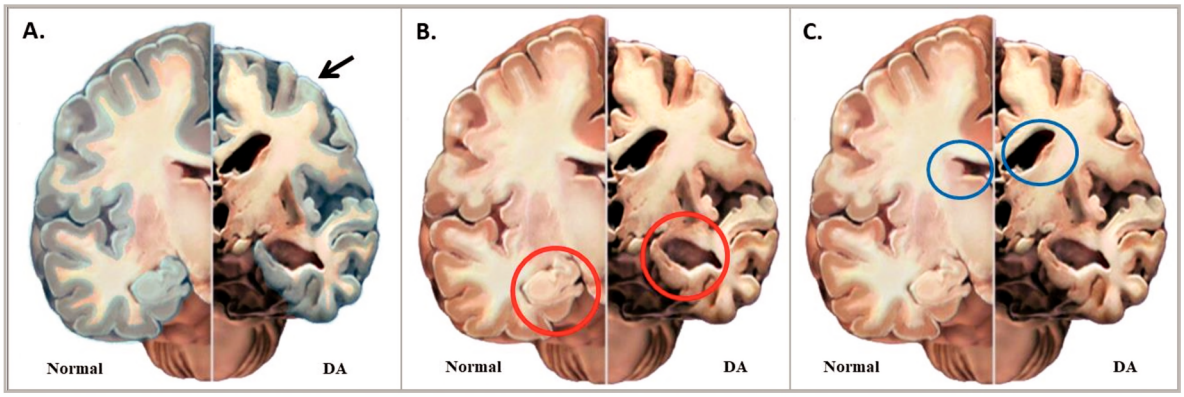

Figura 2. Comparação entre cérebro normal e de um paciente com Doença de Alzheimer. A. Córtex cerebral destacado em cinza (seta). Paciente com doença de Alzheimer (DA) apresentando redução da área do córtex, danificando as regiões envolvidas com pensamentos, planos e lembranças. **B.** Região do hipocampo selecionada pelos círculos vermelhos. Paciente com DA apresentando grave redução dessa área (lado direito da figura), prejudicando a formação da memória recente. **C.** Ventrículos selecionados com círculos azuis. Esses espaços, preenchidos por fluido dentro do cérebro, ficam maiores em pacientes com DA (lado direito da figura). Fonte: Adaptado de <http://www.alz.org/brain_portuguese/10.asp>.

A avaliação de marcadores neuropatológicos levou à definição de duas principais etiologias para a DA. A primeira compreende a hipótese amiloide (Figura 3) (SELKOE, 2016), que define o início da neurodegeneração como fruto da clivagem proteolítica da proteína precursora de amiloide (APP), resultando na produção, agregação e deposição da proteína β-amiloide (HARDY, 2002). A segunda é a hipótese colinérgica, que define a disfunção do sistema colinérgico

como suficiente para produzir deficiências na memória (BARTUS et al., 1999). Cérebros de pacientes com DA mostraram degeneração dos neurônios colinérgicos e atividade reduzida de colina acetiltransferase e a acetilcolinesterase no córtex cerebral (AULD et al., 2002).

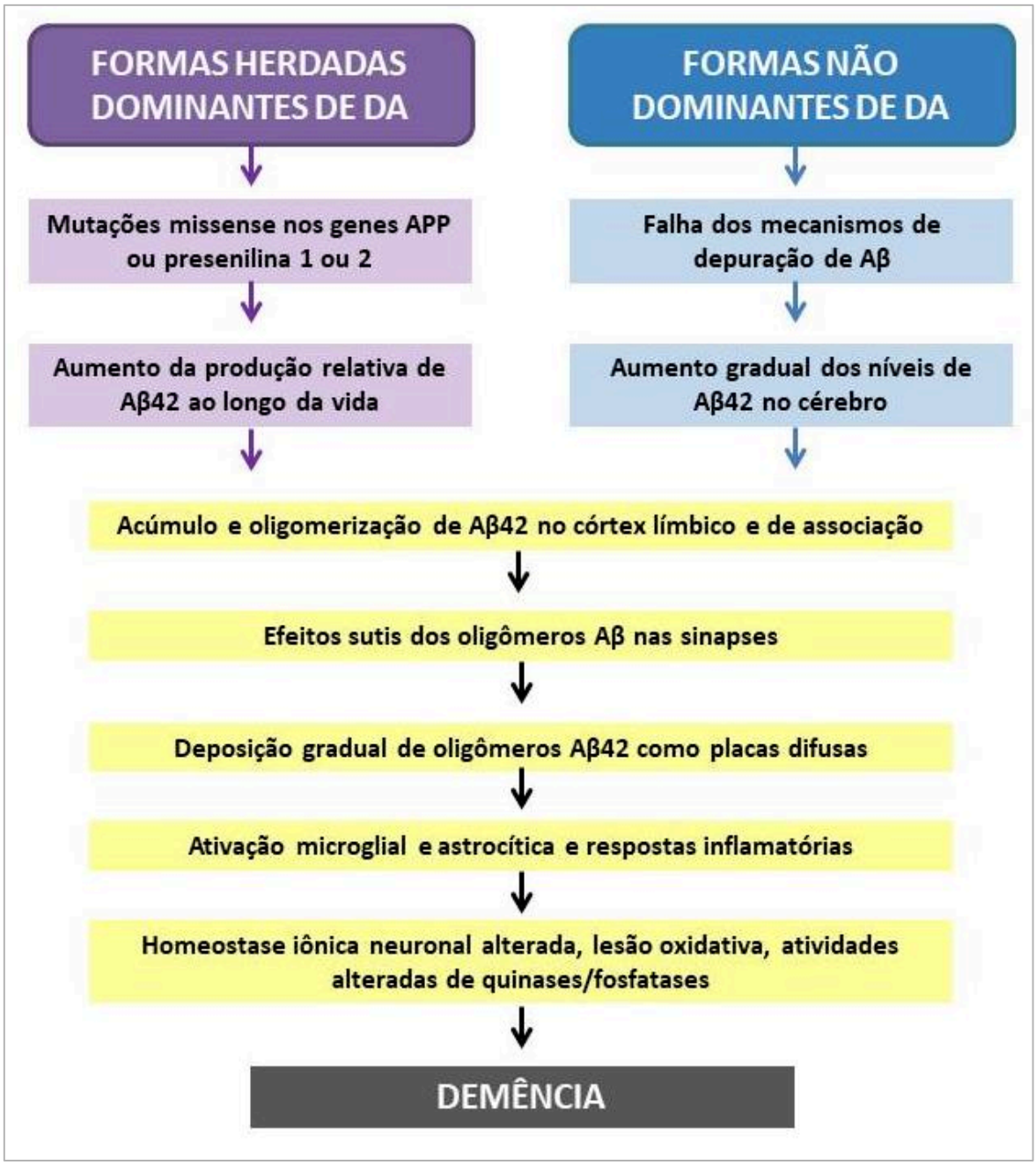

Figura 3. Sequência dos principais eventos patogênicos que levam à Doença de Alzheimer proposto pela hipótese da cascata amilóide. Fonte: RODRIGUES, T. S. (A autora)

1.2 Hipótese amiloide

As placas β-amilóides associadas à AD foram purificadas pela primeira vez na década de 1980 e, após sua análise, verificou-se que se tratava de agregados multiméricos do polipeptídeo Aβ (GLENNER et al., 1984; MASTERS et al., 1985). O cDNA de Aβ mostrou que ele era derivado de uma proteína precursora maior, a Proteína Precursora de Amiloide (APP) (TANZI et al., 1987). O isolamento e sequenciamento dessa proteína de 695 aminoácidos confirmou que a clivagem do seu domínio transmembranar tinha como produto o peptídeo Aβ (KANG et al., 1987).

A APP sofre processamento pós-tradução, envolvendo várias secretases e proteases diferentes, através de duas vias principais (Figura 4). Na via não amiloidogênica, a APP é sequencialmente clivada pelas enzimas α-secretase e γ-secretase. A primeira cliva APP no 17º aminoácido, gerando um grande domínio extracelular (sAPP-α) e um fragmento C-terminal de 83 aminoácidos associado à membrana (C83). APP C83 é então clivado pela γ-secretase gerando o peptídeo P3 e o domínio intracelular de APP (AICD), sendo ambos rapidamente degradados. Na via amiloidogênica, a APP é processada principalmente por β-secretase liberando sAPP-β e gerando um fragmento C terminal associado à membrana de 99 aminoácidos (C99). A γ-secretase ainda cliva C99, liberando AICD e o peptídeo Aβ amiloidogênico, que se agrega formando placas amiloides no cérebro (SARAH et al., 2007).

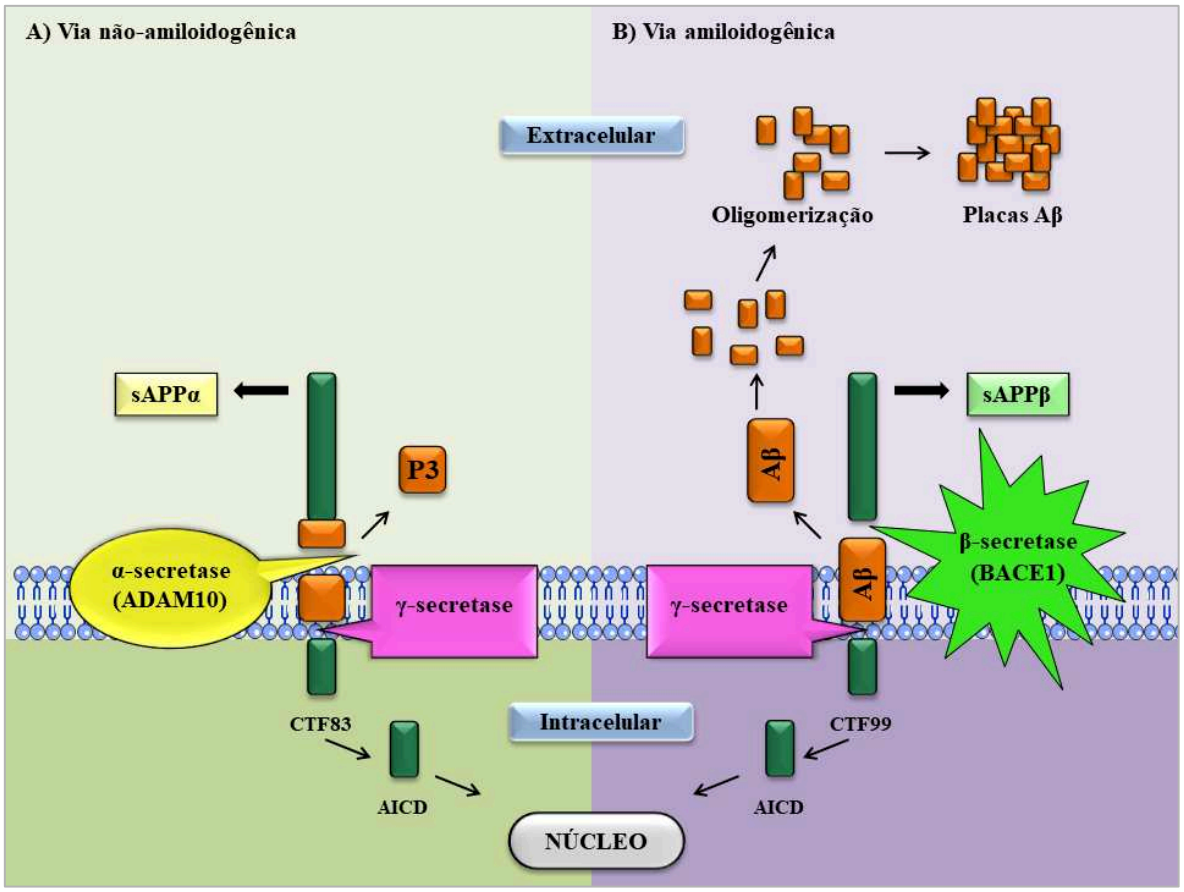

Figura 4. Processamento da proteína APP. Na via não amiloidogênica, a APP é sequencialmente clivada pelas enzimas α-secretase e γ-secretase. A primeira cliva APP no 17º aminoácido, gerando um grande domínio extracelular (sAPP-α) e um fragmento C-terminal de 83 aminoácidos associado à membrana (CTF83). APP C83 é então clivado pela γ-secretase gerando o peptídeo P3 e o domínio intracelular de APP (AICD), sendo ambos rapidamente degradados. Na via amiloidogênica, a APP é processada principalmente por β-secretase liberando sAPP-β e gerando um fragmento C terminal associado à membrana de 99 aminoácidos (CTF99). A γ-secretase ainda cliva CTF99, liberando AICD e o peptídeo Aβ amiloidogênico, que se agrega formando placas amilóides no cérebro. Fonte: RODRIGUES, T. S. (A autora).

A β-secretase, enzima de clivagem do sítio β1 (BACE1) foi identificada e caracterizada pela primeira vez em 1999 (SINHA et al., 1999; VASSAR et al., 1999; YAN et al., 1999; LIN et al.; 2000). BACE1 é uma proteína transmembrana tipo I de 501 aminoácidos, predominantemente expressa em membranas perinucleares pós-Golgi, estruturas vesiculares do citoplasma e superfície celular (EHEHALT et al., 2002).

Desde que os estudos moleculares da DA começaram, pesquisadores se concentraram na compreensão dos diversos e complexos mecanismos dessa patologia. A partir disso, a hipótese amiloide (Aβ) (BEYREUTHER & MASTERS, 1991; HARDY & ALLSOP, 1991; SELKOE, 1991; HARDY & HIGGINS, 1992) tornou-se o modelo dominante da patogênese da DA e está orientando o desenvolvimento de tratamentos potenciais. Importantes descobertas têm reafirmado a influência da agregação amiloide no desenvolvimento de DA, tais como:

- Estudos de neuropatologia da DA na síndrome de Down mostrou que o acúmulo inicial de depósitos Aβ precede a ativação microglial e astrocítica, a formação de emaranhado e a neurodegeneração (MANN et al., 1992; LEMERE et al., 1996a; 1996b);

- A deleção do gene codificador de BACE1 impede a geração do peptídeo Aβ e elimina completamente os danos relacionados às placas beta-amiloides em camundongos transgênicos que expressam mutação na APP ortóloga humana (FARZAN et al., 2000; CAI et al., 2001; LUO et. al, 2001; ROBERDS et al., 2001; OHNO et al., 2004; LAIRD et al., 2005);

- O nível de expressão e a atividade de BACE1 estão elevados em pacientes com DA (HOLSINGER et al., 2002; YANG et al., 2003);

- A superprodução do peptídeo Aβ leva à neurotoxicidade, formação de emaranhados neuronais, dano sináptico e, eventualmente, perda de neurônios nas regiões cerebrais patologicamente afetadas pela DA (SELKOE, 1998; SHANKAR & WALSH, 2009);

- Entre os vários peptídeos Aβ gerados pelas clivagens de múltiplos locais de secretases, o $A\beta_{42}$ (peptídeo Aβ de 42 aminoácidos) provou ser o mais hidrofóbico e amiloidogênico (BURDICK et al., 1992);

- A maioria das mutações relacionadas à DA familiar hereditária aumenta a geração de peptídeos Aβ ou a proporção de $A\beta_{42}/A\beta_{40}$ (BORCHELT et al., 1996; SCHEUNER et al., 1996);

- Níveis aumentados de $A\beta_{42}$ geram oligomerização e formação de placa amiloide (JARRET et al., 1993; IWATSUBO et al., 1994).

Embora o excesso de Aβ cause neurotoxicidade, o $A\beta_{40}$ parece proteger os neurônios contra o dano neuronal induzido pelo $A\beta_{42}$, sendo necessário para a viabilidade dos neurônios centrais (PLANT et al., 2003; ZOU et al., 2003). Estudos mostram que baixas doses (picomolar) de $A\beta_{40}$ podem modular positivamente a plasticidade sináptica e a memória, exercendo importantes funções fisiológicas quando em condições normais (MORLEY et al., 2008). Diante disso, o gatilho para o desenvolvimento da DA seria o aumento excessivo de $A\beta_{42}$ e seu acúmulo em placas β-amiloides, gerando neurotoxicidade e contribuindo para o desencadeamento dos demais mecanismos patogênicos da doença.

De acordo com alguns pesquisadores, a toxicidade do $A\beta_{42}$ é justificada por sua conformação única que compreende um único motivo triplo β em sua estrutura, formado por três folhas β que recobrem seus resíduos 12-18 (β1), 24-33 (β2) e 36-40 (β3). Esta dobra terciária (Figura 5) seria responsável por sua citotoxicidade e agregação, resultando na formação de placas β-amiloides presentes em pacientes com DA (XIAO et al., 2015).

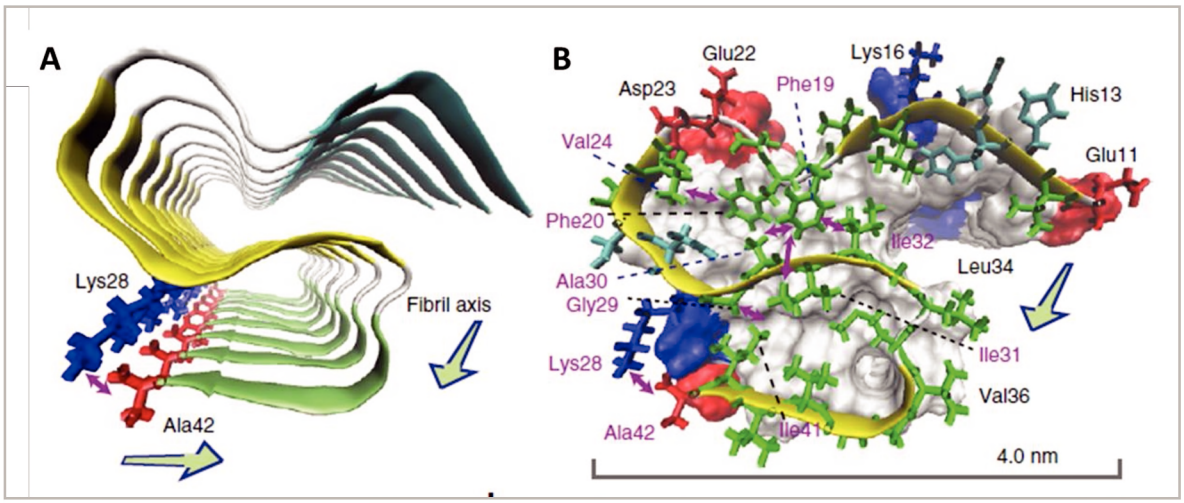

Figura 5. Detalhes estruturais do Aβ (1–42). Os resíduos desordenados 1–10 são omitidos para maior clareza. Setas verdes indicam o eixo da fibrila. **A.** Vista do eixo da fibrila, mostrando três regiões de fita β (ciano, resíduos 12-18; amarelo, 24-33; verde, 36-40) conectadas por regiões giratórias (prata). A ponte salina única entre Lys28 (azul) e Ala42 (vermelho) é mostrada**. B.** Ligações (Van der Waals) da cadeia lateral para a cadeia Aβ única e diagrama de polaridade para o restante das cadeias Aβ. Os resíduos

são destacados como verdes, hidrofóbicos; ciano, polar; vermelho, ácido e azul, básico. As ligações intramoleculares da cadeia lateral são evidenciados por setas roxas e os intermoleculares por setas azuis. Fonte: XIAO et al (2015). Reproduzido com permissão da *Springer Nature.* Número da Licença de Uso: 5080221276326.

Diante de tais descobertas, esse trabalho se concentrará nos mecanismos da Hipótese Amiloide, na tentativa de identificar peptídeos que possam atuar na via amiloidogênica de processamento de APP e servirem de protótipo para novos fármacos de ação terapêutica para prevenir ou tratar a DA.

1.3 BACE1 como alvo terapêutico

Devido às fortes evidências que confirmam a hipótese amiloide como sendo a principal etiologia ligada ao desenvolvimento da DA, diversos estudos têm se concentrado no desenvolvimento de terapias para redução de Aβ, tendo como foco a inibição de BACE1 (YAN & VASSAR, 2014).

A Figura 6 mostra a estrutura 3D de BACE1, evidenciando seu sítio ativo formado pela díade catalítica conservada Asp32 e Asp 228. Na porção N-terminal da molécula (resíduos 67-75) há uma aba que é perpendicular ao sítio ativo, cobrindo-o parcialmente, sendo a região mais flexível da β-secretase. Mudanças nessa aba parecem controlar o acesso ao sítio-alvo, posicionando corretamente o substrato para que ocorra a catálise (XU et al., 2011).

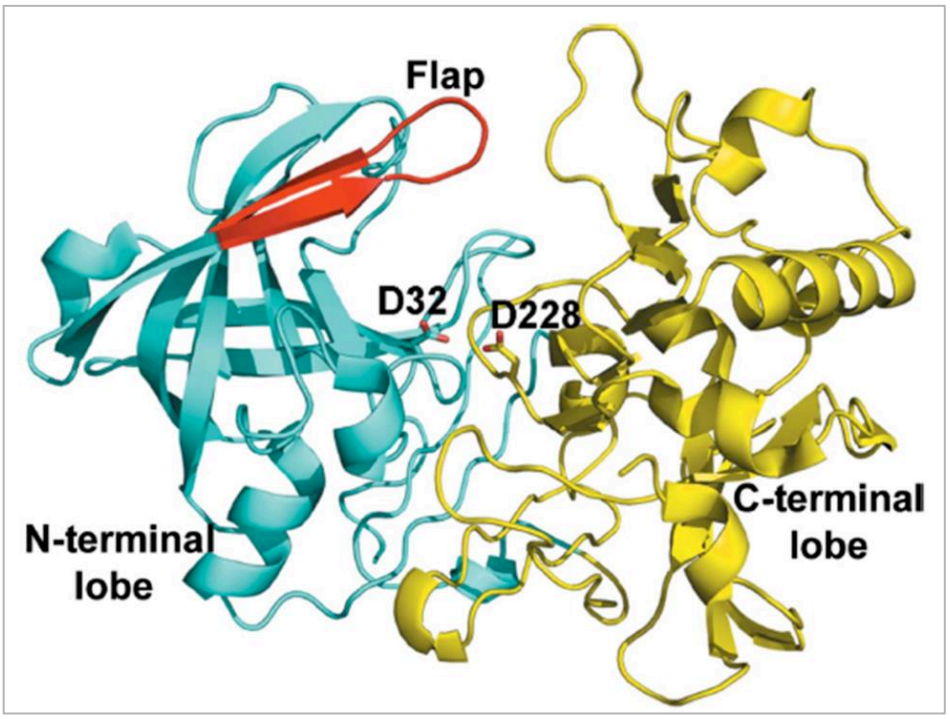

Figura 6. Representação em fita da estrutura tridimensional da BACE1. Os lóbulos dos terminais N e C são coloridos em ciano e amarelo, respectivamente. Os resíduos da díade Asp, Asp32 e Asp228, são apresentados como bastões. Os resíduos 67-78 são coloridos em vermelho e a aba é mostrada em sua conformação "aberta". Fonte: XU et al (2012). Reproduzido com permissão da *International Union of Crystallography* (IUCr Journal), DOI: 10.1107/S0907444911047251.

Pesquisas utilizando camundongos transgênicos com superexpressão de APP humana mostraram que a deleção genética de BACE1 elimina a produção de Aβ e, consequentemente, reduz as alterações cognitivas e comportamentais relacionadas à DA (DOMINGUEZ et al., 2005; OHNO et al., 2007; MCCONLOGUE et al., 2007). Além disso, a identificação de uma rara mutação humana no sítio de clivagem de APP por BACE1 resultou em diminuição de 40% da produção de Aβ em ensaios *in vitro*, redução de cinco a sete vezes no risco de desenvolver DA e melhoria da função cognitiva em idosos sem DA (JONSSON et al., 2012; BENILOVA et al., 2014; MALONEY et al., 2014). A deleção de β-secretase em camundongos parece não gerar efeitos evidentes nesses animais, sugerindo que os inibidores de BACE1 podem não apresentar efeitos colaterais graves para o organismo (LUO et al., 2001). A inibição da atividade de BACE1 pode impedir a produção de $A\beta_{42}$, prevenir o desenvolvimento dessa patologia no

cérebro e resgatar déficits de memória em camundongos (OHNO et al., 2004; 2007; LAIRD et al., 2005; MCCONLOGUE et al., 2007).

Apesar dessas descobertas já terem completado décadas, os pesquisadores ainda buscam, sem muito sucesso, inibidores de BACE1 que sejam permeáveis às células, biodisponíveis por via oral e ativos no sistema nervoso central. Além da busca por peptídeos bioativos que possam interagir com BACE1 inibindo sua atividade, essas moléculas devem conseguir penetrar facilmente na barreira hematoencefálica. A busca frustrada por tais moléculas só confirmam o fato das pesquisas com essa finalidade serem extremamente necessárias, além de desafiadoras (LUO et al., 2001).

1.4 Tratamentos medicamentosos para doença de Alzheimer

Os tratamentos medicamentosos existentes para pacientes com DA compreendem três inibidores de colinesterase (rivastigmina, donepezil e galantamina) e um que afeta o sistema glutamatérgico (memantina) (CUMMINGS et al., 2014; GODYN et al., 2016). Nenhum desses fármacos, porém, representa cura para a DA. Esses tratamentos não impedem a progressão da demência, mas desaceleram, temporariamente, a perda da função cognitiva ao diminuir a atividade da colinesterase, resultando em níveis mais elevados de acetilcolina e melhoria da função cerebral (CUMMINGS et al., 2014; GODYN et al., 2016).

Mais de duzentos compostos alcançaram a Fase II de ensaio clínico desde 2003, mas nenhum novo medicamento foi aprovado para o tratamento da DA (CUMMINGS et al., 2014; GODYN et al., 2016). A maioria dos ensaios clínicos que apresentou resultados positivos na Fase II, não teve sucesso na Fase III, devido principalmente à falta de eficácia terapêutica ou existência de efeitos adversos graves (CUMMINGS et al., 2014).

Em 2011, houve um avanço significativo no desenvolvimento de inibidores de BACE1. May e colaboradores (2011) identificaram um inibidor de BACE1 moderamente potente chamado LY2811376, que produziu mudanças farmacodinâmicas robustas em modelos animais e voluntários saudáveis. Apesar dos testes clínicos desta molécula terem sido interrompidos devido ao surgimento

de efeitos adversos, seus dados forneceram suporte para o uso de pequenas moléculas bioativas para tratar a DA (MAY et al., 2011).

Outros testes com potenciais inibidores de BACE1 também falharam nas fases dos ensaios clínicos. O inibidor de BACE1, oralmente ativo, BI 1181181, falhou na Fase I devido à baixa biodisponibilidade oral e baixa penentração da barreira hematoencefálica. Os inibidores RG7129 (Fase I), LY2811376 (Fase I) e LY2886721 (Fase II) falharam nos ensaios devido à toxicidade hepática que provocaram (LILLY, 2013; KENNEDY et al., 2016).

Em abril de 2012, a Merck divulgou na Academia Americana de Neurologia, os resultados da Fase I de uma molécula inibidora de BACE1 chamada Verubecestate (MK-8931) (KENNEDY et al., 2016). MK-8931 foi inicialmente testada em 88 voluntários saudáveis na Fase I do ensaio clínico, que foi realizada de forma randomizada, duplo-cega e controlada por placebo. Posteriormente, conduziram outro ensaio de Fase I em 32 pacientes com DA a fim de verificar a segurança, tolerabilidade, farmacocinética, e farmacodinâmica da molécula MK-8931 (NCT01496170). Os resultados de MK-8931 na fase I encorajaram a realização das Fases I e II dos ensaios clínicos, que foram iniciados no final de 2012. Em fevereiro de 2017, a Merck interrompeu o teste de Fase III de Verubecestate, em pacientes com DA leve e moderada, devido à falta de eficácia (KENNEDY et al., 2016).

Estudos de Fase I randomizados, duplo-cego e controlados por placebo em jovens saudáveis e idosos estabeleceram a segurança de um novo inibidor de BACE1 chamado AZD3293 que foi desenvolvido pela AstraZeneca (EKETJALL et al., 2016). Foi relatado que administração de AZD3293 reduziu os níveis de peptídeos Aβ no líquido cefalorraquidiano. Em setembro de 2014, a AstraZeneca e a Elli Lilly lançaram as Fases II e III, para testar a AZD3293 em pacientes com comprometimento cognitivo leve e DA leve (EKETJALL et al., 2016).

Até o momento, ainda não há terapia eficaz disponível para curar ou inibir significativamente a progressão dos sintomas da DA. A busca por moléculas potencialmente bioativas que possam inibir BACE1 é, ainda, uma das principais abordagens terapêuticas para prevenir ou tratar a doença de Alzheimer. No desenvolvimento desse trabalho, buscamos peptídeos de ação antineurodegenerativa que possam interagir com os alvos terapêuticos BACE1 e

β-amiloide, apresentando bioatividade potencial para tratar a Doença de Alzheimer.

2 PEPTÍDEOS BIOATIVOS

2.1 Definição

Peptídeos bioativos são definidos como sequências de resíduos de aminoácidos de uma proteína capazes de exercer algum efeito biológico nas funções do corpo. Alguns desses peptídeos podem impactar positivamente na saúde humana (KITTS & WEILER, 2003), regulando funções corporais importantes por meio de suas inúmeras atividades, incluindo funções anti-hipertensivas, antimicrobianas, antitrombóticas, imunomoduladoras, opióides, antioxidantes (CHAKRABARTI et al., 2014; SANCHEZ & VAZQUEZ, 2017).

Embora a estrutura e a relação funcional dos peptídeos bioativos não estejam bem estabelecidas, a maioria deles compartilha algumas propriedades comuns. Por exemplo, a maioria desses peptídeos contém de 2 a 20 aminoácidos e, geralmente, são ricos em aminoácidos hidrofóbicos (KITTS & WEILER, 2003; MOLLER et al., 2008).

2.2 Obtenção de peptídeos bioativos

Nos últimos anos, houve aumento das pesquisas que buscam sequências de peptídeos bioativos que possam reduzir ou prevenir o risco de doenças crônicas e fornecer proteção imunológica (KORHONEN et al., 2006). Esses peptídeos podem ser produzidos por hidrólise enzimática (usando enzimas proteolíticas de plantas ou microrganismos), hidrólise com enzimas digestivas (digestão gastrointestinal simulada) ou por fermentação.

Alguns estudos utilizaram, também, uma combinação desses métodos para produzir peptídeos com atividade biológica (KORHONEN et al., 2006). Esses peptídeos bioativos podem ser sintetizados quimicamente, visto que sua

quantidade encontrada na natureza é baixa e há interesse comercial crescente e constante em produzi-los (PEREZ ESPITIA et al., 2012).

No método de **hidrólise enzimática,** a proteína de interesse é submetida a tratamento enzimático em pH e temperatura específicas. Exemplos:

- El-Fattah et al.(2017): peptídeos bioativos com atividades inibidoras da ECA foram produzidos a partir da hidrólise do leite usando protease de *Aspergillus oryzae*.

O método de **fermentação** envolve o uso de culturas de microrganismos, como leveduras, fungos ou bactérias para hidrolisar as proteínas de interesse e gerar peptídeos mais curtos. O grau de hidrólise depende do tempo de fermentação, da cepa microbiana e da fonte de proteína. Exemplos:

- Gobbetti et al. (2000): peptídeos inibidores da enzima de conversão da angiotensina (ACE) foram gerados a partir da hidrólise do leite, usando as cepas *Lactobacillus lactis* e *Lactobacillus delbrueckii*;

- Ahn et al. (2009) mostraram que a atividade inibitória de ACE por peptídeos derivados de proteína de soro de leite fermentados com *Lactobacillus brevis* era mais forte do que aqueles fermentados com *L. lactis* , *L. plantarum* e *L. acidophilus*.

- Sanjukta et al. (2015) demonstraram que proteínas de soja fermentadas por *Bacillus subtilis* MTCC5480 produziram maior grau de hidrólise em comparação com *B. subtilis* MTCC1747.

Vários estudos usaram a técnica de **digestão gastrointestinal simulada**, *in vitro,* para produzir peptídeos bioativos a partir de proteínas presentes em alimentos. Nesse método, os pesquisadores tentaram identificar a atividade dos peptídeos que podem ser produzidos em nosso corpo após o consumo de um determinado alimento ou proteína alimentar (MORA et al., 2017; ASPRI et al., 2018).

A absorção do trato gastrointestinal é essencial para que um peptídeo bioativo exerça sua ação biológica. Acreditava-se que todos os peptídeos e proteínas eram digeridos até seus aminoácidos constituintes e apenas esses

aminoácidos eram capazes de atravessar a barreira epitelial intestinal. No entanto, vários estudos mostraram que, em condições normais, muitos peptídeos atravessam o epitélio intestinal, entram na circulação e exercem seus efeitos sistêmicos (MUHEEM et al., 2016; NG et al., 2018).

Nesse estudo, a amostra de tratamento (secretoma de bactérias presentes no microbioma do alimento larval de abelhas sem ferrão) será ingerida pelas moscas de linhagens transgênicas de *Drosophila melanogaster* misturada ao alimento. Dessa forma, o conteúdo proteico do secretoma poderá ser clivado por enzimas digestivas do trato gastrointestinal da mosca, gerando peptídeos bioativos.

3 ABELHAS SEM FERRÃO

3.1 Características gerais

Existem aproximadamente 500 espécies de abelhas sem ferrão, localizadas principalmente na América Latina, Austrália, África e Ásia (RASMUSSEN & CAMERON, 2010). São da ordem Hymenoptera, tribo Meliponini e podem ser classificadas em dois gêneros: *Melipona e Tetragonisca* (MICHENER, 2013). A Figura 7 mostra um indivíduo de cada uma das espécies utilizadas no presente estudo.

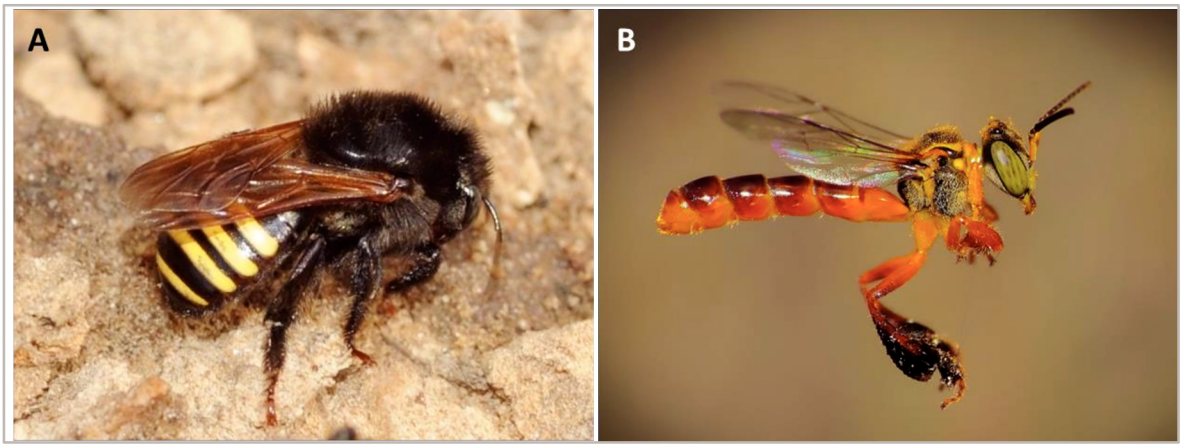

Figura 7. Abelhas sem ferrão nativas brasileiras. A. Abelha *Melipona quadrifasciata* (gênero *Melipona*), popularmente conhecida como Mandaçaia. **B.** Abelha *Tetragonisca*

angustula (gênero *Tetragonisca*), popularmente conhecida como Jataí. Fonte:< https://www.criarabelhas.com.br/>.

As abelhas sem ferrão são insetos eussociais que compõem um grupo complexo e diversificado, com grande número de espécies e vários padrões comportamentais (KEER et al., 2001; MICHENER, 2007). Elas formam colônias perenes, instalando-se em cavidades pré-existentes, tais como troncos de árvores ou ninhos abandonados por outros animais (KERR et al., 1996; 2001) onde armazenam alimento e mantem sua prole protegida (MICHENER, 2013). Elas constroem continuamente células de cria, formando favos horizontais ou cachos (KERR et al, 1996).

O aprovisionamento das células de cria (Figura 8) é massal, com material semi líquido, que consiste de pólen, secreção glandular e néctar ou mel, sobre o qual o ovo é posicionado verticalmente, pela rainha. Após a oviposição, a célula é, imediatamente, fechada pelas operárias e aberta apenas para eclosão do imago (MICHENER, 1974; ROUBIK, 1989).

O pólen e o néctar fornecem carboidratos e proteínas para a dieta das abelhas adultas e alimentam as larvas (MICHENER, 1974; ROUBIK, 1989). O pólen é armazenado em potes de cera e, em seguida, as operárias regurgitam uma substância glandular que auxiliará na fermentação dele para consumo (KERR et al., 1996). O néctar é desidratado por ventilação pelas operárias receptoras, sendo em seguida, armazenado em potes de cera.

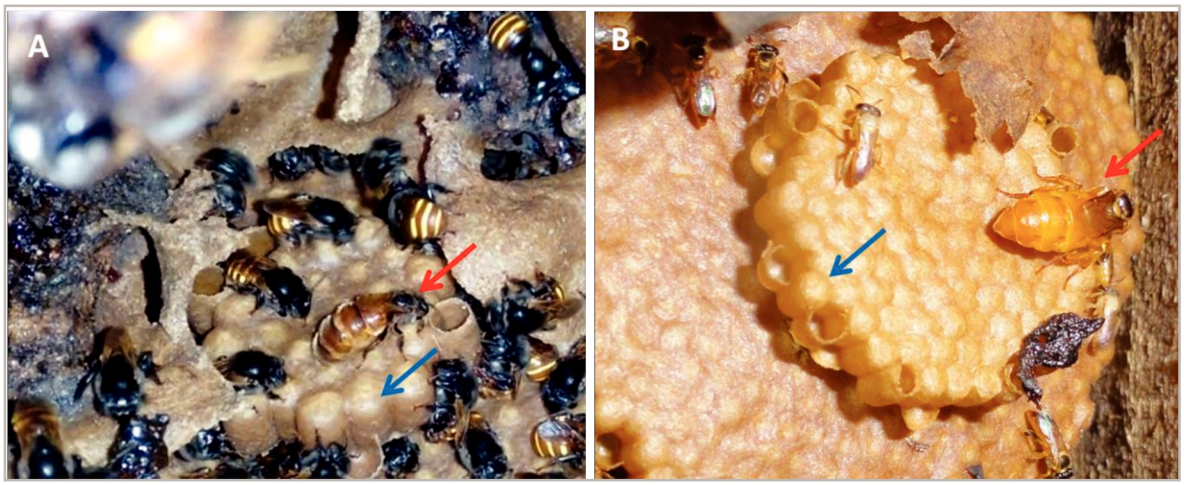

Figura 8. Células de cria de abelhas sem ferrão nativas brasileiras. A. Abelha rainha de *Melipona quadrifasciata* (seta vermelha) e células de cria (seta azul). **B.** Abelha *Tetragonisca angustula*, (seta vermelha) e células de cria (seta azul). Fonte:< https://www.criarabelhas.com.br/>.

3.2 Alimento larval de abelhas brasileiras sem ferrão

O alimento larval das abelhas sem ferrão é constituído de mistura de secreção glandular, mel e pólen. Essa mistura, que é colocada dentro das células de cria para alimentar as larvas de abelhas (Figura 9) é ainda menos explorada que os demais produtos das abelhas sem ferrão, tais como mel e própolis. O ambiente escuro, quente e úmido da célula de cria contribui para o crescimento de microrganismos (KERR et al, 1996).

Figura 9. Colmeia de abelha sem ferrão. Células de cria em colmeia de abelhas sem ferrão Manguadari contendo alimento larval e o ovo posto pela abelha-rainha. Fonte: SILVA et at (2014).

O pólen, um dos constituintes do alimento larval, é fermentado pela secreção glandular das abelhas, sendo uma ótima fonte de microrganismos presentes no intestino das abelhas. Estudos mostram que, dos microrganismos encontrados no pólen, cerca de 30% são bactérias gram-positivas (*Bacillus, Bacteridium, Streptococcus e Clostridium spp*) e 70% bactérias gram-negativas (*Achromobacter, Citrobacter, Enterobacter, Erwinia, Escherichia coli, Flavobacterium, Klebsiella, Proteus e Pseudomonas*) (GILLIAM et al., 1987; 1990; EL-LEITHY & EL-SIBAEL, 1992).

Nosso estudo será o primeiro a avaliar o secretoma de bactérias isoladas do alimento de larvas de abelhas brasileiras sem ferrão, tais como *Melipona quadrifasciata e Tetragonisca angustula*, em busca de peptídeos bioativos que possam servir como protótipo para novos fármacos para tratamento ou prevenção da DA. Para verificar a ação antineurodegenerativa dos secretomas bacterianos, utilizaremos linhagens transgênicas do organismo modelo *Drosophila melanogaster.*

4 *DROSOPHILA MELANOGASTER*

4.1 Características gerais

Drosophila melanogaster é um inseto holometábolo, pequeno (2-3 milímetros), encontrado em frutas em decomposição, sendo por isso conhecida, popularmente, como mosca da fruta (LYNCH et al., 2012).

A *D. melanogaster* possui ciclo de vida rápido (Figura 10). O desenvolvimento embrionário, após a fertilização e formação do zigoto, ocorre dentro da membrana do ovo, que eclode em larva. O período larval se divide em três estágios. No terceiro e último estágio (3° instar – L3), a larva pode alcançar o comprimento de 4,5 milímetros, desenvolvendo-se para o próximo estágio, de pupa. A 25°C, o ciclo de vida se completa em cerca de 10-12 dias, quando a pupa eclode em adulto. As moscas produzem grande número de descendentes em um único cruzamento, além de serem de fácil manutenção e baixo custo (GRAF et al., 1996; JENNINGS, 2011).

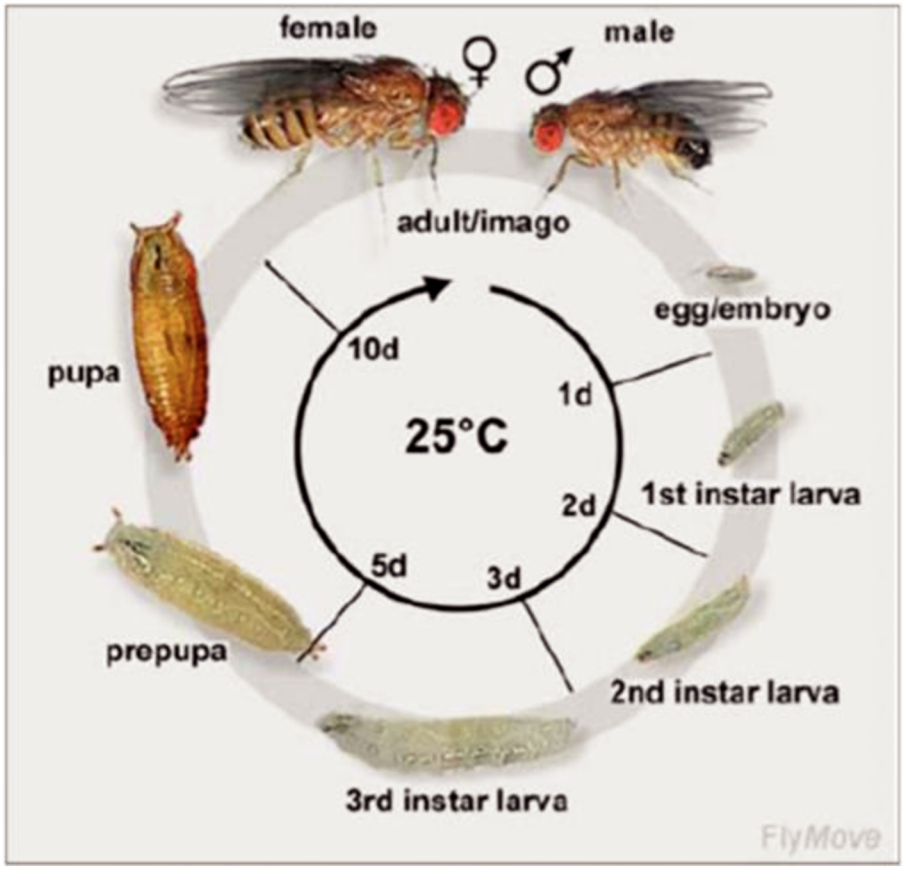

Figura 10. Ciclo de vida da *Drosophila melanogaster*. Fonte: <http://www.sc.didaxis.pt/hereditariedade/drosophila.htm>.

A mosca da fruta possui quatro pares de cromossomos (2n = 8) (Figura 11), sendo três pares autossômicos e um par de cromossomos sexuais (DE BELLE & HEISENBERG, 1996).

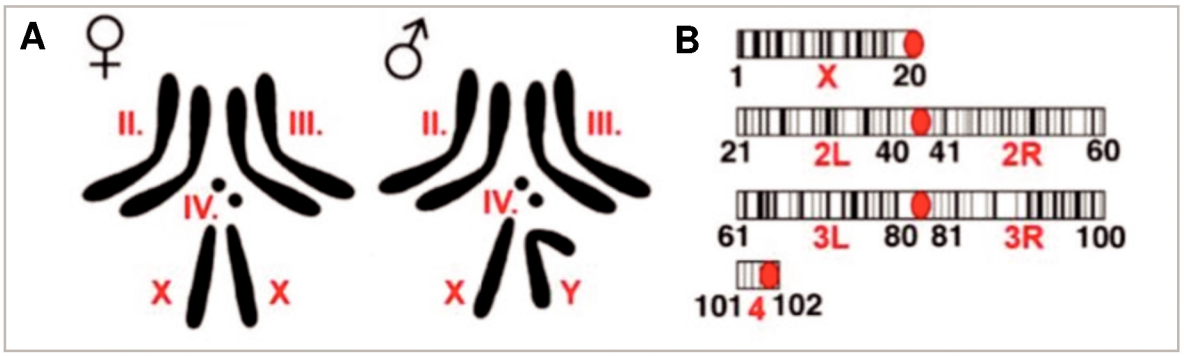

Figura 11. Representação dos cromossomos de célula da glândula salivar de *Drosophila melanogaster*. A. Esquema de cromossomos de célula da glândula salivar. **B.** Os números em preto indicam loci gênicos. Os cromossomos 2 e 3 são subdivididos

em braços esquerdo (**L**) e direito (**R**) e centrômero (ponto vermelho). Fonte: DE BELLE e HEISENBERG (1996).

Os machos são identificados visualmente (Figura 12) por uma mancha escura na extremidade posterior do abdômen e pelo apêndice sexual (semelhante a um pente) localizado nas patas dianteiras, como linhas pretas e grossas. Estes são aferroados na fêmea quando há a tentativa de acasalar. Na mosca macho, os dois últimos segmentos do abdome são mais escuros que os de uma fêmea. Machos têm uma faixa grossa e preta, enquanto que fêmeas tem uma faixa mais escura e uma mais clara acima dessa (AHUJA & SINGH, 2008; CHILDRESS & HALDER, 2008).

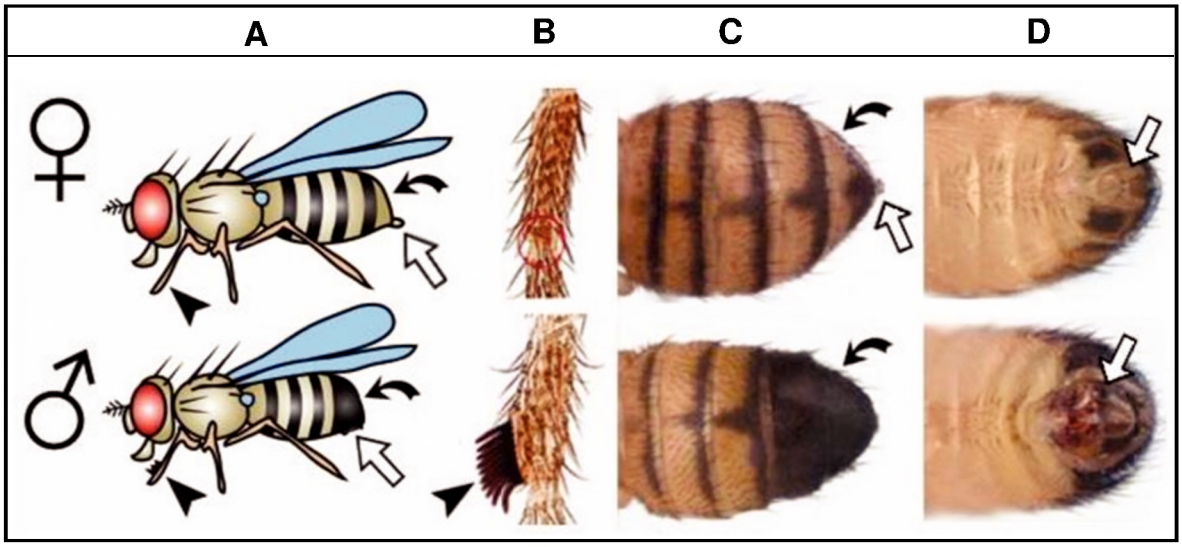

Figura 12. Diferenças entre macho e fêmea de *Drosophila melanogaster.* As imagens mostram as fêmeas (parte superior) e os machos (parte inferior). **A.** Visão lateral do corpo inteiro (1ª coluna). As fêmeas são ligeiramente maiores que os machos. **B.** Visão ampliada das patas dianteiras. Apenas machos exibem apêndice sexual no primeiro par de patas (ponta de seta). **C.** Vista dorsal. As fêmeas exibem listras escuras separadas na ponta posterior do abdômen, que são fundidas em machos (setas curvas). **D.** Visão ventral do abdômen. As placas anais (setas brancas) são mais escuras e complexas nos machos e nas fêmeas, exibem uma extensão tipo pino. O abdômen e a placa anal ainda estão pálidos em machos recém-eclodidos e podem ser confundidos como indicadores de fêmea, à primeira vista. Durante um período muito curto após a eclosão, as moscas exibem um ponto esverdeado escuro, visível a olho nu, em seu abdômen, o mecônio (não

mostrado) que é tomado como um indicador da virgindade da fêmea, mesmo que machos férteis estejam presentes. Fonte: CHILDRESS & HALDER (2008), com modificações.

4.2 *Drosophila melanogaster* como organismo modelo

A *D. melanogaster* vem sendo utilizada nas ciências biológicas para o desenvolvimento de estudos científicos e foi um dos primeiros organismos a ter seu genoma sequenciado. Após a conclusão do sequenciamento do genoma humano, a homologia observada entre os dois genomas reforçou o papel dessa mosca como organismo modelo para o entendimento da biologia humana, bem como dos mecanismos de certas doenças (ADAMS et al., 2000).

Estima-se que, aproximadamente 75% dos genes relacionados à doença em humanos possuem ortólogos funcionais em *D. melanogaster*. A homologia entre a sequência desses genes é de cerca de 40% de identidade, sendo de 80% – 90% em domínios funcionais conservados (ADAMS et al., 2000). Estudos na mosca da fruta alteraram substancialmente as estimativas da relação evolutiva entre organismos vertebrados e invertebrados (Figura 13).

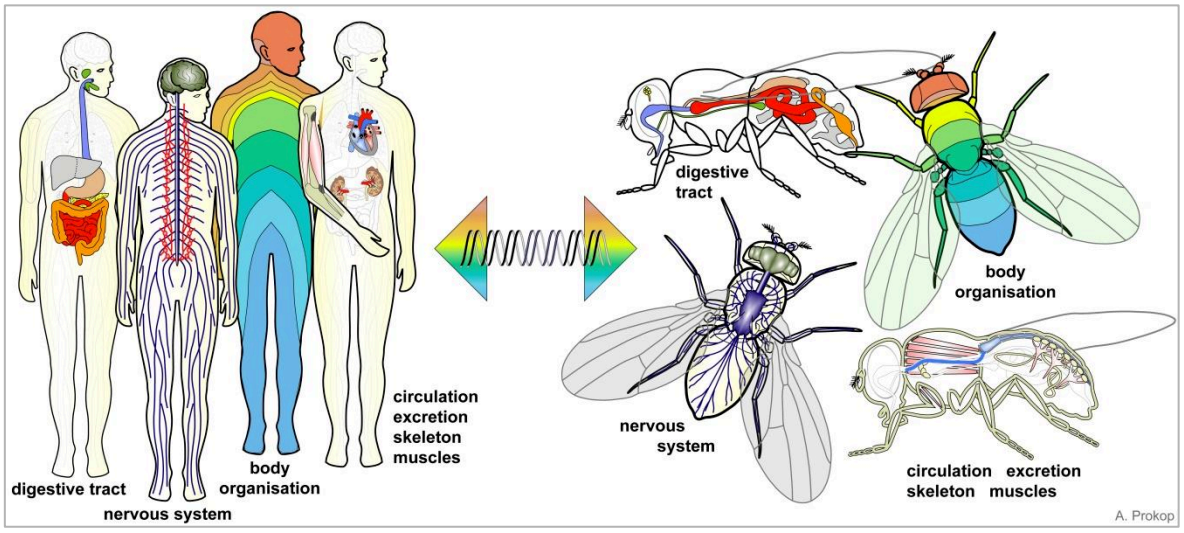

Figure 13. Homologia entre sistema humano e *Drosophila melanogaster.* Para quase todos os órgãos dos humanos existe uma correspondência nas moscas, e os genes comuns regulam seu desenvolvimento, organização e função. Fonte: < https://droso4schools.wordpress.com/organs/>.

Nos últimos 50 anos, o estudo genético em *D. melanogaster* foi aplicado com sucesso para decifrar os principais mecanismos subjacentes a inúmeros processos, incluindo desenvolvimento (LAWRENCE, 1992), sinalização (CADIGAN & PEIFER, 2009), ciclo celular (LEE & ORR-WEAVER, 2003), desenvolvimento, função e comportamento do sistema nervoso (WEINER, 2000; BELLEN et al., 2010) e, até mesmo, aspectos moleculares de doenças humanas (BIER, 2005).

A semelhança dos aspectos da biologia celular entre *Drosophila* e humanos varia da expressão gênica à sinaptogênese, conectividade neural, sinalização e morte celular (SANG & JACKSON, 2005). *D. melanogaster* apresenta um sistema nervoso complexo, com capacidade de desenvolver comportamentos como aprendizagem e memória, o que é atraente para estudos de disfunções neuronais e doenças neurodegenerativas (CHAN & BONINI, 2000).

Várias linhagens dessa mosca têm sido usadas para estudar doenças neurodegenerativas, já que seu sistema nervoso inclui olhos, órgãos olfativos, gustativos, órgãos auditivos, cordão nervoso ventral (análogo à medula espinhal), neurônios sensoriais periféricos para nocicepção e cérebro (HIRTH, 2010). Atualmente, existem testes validados para avaliar a neurodegeneração em *Drosophila*, como a avaliação da vacuolização do cérebro central, através de coloração histológica e medidas de desempenho locomotor, pelo teste de escalada (MCGURK, 2015; GEVEDON et al., 2019).

A utilização da mosca-da-fruta reduz significativamente os custos para estudos que visam o entendimento de mecanismos moleculares e fisiológicos nos mamíferos, auxiliando na identificação de novos alvos para terapia e triagem de moléculas biologicamente ativas com potencial farmacológico (REITER et al., 2001; LLOYD & TAYLOR, 2010).

4.3 Sistema GAL4/UAS

Centros de estoque de *D. melanogaster* como o *Bloomington* (Estados Unidos), mantêm disponível o acesso aos transgênicos. As linhagens são mantidas e classificadas conforme sua aplicação e construção gênica (COOK et al., 2010).

As linhagens *drivers* são construídas para o direcionamento da expressão de um gene de interesse a um tecido específico. As linhagens GMR-GAL4 e elav-GAL4 possuem a expressão de GAL4 controlada por promotores gênicos como o repórter múltiplo ocular (*Glass multiple reporter*) para o olho (LI et al., 2012) e elav, para o cérebro, respectivamente.

Nas linhagens *responders*, a transcrição do gene alvo está sob o comando de uma sequência de ativação antecedente (UAS) dependente de GAL4 (COOK et al., 2010) como a linhagem UAS-BACE1, APP, para o genes ligados à Doença de Alzheimer.

GAL4 é um fator de transcrição identificado na levedura *Saccharomyces cerevisiae* (ELLIOT & BRAND, 2008; ROOTE & PROKOP, 2013). Essa proteína é composta por 881 aminoácidos e a sua indução por galactose ativa genes como GAL10 e GAL1, situados posteriormente às sequências de ativação antecedentes (UAS) ou acentuadores (enhancer) (DUFFY, 2002; CARROLL, 2008). GAL4 possui pelo menos dois domínios, um para ligação ao DNA e outro para ativação da transcrição. Os acentuadores (UAS) eucarióticos podem agir a grandes distâncias dos promotores dos genes, para modular a transcrição (CARROLL, 2008).

UAS e GAL4 não existem naturalmente em *Drosophila* (ELLIOT & BRAND, 2008; ROOTE & PROKOP, 2013). Estudos demonstraram que a expressão de GAL4 é capaz de induzir a transcrição de um gene repórter sob o controle de UAS, em *D. melanogaster* (DUFFY, 2002).

A utilização do sistema GAL4/UAS em *Drosophila,* para estudo de expressão gênica, começou em 1993. A ativação do sistema acontece pelo cruzamento entre linhagens expressando GAL4 (*drivers*) com linhagens contendo o elemento UAS (*responder*). Como resultado do cruzamento, a progênie expressa o gene ligado ao UAS sob um padrão de expressão dirigido por GAL4 (ELLIOT & BRAND, 2008; ROOTE & PROKOP, 2013). Os genes de interesse podem ser repórteres, diferentes isoformas de outras espécies ou RNAs de interferência. De modo geral, o sistema GAL4/UAS possibilita o estudo da expressão gênica mediante análise temporal e espacial, sendo considerada uma das técnicas mais eficientes para análise de funções gênicas (DUFFY, 2002).

Nesse estudo o sistema GAL4/UAS foi utilizado para a construção de duas linhagens para o estudo da DA:

1. **GMR-GAL4 > UAS-BACE1, APP:** Machos portando o *responder* UAS (UAS-BACE1, APP) foram cruzados com fêmeas expressando o *driver* GAL4 (GMR-GAL4). Parte da progênie (F1) resultante do cruzamento apresenta superexpressão de BACE1 e APP direcionado para o olho da mosca (Figura 14A). As moscas dessa linhagem apresentam o fenótipo de olho rugoso, como mostra a Figura 15.

2. **elav-GAL4 > UAS-BACE1, APP:** Machos portando o *responder* UAS (UAS-BACE1, APP) foram cruzados com fêmeas expressando o *driver* GAL4 (elav-GAL4). Parte da progênie (F1) resultante do cruzamento apresenta superexpressão de BACE1 e APP direcionado para o cérebro da mosca (Figura 14B). As moscas dessa linhagem apresentam o fenótipo de Alzheimer tardio.

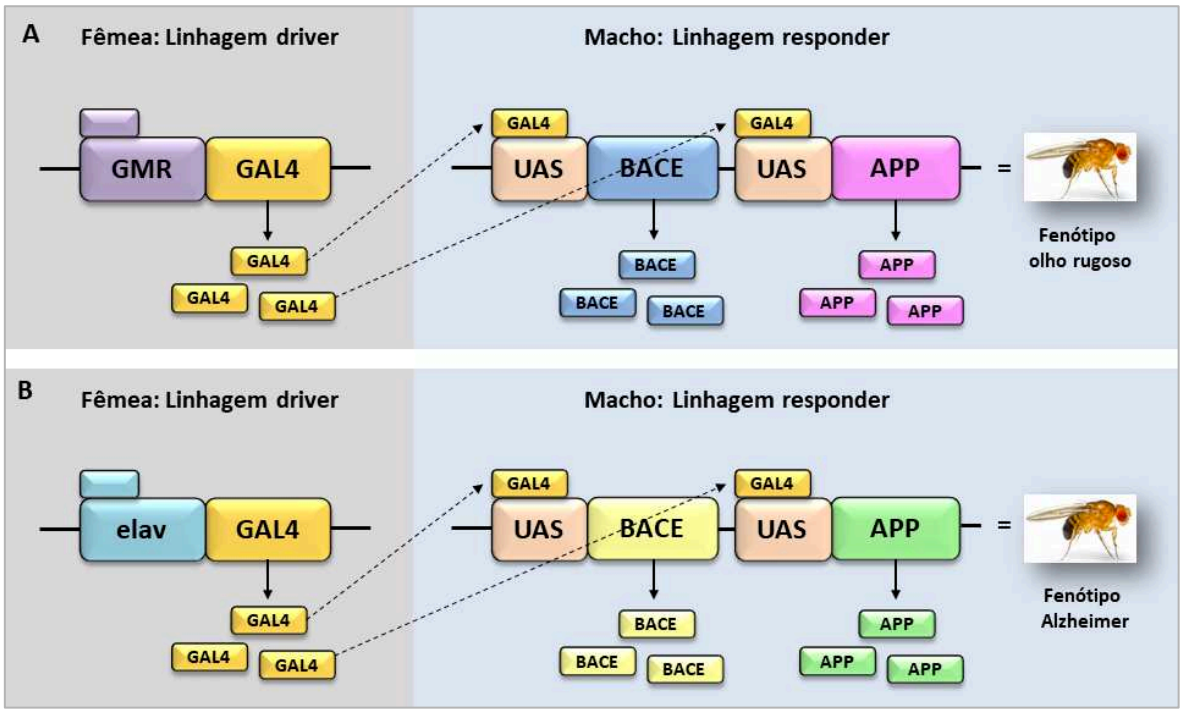

Figura 14. Utilização do sistema GAL4/UAS em *Drosophila melanogaster*, para obtenção das linhagens utilizadas em nosso estudo. **A.** Obtenção da linhagem GMR-

GAL4 > UAS, BACE1, APP. **B.** Obtenção da linhagem elav-GAL4 > UAS, BACE1, APP. Fonte: RODRIGUES, T. S. (A autora).

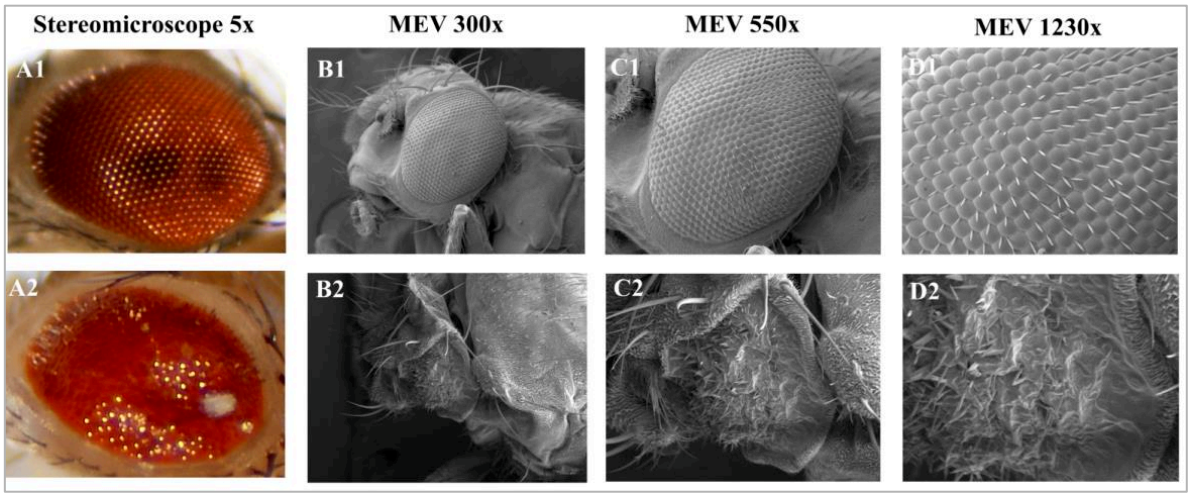

Figura 15. Padrão fenotípico de olhos enrugados e normais em *Drosophila melanogaster.* A1, B1, C1 e D1. Indivíduo da linhagem transgênica GMR-GAL4 > UAS-BACE1, UAS-APP, com olho rugoso. **A2, B2, C2 e D2.** Indivíduo da linhagem selvagem *Canton S*, apresentando olho normal. Imagens A1 e A2 capturadas por estereomicroscópio em aumento de 4x. Imagens B1-B2, C1-C2, D1-D2, capturadas por microscópio eletrônico de varredura nos aumentos 300x, 550x e 1230x, respectivamente.

4.4 Sistema nervoso de *Drosophila melanogaster*

O sistema nervoso da mosca e do homem é subdividido em segmentos que compreendem **nervos motores**, que conduzem as informações do sistema nervoso central para os músculos e glândulas e **nervos sensoriais,** que conduzem informações dos órgãos sensoriais para o sistema nervoso central (SNC) (Figuras 16 e 17) (PROKOP, 2015). Ambos os organismos apresentam:

- Corpos celulares dos neurônios que constituem os nervos sensoriais localizados fora do SNC: em humanos, principalmente nos gânglios da raiz dorsal e nas moscas, nos órgãos sensoriais na superfície do corpo.
- Órgãos sensoriais para visão, olfato, paladar, audição, equilíbrio, informação mecânica, temperatura, estímulos nocivos;
- Subdivisão do SNC em cérebro e medula ventral/espinal;
- Comportamentos coordenados pelo SNC;

- Cérebros altamente especializados e subdivididos em centros funcionais (visão, olfato, coordenação motora, aprendizagem, etc.).

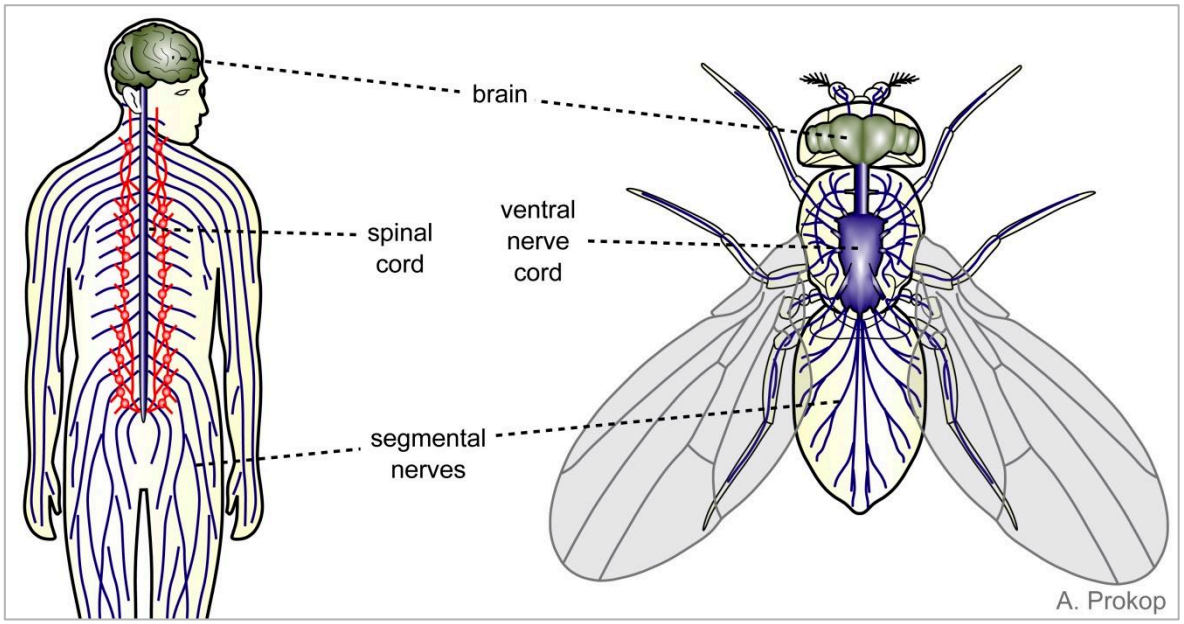

Figura 16. Sistema nervoso do homem e *Drosophila melanogaster.* Organização do sistema nervoso em cérebro na cabeça, medula ventral / espinhal no tronco e nervos segmentares. Fonte: < https://droso4schools.wordpress.com/organs/>.

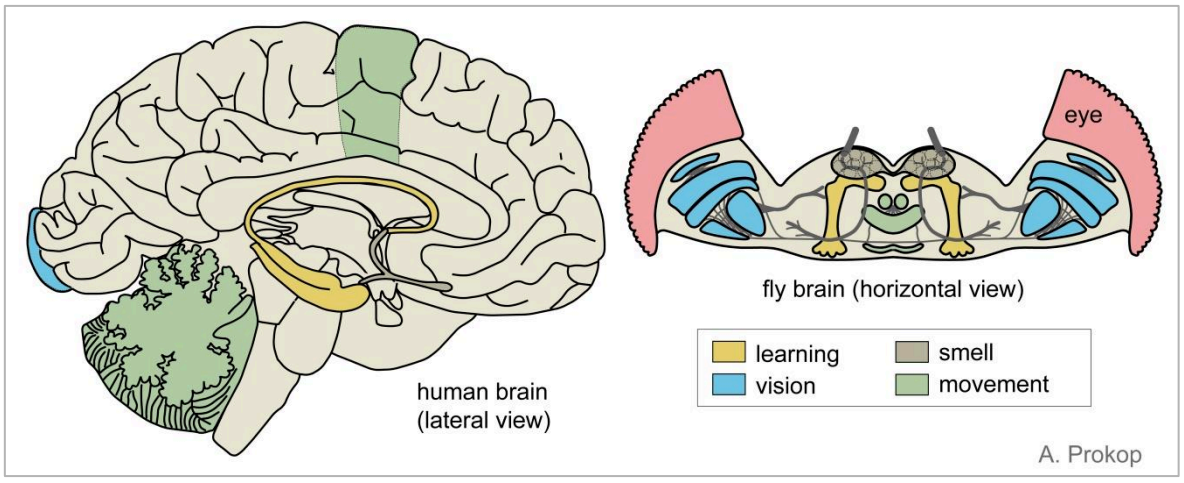

Figura 17. Cérebro humano e de *Drosophila melanogaster*. Organização do cérebro humano e de *Drosophila melanogaster*, esquematizando a analogia entre as estruturas dos dois organismos (em cores). Fonte: Fonte: < https://droso4schools.wordpress.com/organs/>.

4.5 Sistema digestivo de *Drosophila melanogaster*

Drosophila e humanos possuem trato gastrointestinal organizado de forma semelhante (Figura 18). Nas moscas, esse sistema é dividido em estômago e intestino anterior, médio e posterior. *Drosophila* também possui glândulas acessórias que se assemelham àquelas encontradas em humanos. Podemos destacar as glândulas salivares, que produzem saliva para a pré-digestão do alimento; o corpo gorduroso, que desempenha função semelhante ao fígado humano, sendo encontrado em todo o abdômen da mosca e um grupo de células localizadas no cérebro da mosca que desempenha função similar ao pâncreas humano (THOMPSON et al., 1992).

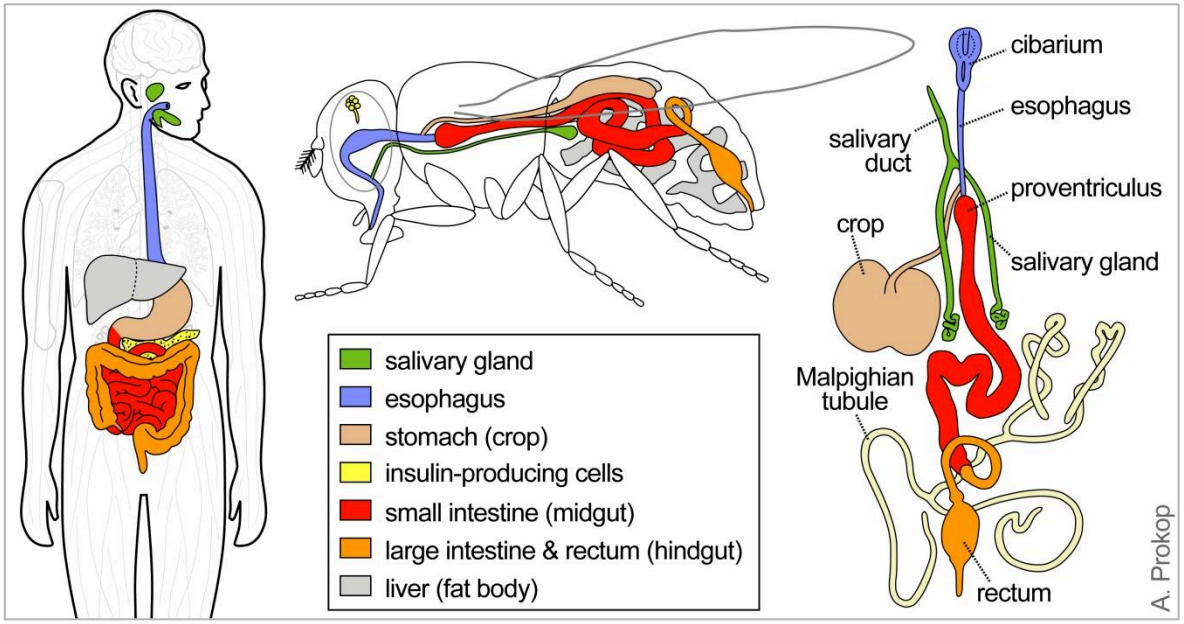

Figura 18. Comparação entre o sistema gastrointestinal da *Drosophila melanogaster* e do homem. As cores indicam estruturas homólogas e funcionalmente relacionadas do canal alimentar. Fonte: < https://droso4schools.wordpress.com/organs/>.

Em mamíferos, após a ingestão, o alimento passa pelo esôfago e depois estômago, onde o alimento se acumula. Após esta etapa, o alimento passa para o intestino delgado, ocorrendo a absorção de nutrientes e para o intestino grosso onde há absorção de nutrientes, água e eletrólitos. Por fim, atinge o reto e o ânus, onde ocorre a excreção (THOMPSON et al., 1992).

Em *Drosophila,* o alimento passa pelo intestino anterior onde é armazenado e move-se para o intestino médio, para início da absorção de nutrientes (EDGECOMB et al., 1994). Posteriormente, o alimento passa pelo intestino grosso e reto, para absorção de nutrientes, água e eletrólitos e atinge o ânus, para excreção (DEMEREC, 1950).

5 TECNOLOGIAS "ÔMICAS"

5.1 Espectrometria de massa para análise proteica

A espectrometria de massa (MS) consiste no estudo de íons na fase gasosa, caracterizando-os por sua razão massa carga (m/z) (HOFFMAN & STROOBANT, 2007). Essa técnica apresenta um amplo espectro de aplicações envolvendo identificação e/ou quantificação de compostos e elucidação de propriedades químicas e estruturais de moléculas, em diversas áreas do conhecimento, destacando-se sua utilização nas áreas biotecnológicas e biomédicas.

O uso de espectrometria de massa na área de biologia, mais especificamente em proteômica (AEBERSOLD & MANN, 2016) foi impulsionado, no final da década de 80, pelo advento das técnicas de ionização 'suave' denominadas ESI (Ionização por Eletrospray) (FENN et al., 1989) e MALDI (Dessorção a Laser Assistida por Matriz) (KARAS & HILLENKAMP, 1988) possibilitando a ionização de macromoléculas como, peptídeos, proteínas e ácidos nucleicos, sem fragmentação durante esse processo ou necessidade de derivatização (AEBERSOLD & GOODLETT, 2001; GRIFFITHS, 2008).

O interesse na aplicação de espectrometria de massa para caracterização de proteínas e o desenvolvimento dessa técnica de ionização promoveu a evolução dos analisadores de massas sendo que, a partir da década de 90, se tornaram disponíveis comercialmente, instrumentos com capacidade de experimentos de espectrometria de massa sequencial (MSn), bem como instrumentos contendo plataformas com diversas geometrias, combinando diferentes analisadores como tempo de voo - tempo de voo (TOF-TOF), quadrupolo - tempo de voo (Q-TOF) (MORRIS et al., 1996), ressonância

ciclotrônica de íons com transformada de Fourier (FTICR) (KINTER, 2005; ALTELAAR et al., 2012), armadilha de íons - orbitrap (LTQ-Orbitrap) (HU et al., 2005) e quadrupolo - orbitrap (Q-Orbitrap) (MICHALSKI et al, 2011).

Paralelamente, o acoplamento de técnicas de separação permitiu a análise de misturas complexas, como os peptídeos resultantes da digestão enzimática de amostras biológicas (Figura 19) (AEBERSOLD & GOODLETT, 2001). Além disso, o desenvolvimento de ferramentas de bioinformática para buscas em bancos de dados possibilitou a análise de estudos proteômicos (WASHBURN et al, 2001), promovendo aumento significativo da aplicabilidade da técnica. Dessa forma, o emprego de MS para a análise de proteínas tornou-se rotineiro, especialmente no caso de sequenciamento e identificação de proteínas (AEBERSOLD & GOODLETT, 2001; GRIFFITHS, 2008), determinação da massa molecular de proteínas e complexos proteicos intactos (SHARON & ROBINSON, 2007), identificação e localização de modificações pós-traducionais (CRAVATT et al., 2007) e quantificação absoluta e relativa de proteínas (KELLIE et al., 2010; MOHR et al., 2017).

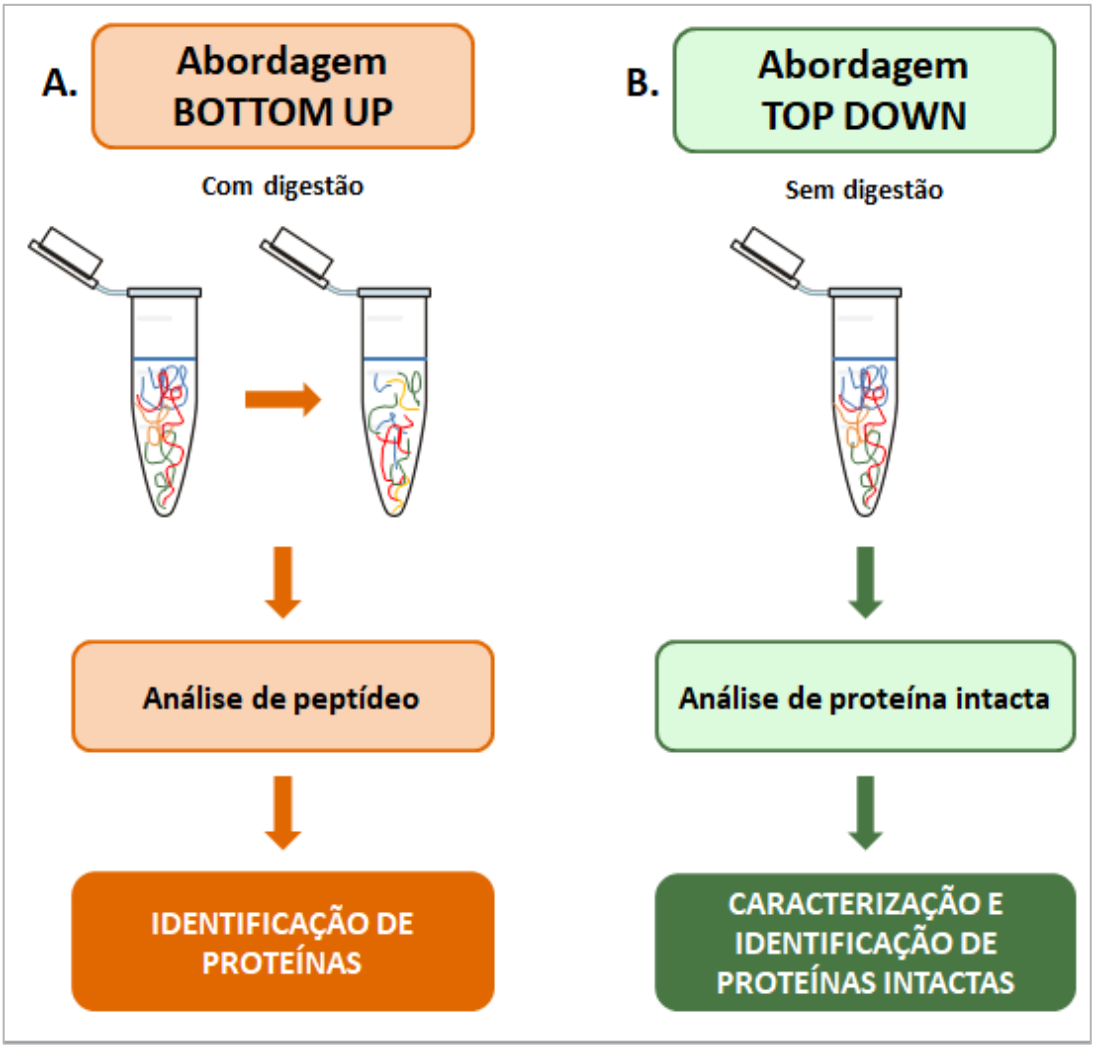

Figura 19. Esquema das abordagens *Bottom Up* e *Top Down* para a identificação de proteínas. Na abordagem *Bottom Up* **(A)** a digestão enzimática é utilizada para clivar proteínas intactas em peptídeos. Os peptídeos são analisados por espectrometria de massa em tandem. A identificação pode ocorrer através da identificação de peptídeos *in silico* a um banco de dados de proteínas por um algoritmo de pesquisa. Na abordagem *Top Down* **(B),** proteínas intactas são analisadas diretamente no espectrômetro de massa, sem digestão enzimática. O precursor resultante e as massas do fragmento são então combinados com as sequências candidatas de um banco de dados de proteínas. Fonte: KELIE et al (2010).

Essa abrangente aplicação de espectrometria de massa para a caracterização de proteínas é consequência de vantagens intrínsecas da técnica, dentre elas a alta sensibilidade, rapidez, versatilidade, facilidade de operação e aplicabilidade universal, uma vez que não há limite conhecido de tamanho da proteína e complexidade do sistema a ser estudado, assim como não é

necessário um elevado grau de pureza das amostras (HOFFMANN & STROOBANT, 2007; GIANI et al., 2019).

5.2 Sequenciamento de DNA de Nova Geração (NGS)

Um genoma é a informação genética completa de um organismo ou célula. Os ácidos nucléicos de fita simples ou dupla armazenam essas informações em uma sequência linear ou circular. Os sequenciadores automáticos podem gerar sequências, conhecidas como leituras (*reads*), compreendidas em intervalos definidos de comprimentos, geralmente mais curtos do que o tamanho dos genomas investigados. A sequência completa do genoma deve ser deduzida da sobreposição desses fragmentos mais curtos, um processo definido como montagem do genoma *de novo*. Historicamente, principalmente devido às restrições de tempo e custo, apenas um indivíduo por espécie foi abordado e sua sequência geralmente representa o genoma de 'referência' para a espécie (HEATHER & CHAIN, 2016).

Os genomas de referência orientam o ressequenciamento na mesma espécie, atuando como um modelo para mapeamento de leitura. Eles podem ser anotados para entender a função do gene ou usados para projetar experimentos de manipulação de genes. Sequências de diferentes espécies podem ser alinhadas e comparadas para estudar a evolução molecular (HEATHER & CHAIN, 2016).

O alto custo por base e baixo rendimento das plataformas de sequenciamento de eletroforese capilar (CE) levou ao desenvolvimento das chamadas tecnologias de sequenciamento de nova geração (NGS) que forneceram um rendimento muito maior a um custo substancialmente mais baixo (HEAD et al., 2014). Do ponto de vista técnico, a nova geração de abordagens de sequenciamento resultou de uma combinação de avanços na microfabricação, imagens de alta resolução e poder computacional (HEAD et al., 2014).

Todas as abordagens NGS dependem de uma preparação de 'biblioteca' usando DNA nativo ou amplificado. Em um protocolo clássico, após a fragmentação do DNA e seleção do tamanho do fragmento, os adaptadores são ligados às extremidades de cada fragmento, seguido, geralmente, por uma etapa

de amplificação do DNA. A biblioteca resultante é carregada em uma célula de fluxo e sequenciada em reações de sequenciação paralela maciça (FORDE & O'TOOLE, 2013). Cada reação envolve, geralmente, a incorporação gradativa, mediada por polimerase, de desoxinucleotídeos marcados com fluorescência em uma cadeia de DNA alongada, imobilizada em uma superfície.

Em 2004, antes da introdução das tecnologias NGS, 192 sequências de genoma bacteriano foram totalmente concluídas e publicadas (FORDE & O'TOOLE, 2013). Até março de 2021, aproximadamente 420.000 sequências de genoma bacteriano foram concluídas, publicadas e depositadas em bancos de dados online (Figura 20).

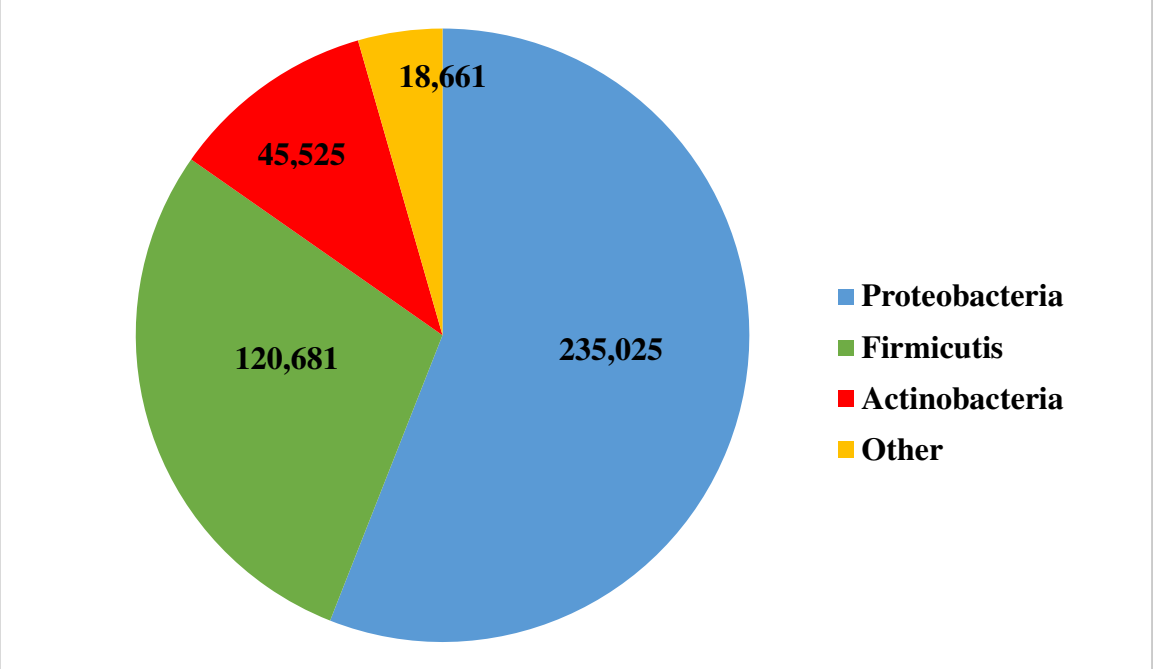

Figura 20. Genomas bacterianos publicados. Distribuição filogenética de projetos de sequenciamento de genoma bacteriano concluídos até março de 2021. Dados consultados em: <https://www.ncbi.nlm.nih.gov/>. Fonte: RODRIGUES, T.S. (A autora).

6 OBJETIVOS

6.1 Objetivo geral

O objetivo desse trabalho foi analisar o secretoma de bactérias isoladas do alimento larval de abelhas sem ferrão brasileiras, das espécies *Melipona quadrifasciata* e *Tetragonisca angustula*, em *Drosophila melanogaster* modelo para Doença de Alzheimer.

6.2 Objetivos específicos

Após tratar larvas (L1) da linhagem transgênica GMR,GAL4;UAS-BACE1,UAS-APP (modelo olho rugoso) e adultos da linhagem transgênica elav-GAL4; UAS-BACE1,UAS-APP (modelo de Alzheimer) de *D. melanogaster*, com os secretomas bacterianos:

- Verificar a toxicidade dos secretomas bacterianos em linhagens transgênicas de *Drosophila melanogaster*, através de teste de sobrevivência e análise da taxa de eclosão;
- Avaliar o fenótipo de olho rugoso de moscas da linhagem GMR-GAL4; UAS-BACE1, UAS-APP, por estereomicroscópio, microscopia eletrônica de varredura e secções histológicas;
- Avaliar a taxa de escalada de moscas da linhagem transgênica elav-GAL4; UAS-BACE1, UAS-APP;
- Quantificar os níveis de β-amiloide dos cérebros de moscas da linhagem transgênica elav-GAL4; UAS-BACE1, UAS-APP;
- Realizar análise histológica do cérebro de moscas da linhagem transgênica elav-GAL4; UAS-BACE1, UAS-APP;
- Realizar a análise proteômica dos secretomas bacterianos que apresentaram melhor efeito antineurodegenerativo nos testes com *D. melanogaster.*
- Realizar análises *in silico* dos peptídeos encontrados na análise proteômica, a fim de prever a bioatividade potencial, bem como o docking molecular entre suas sequências e os alvos terapêuticos BACE1 e β-amiloide.
- Identificar peptídeos que sirvam de protótipo para novos fármacos que possam prevenir ou tratar a Doença de Alzheimer.

REFERÊNCIAS

ADAMS, M. D. et al. The genome sequence of *Drosophila melanogaster*. **Science (New York, N.Y.)**, v. 287, n. 5461, p. 2185–95, 2000. https://doi.org/10.1126/science.287.5461.2185

AEBERSOLD, R.; GOODLETT, D. R. **Mass spectrometry in proteomics**. Chemical Review, p. 269–296, 2001. https://doi.org/10.1021/cr990076h

AEBERSOLD, R.; MANN, M. Mass-spectrometric exploration of proteome structure and function. **Nature,** v. 537, n. 7620, p. 347–355, 2016. https://doi.org/10.1038/nature19949

AGUZZI, A., O'CONNOR, T. Protein aggregation diseases: pathogenicity and therapeutic perspectives. **Nat Rev Drug Discov**. v. 9, p. 237–248, 2010. https://doi.org/10.1038/nrd3050

AHN, J. E. et al. Angiotensin I-Converting Enzyme (Ace) Inhibitory Peptides From Whey Fermented By Lactobacillus Species. **J. Food Biochem.** v. 233, p. 587–602, 2009. https://doi.org/10.1111/j.1745-4514.2009.00239.x

AHUJA, A.; SINGH, R. S. Variation and Evolution of Male Sex Combs in *Drosophila*: Nature of Selection Response and Theories of Genetic Variation for Sexual Traits. **Genetics**, v. 179, n. 1, p. 503–509, 2008. https://doi.org/10.1534/genetics.107.086363

ALTELAAR, A. F. M.; MUNOZ, J.; HECK, A. J. R. Next-generation proteomics: towards an integrative view of proteome dynamics. **Nature reviews Genetics**, v. 14, n. 1, p. 35–48, 2012. https://doi.org/10.1038/nrg3356

ALZHEIMER ASSOCIATION. Facts and numbers about Alzheimer disease. **Alzheimers Dement.** v. 14, p. 367–429. 2018.

ALZHEIMER'S DISEASE INTERNATIONAL. **World Alzheimer Report 2015: The Global Impact of Dementia**. Alzheimer's Disease International, London, Copyright, Alzheimer's Disease International, 2015

ALZHEIMER'S DISEASE INTERNATIONAL. **World Alzheimer Report 2019: Attitudes to dementia**. Alzheimer's Disease International, London, Copyright, Alzheimer's Disease International, 2019.

ASPRI, M. et al. Bioactive properties of fermented donkey milk, before and after in vitro simulated gastrointestinal digestion. **Food Chem.** v. 268, p. 476–484, 2018. https://doi.org/10.1016/j.foodchem.2018.06.119

AULD, D. S. et al. Alzheimer's disease and the basal forebrain cholinergic system: relations to beta-amyloid peptides, cognition and treatment strategies. **Prog**

Neurobiol. v. 68, n. 3, p. 209-45, 2002. https://doi.org/10.1016/S0301-0082(02)00079-5

BARTUS, R. T.; EMERICH, D. F. Cholinergic markers in Alzheimer disease. **JAMA**. v. 282, n. 23, p. 2208-9, 1992. https://doi.org/10.1001/jama.282.23.2208

BELLEN, H. J.; TONG, C.; TSUDA, H. 100 years of *Drosophila* research and its impact on vertebrate neuroscience: a history lesson for the future. **Nature Reviews Neuroscience**, v. 11, n. 7, p. 514–522, 2010. https://doi.org/10.1038/nrn2839

BENILOVA, I. et al. The Alzheimer disease protective mutation A2T modulates kinetic and thermodynamic properties of amyloid-b (Ab) aggregation. **J. Biol. Chem.** v. 289, p. 30977–30989, 2014. https://doi.org/10.1074/jbc.M114.599027

BEYREUTHER, K.; MASTERS, C. L. Amyloid precursor protein (APP) and beta A4 amyloid in the etiology of Alzheimer's disease: precursor-product relationships in the derangement of neuronal function. **Brain. Pathol.** v. 1, p. 241 – 251, 1991. https://doi.org/10.1111/j.1750-3639.1991.tb00667.x

BIER, E. *Drosophila*, the golden bug, emerges as a tool for human genetics. **Nature Reviews Genetics**, v. 6, n. 1, p. 9–23, 2005. https://doi.org/10.1038/nrg1503

BOFF, M.S.; SEKYIA, F.S.; BOTTINO, C.M.C. Prevalence of dementia among Brazilian population: systematic review. **São Paulo Medical Journal.** v. 129, n.1, p. 46-50, 2011. https://doi.org/10.1590/S1516-31802011000100009

BORCHELT, D. R. et al. Familial Alzheimer's disease-linked presenilin 1 variants elevate A-beta 1–42/1–40 ratio in vitro and in vivo. **Neuron.** 1996, v. 17, p. 1005–1013, 1996. https://doi.org/10.1016/S0896-6273(00)80230-5

BURDICK, D. Assembly and aggregation properties of synthetic Alzheimer's A4/beta amyloid peptide analogs. **J. Biol. Chem.** v. 267, p. 546–554, 1992. https://doi.org/10.1016/S0021-9258(18)48529-8

CADIGAN, K. M.; PEIFER, M. Wnt signaling from development to disease: Insights from model systems. **Cold Spring Harbor Perspectives in Biology**, v. 1, n. 2, p. 2881–2881, 2009. https://doi.org/10.1101/cshperspect.a002881

CAI, H. et al. BACE1 is the major beta-secretase for generation of Abeta peptides by neurons. **Nat. Neurosci.** v. 4, p. 233–234, 2001. https://doi.org/10.1038/85064

CARROLL, A. F. **Introdução à genética**, 9ª. Rio de Janeiro: 2008.

CAVALCANTI, J. L. S.; ENGELHARDT, E. Aspects of the pathophysiology of sporadic alzheimer's disease. **Brazilian Journal of Neuropathology.** v. 48, p. 21-29, 2012.

CHAKRABARTI, S.; JAHANDIDEH, F.; WU, J. Food-derived bioactive peptides on inflammation and oxidative stress. **Biomed. Res. Int.** 608979, 2014. https://doi.org/10.1155/2014/608979

CHAN, H. Y.; BONINI, M. N. *Drosophila* models of human neurodegenerative disease. **Cell death differ.** v. 7, p. 1075-1080, 2000. https://doi.org/10.1038/sj.cdd.4400757

CHILDRESS, J.; HALDER, G. Appendix: Phenotypic Markers in *Drosophila.* In: DAHMANN, C. (Ed.). ***Drosophila* Methods and Protocols: Humana Press**. p. 27-44, 2008.

COOK, K. R. et al. New research resources at the Bloomington *Drosophila* Stock Center. **Fly**, v. 4, n. 1, p. 88–91, 2010. https://doi.org/10.4161/fly.4.1.11230

CRAVATT, B. F.; SIMON, G. M.; YATES, J. R. The biological impact of massspectrometry-based proteomics. **Nature,** v. 450, n. 7172, p. 991–1000, 2007. https://doi.org/10.1038/nature06525

CUMMINGS, J. L.; MORSTORF, T.; ZHONG, K. Alzheimer's disease drug-development pipeline: few candidates, frequent failures. **Alzheimers Res. Ther.** v. 6, p. 37, 2014. https://doi.org/10.1186/alzrt269

DE BELLE, J. S.; HEISENBERG, M. Expression of *Drosophila* mushroom body mutations in alternative genetic backgrounds: a case study of the mushroom body miniature gene (mbm). **Proceedings of the National Academy of Sciences of the United States of America**, v. 93, n. 18, p. 9875–80, 3 1996. https://doi.org/10.1073/pnas.93.18.9875

DEMEREC, M. **Biology of Drosophila.** New York: JohnWiley & Sons. ed. 1950.

DOMINGUEZ, D. et al. Phenotypic and biochemical analyses of BACE1- and BACE2-deficient mice. **J. Biol. Chem.** v. 280, p. 30797–30806, 2005. https://doi.org/10.1074/jbc.M505249200

DUFFY, J. B. GAL4 system in *Drosophila:* A fly geneticist's swiss army knife. **Genesis**, v. 34, n. 1–2, p. 1–15, 2002. https://doi.org/10.1002/gene.10150

EASTWOOD, R.; REISBERG, B. Mood and behaviour. In: Gauthier S, editor. **Clinical diagnosis and management of Alzheimer's disease**. London: Martin Dunitz; p. 175-90, 1996.

EDGECOMB, R.S.; HARTH, C. E.; SCHNEIDERMAN, A. M. Regulation of feeding behavior in adult *Drosophila melanogaster* varies with feeding regime and nutritional state**. J. Exp. Biol.** v. 197, p. 215–35, 1994. https://doi.org/10.1242/jeb.197.1.215

EHEHALT, R. et al. Splice variants of the beta-site APP-cleaving enzyme BACE1 in human brain and pancreas. **Biochem. Biophys. Res. Commun.** v. 293, p. 30–37, 2002. https://doi.org/10.1016/S0006-291X(02)00169-9

EKETJÄLL, S. et al. AZD3293: A Novel, Orally Active BACE1 Inhibitor with High Potency and Permeability and Markedly Slow Off-Rate Kinetics. **J. Alzheimers Dis.** v. 50, n. 4, p. 1109-23, 2016. https://doi.org/10.3233/JAD-150834

EL-FATTAH, A. M. A. et al. Bioactive peptides with ACE-I and antioxidant activity produced from milk proteolysis. **Int. J. Food Prop.** v. 20, p.3033–3042, 2017. https://doi.org/10.1080/10942912.2016.1270963

EL-LEITHY, M.; EL-SIBAEL, K. Role of microorganisms isolated from bees, its ripening and fermentation of honey. **Egyptian Journal of Microbiology** v. 75, p. 679-681, 1992.

ELLIOTT, D. A.; BRAND, A. H. The GAL4 System. In: DAHMANN, C. (Eds) **Methods in molecular biology (Clifton, N.J.)**. Humana Press. v. 420, p. 79–95, 2008. https://doi.org/10.1007/978-1-59745-583-1_5

FARZAN, M. et al. BACE2, a beta -secretase homolog, cleaves at the beta site and within the amyloid-beta region of the amyloid-beta precursor protein. **Proc. Natl. Acad. Sci. USA.** v. 97, p. 9712–9717, 2000. https://doi.org/10.1073/pnas.160115697

FENN, J. et al. Electrospray Ionization for Mass Spectrometry of Large Biomolecules. **Science,** v. 246, n. 4926, p. 64–71, 1989. https://doi.org/10.1126/science.2675315

FORDE, B. M.; O'TOOLE, P. W. Next-generation sequencing technologies and their impact on microbial genomics. **Brief. Funct. Genomics.** v. 12, n. 5, p.440-53, 2013. https://doi.org/10.1093/bfgp/els062

GEVEDON, O. et al. In Vivo Forward Genetic Screen to Identify Novel Neuroprotective Genes in Drosophila melanogaster**. J. Vis. Exp.** v. 149, 2019. https://doi.org/10.3791/59720

GIANI, A. M. et al. Long walk to genomics: History and current aproximas to genome sequencing and assembly. **Comput. Struct. Biotechnol. J.** v. 18, p. 9-19, 2019. https://doi.org/10.1016/j.csbj.2019.11.002

GILLIAM, M.; PREST, B. Microbiology of feces of the larval honey bee, *Apis mellifera,* **Journal of Invertebrate Pathology** v. 49; p. 70–75, 1987. https://doi.org/10.1016/0022-2011(87)90127-3

GILLIAM, M.; ROUBIK, D. W.; LORENZ, B. J. Microorganisms associated with pollen, honey, and brood provisions in the nest of a stingless bee, *Melipona fasciata*. **Apidologie** v. 21, p. 89-97, 1990. https://doi.org/10.1051/apido:19900201

GLENNER, G. G.; WONG, C. W. Alzheimer's disease: initial report of the purification and characterization of a novel cerebrovascular amyloid protein. **Biochem. Biophys. Res. Commun.** v. 120, p. 885–890, 1984. https://doi.org/10.1016/S0006-291X(84)80190-4

GOBBETTI, M. et al. Production of Angiotensin-I-Converting-Enzyme- Inhibitory Peptides in Fermented Milks Started by Lactobacillus delbrueckii subsp. bulgaricus SS1 and Lactococcus lactis subsp. cremoris FT4. **Appl. Environ. Microbiol.** v. 66, p. 3898–3904, 2000. https://doi.org/10.1128/AEM.66.9.3898-3904.2000

GODYN, J. et al. Therapeutic strategies for Alzheimer's disease in clinical trials. **Pharmacol. Rep.** v. 68, p. 127–138, 2016. https://doi.org/10.1016/j.pharep.2015.07.006

GRAF, U. et al. Somatic mutation and recombination test in *Drosophila melanogaster.* **Environmental mutagenesis**, v. 6, p. 9–13, 1996.

GRIFFITHS, J. A Brief History of Mass Spectrometry. **Analytical Chemistry**, v. 80, p. 5678–5683, 2008. https://doi.org/10.1021/ac8013065

HARDY, J, ALLSOP, D. Amyloid deposition as the central event in the aetiology of Alzheimer's disease. **Trends in Pharmac.** v. 12, p. 383 – 388, 1991. https://doi.org/10.1016/0165-6147(91)90609-V

HARDY, J. A.; HIGGINS, G. Alzheimer's disease: the amyloid cascade hypothesis. **Science**. v. 256, p. 184 – 185, 1992. https://doi.org/10.1126/science.1566067

HARDY, J.; SELKOE, D. J. The amyloid hypothesis of Alzheimer's disease: progress and problems on the road to therapeutics. **Science.** v. 297, n. 5580, p. 353-6, 2002. https://doi.org/10.1126/science.1072994

HASSAN KHAN, M. Molecular interactions of cholinesterase inhibitors using *in silico* methods: current state and future perspectives. **New Biotechnol.** v. 5, p. 331–346, 2009. https://doi.org/10.1016/j.nbt.2009.03.008

HEAD, S. R. et al. Construção de biblioteca para sequenciamento de última geração: visões gerais e desafios. Biotechniques. v. 56, p. 61–4, 2014.

HEATHER, J. M.; CHAIN, B. A sequência de sequenciadores: a história do DNA de sequenciamento. **Genômica.** v. 107, p. 1–8, 2016.

HIRTH, F. On the origin and evolution of the tripartite brain. **Brain. Behav. Evol.** v. 76, p. 3–10, 2010. https://doi.org/10.1159/000320218

HOFFMANN, E. DE; STROOBANT, V. **Mass Spectrometry: Principles and Applications**. 3rd. ed. Bruxellas, Bélgica: John Wiley & Sons, 2007.

HOLSINGER, R. M. et al Increased expression of the amyloid precursor beta-secretase in Alzheimer's disease. **Ann. Neurol.** v. 51, p. 783–786, 2002. https://doi.org/10.1002/ana.10208

HU, Q. et al. The Orbitrap: A new mass spectrometer. **Journal of Mass Spectrometry**, v. 40, n. 4, p. 430–443, 2005. https://doi.org/10.1002/jms.856
HUANG, Y.; DE MUCKE, L. Alzheimer's mechanisms and therapeutic therapies. **Cell.** v. 148, n. 6, p. 1204–1222, 2012. https://doi.org/10.1016/j.cell.2012.02.040

IWATSUBO, T. et al. Visualization of A beta 42(43) and A beta 40 in senile plaques with end-specific A beta monoclonals: evidence that an initially deposited species is A beta 42(43) **Neuron.** v. 13, p. 45–53, 1994. https://doi.org/10.1016/0896-6273(94)90458-8

JARRETT, J. T.; BERGER, E. P.; LANSBURY, P. T. J. The carboxy terminus of the beta amyloid protein is critical for the seeding of amyloid formation: implications for the pathogenesis of Alzheimer's disease. **Biochemistry**. v. 332, p. 4693–4697, 1993. https://doi.org/10.1021/bi00069a001

JENNINGS, B. H. *Drosophila:* a versatile model in biology & medicine. **Materials Today**, v. 14, n. 5, p. 190–195, 2011. https://doi.org/10.1016/S1369-7021(11)70113-4

JONSSON, T. et al. Stefansson, A mutation in APP protects against Alzheimer's disease and age-related cognitive decline. **Nature** v. 488, p. 96–99, 2012. https://doi.org/10.1038/nature11283

KANG, J. et al. The precursor of Alzheimer's disease amyloid A4 protein resembles a cell-surface receptor. **Nature.** v. 325, p. 733–736, 1987. https://doi.org/10.1038/325733a0

KARAS, M.; HILLENKAMP, F. Laser desorption ionization of proteins with molecular masses exceeding 10,000 daltons. **Analytical chemistry,** v. 60, n. 20, p. 2299–2301,1988. https://doi.org/10.1021/ac00171a028

KELLIE, J. F. et al. The emerging process of Top Down mass spectrometry for protein analysis: biomarkers, protein-therapeutics, and achieving high throughput. **Mol Biosyst**. v. 6, n. 9, p. 1532-9, 2010. https://doi.org/10.1039/c000896f

KENNEDY, M. E. et al. The BACE1 inhibitor verubecestat (MK-8931) reduces CNS beta-amyloid in animal models and in Alzheimer's disease patients. **Sci .Transl. Med**. v. 8, p. 363ra150, 2016.

KERR, W. E.; PETRERE JR. M.; DINIZ FILHO, J. A. F. Biological information and estimate of the ideal hive size for the Maranhão bee (Melipona compressipes fasciculata Smith - Hymenoptera, Apidae). **Revista Brasileira de Zoologia,** 18, 1, 45-52, 2001. https://doi.org/10.1590/S0101-81752001000100003

KERR, W. E.; CARVALHO, G. A.; NASCIMENTO, V. A. (Org.). **Abelha Urucu**: Biologia, Manejo e Conservação. Paracatu: Fundação Acangaú. 1996.

KINTER, M. N. E. S. **Protein Sequencing and Identification Using Tandem Mass Spectrometry.** John Wiley ed. [s.l.] John Wiley & Sons, 2005.

KITTS, D. D.; WEILER, K. Bioactive proteins and peptides from food sources. Applications of bioprocesses used in isolation and recovery. **Curr. Pharm. Des.** v. 9, p. 1309–1323, 2003. https://doi.org/10.2174/1381612033454883

KORHONEN, H.; PIHLANTO, A. Bioactive peptides: Production and functionality. **Int. Dairy J.** v. 16, p. 945–960, 2006. https://doi.org/10.1016/j.idairyj.2005.10.012

LAIRD, F. M. et al. BACE1, a major determinant of selective vulnerability of the brain to amyloid-beta amyloidogenesis, is essential for cognitive, emotional, and synaptic functions. **J. Neurosci.** v. 25, p. 11693–11709, 2005. https://doi.org/10.1523/JNEUROSCI.2766-05.2005

LAWRENCE, P. A. The making of a fly: the genetics of animal design. **The making of a fly: the genetics of animal design.** 1992.

LEE, L. A.; ORR-WEAVER, T. L. Regulation of cell cycles in *Drosophila* development: intrinsic and extrinsic cues. **Annual Review of Genetics**, v. 37, n. 1, p. 545–578, 2003. https://doi.org/10.1146/annurev.genet.37.110801.143149

LEMERE, C. A. et al. Sequence of deposition of heterogeneous amyloid b-peptides and Apo E in Down syndrome: implications for initial events in amyloid plaque formation. **Neurobiol. Dis.** v. 3, p.16 – 32, 1996a. https://doi.org/10.1006/nbdi.1996.0003

LEMERE, C. A. THE E280A presenilin 1 Alzheimer mutation produces increased Ab42 deposition and severe cerebellar pathology. **Nature Med.** v. 2, p. 1146 – 1150, 1996b. https://doi.org/10.1038/nm1096-1146

LI, W. Z. et al. A broad expression profile of the GMR-GAL4 driver in *Drosophila melanogaster.* **Genetics and molecular research : GMR**, v. 11, n. 3, p. 1997–2002, 2012. https://doi.org/10.4238/2012.August.6.4

Lilly Halts Phase 2 Trial of BACE inhibitor due to liver toxicity. 2013. http://www.alzforum.org/news/research-news/lilly-halts-phase-2-trial-bace-inhibitor-due-liver-toxicity.

LIN, X. et al. Human aspartic protease memapsin 2 cleaves the beta-secretase site of beta-amyloid precursor protein. **Proc. Natl. Acad. Sci. USA.** v. 97, p. 1456–1460, 2000. https://doi.org/10.1073/pnas.97.4.1456

LINDEBOOM, J.; WEINSTEIN, H. Neuropsychology of cognitive ageing, minimal cognitive impairment, Alzheimer's disease, and vascular cognitive impairment. **Eur**

J Pharmacol. v. 490, n. 1-3, p. 83-6, 2004. https://doi.org/10.1016/j.ejphar.2004.02.046

LLOYD, T. E.; TAYLOR, J. P. Flightless flies: *Drosophila* models of neuromuscular disease. **Annals of the New York Academy of Sciences**, v. 1184, p. e1-20, 2010. https://doi.org/10.1111/j.1749-6632.2010.05432.x

LUO, Y. et al. Mice deficient in BACE1, the Alzheimer's beta-secretase, have normal phenotype and abolished beta-amyloid generation. **Nat. Neurosci.** v. 4, p. 231–232, 2001. https://doi.org/10.1038/85059

LYNCH, J. A.; EL-SHERIF, E.; BROWN, S. J. Comparisons of the embryonic development of *Drosophila, Nasonia*, and *Tribolium.* **Wiley Interdisciplinary Reviews: Developmental Biology**, v. 1, n. 1, p. 16–39, 2012. https://doi.org/10.1002/wdev.3

MALONEY, J. A. et al. Molecular mechanisms of Alzheimer disease protection by the A673 allele of amyloid precursor protein. **Neurobiology.** v. 289, n. 45, p. 30990-31000, 2014. https://doi.org/10.1074/jbc.M114.589069

MANN, D. M. A. et al. The time course of pathological events in Down's Syndrome with particular reference to the involvement of microglial cells and deposits of b/A4. **Neurodegener.** v. 1, p. 201 – 215, 1992.

MASTERS, C. L. et al. Amyloid plaque core protein in Alzheimer disease and Down syndrome. **Proc. Natl. Acad. Sci**. **USA.** v. 82:4245, p. 4249, 1985. https://doi.org/10.1073/pnas.82.12.4245

MAY, P. C. et al. Redução central robusta de beta-amiloide em humanos com um inibidor da beta-secretase não peptídico disponível por via oral. **J. Neurosci.** v. 31, p. 16507–16516, 2011.

MCCONLOGUE, L. et al. Partial reduction of BACE1 has dramatic effects on Alzheimer plaque and synaptic pathology in APP transgenic mice. **J. Biol. Chem.** v. 282, p. 26326–26334, 2007. https://doi.org/10.1074/jbc.M611687200

MCGURK, L.; BERSON, A.; BONINI, N.M. Drosophila as an *In Vivo* Model for Human Neurodegenerative Disease. **Genetics.** v. 201, p. 377–402, 2015. https://doi.org/10.1534/genetics.115.179457

MICHALSKI, A. et al. Mass Spectrometry-based Proteomics Using Q Exactive, a Highperformance Benchtop Quadrupole Orbitrap Mass Spectrometer. **Molecular & cellular proteomics**, v. 10, n. 9, p. M111.011015, 2011. https://doi.org/10.1074/mcp.M111.011015

MICHENER, C. D. **The bess of the world**. 2nd edition. The Johns Hopkins University Press, Baltimore, 2007.

MICHENER, C. D. **The Social Behavior of the Bees**. Massachussets: Harvard University Press, Cambridge. 1974.

MICHENER, C. D: Pot-Honey: **A Legacy of Stingless Bees.** New York, Springer, 2013.

MOHR, S. et al. Hoxa9 and Meis1 Cooperatively Induce Addiction to Syk Signaling by Suppressing miR-146a in Acute Myeloid Leukemia. **Cancer Cell,** v. 31, n. 4, p. 549– 562.e11, 2017. https://doi.org/10.1016/j.ccell.2017.03.001

MOLLER, N.P. et al. Bioactive peptides and proteins from foods: Indication for health effects. **Eur. J. Nutr.** v. 47, p. 171–182, 2008. https://doi.org/10.1007/s00394-008-0710-2

MORA, L. et al. Effect of cooking and simulated gastrointestinal digestion on the activity of generated bioactive peptides in aged beef meat. **Food Funct.** v. 8, p. 4347–4355, 2017. https://doi.org/10.1039/C7FO01148B

MORLEY, J. E. et al. A physiological role for amyloid-beta protein: enhancement of learning and memory. **J. Alzheimer's Dis**. v. 19, p. 441–449, 2008. https://doi.org/10.1038/npre.2008.2119.1

MORRIS, H. R. et al. High sensitivity collisionally-activated decomposition tandem mass spectrometry on a novel quadrupole/orthogonal-acceleration time-of-flight mass spectrometer. **Rapid communications in mass spectrometry**, v. 10, n. 8, p. 889–896, 1996. https://doi.org/10.1002/(SICI)1097-0231(19960610)10:8<889::AID-RCM615>3.0.CO;2-F

MUHEEM, A. et al. A review on the strategies for oral delivery of proteins and peptides and their clinical perspectives. **Saudi Pharm. J.** v. 24, p. 413–428, 2016. https://doi.org/10.1016/j.jsps.2014.06.004

NG, D.H.C.; EMBLETON, N.D.; MCGUIRE, W. Hydrolyzed formula compared with standard formula for preterm infants. **JAMA** v. 319, p. 1717–1718, 2018. https://doi.org/10.1001/jama.2018.3623

NITRINI, R. ET al. Incidence of dementia in a Brazilian population living in a community. **Alzheimer Dis Assoc Disord.** v. 18, p. 241–46, 2004.

OHNO, M. et al. BACE1 deficiency rescues memory deficits and cholinergic dysfunction in a mouse model of Alzheimer's disease. **Neuron.** v. 41, p. 27–33, 2004. https://doi.org/10.1016/S0896-6273(03)00810-9

OHNO, M. et al. BACE1 gene deletion prevents neuron loss and memory deficits in 5XFAD APP/PS1 transgenic mice. **Neurobiol. Dis.** 26, 134–145, 2007. https://doi.org/10.1016/j.nbd.2006.12.008

PEREZ ESPITIA, P.J. et al. Bioactive Peptides: Synthesis, Properties, and Applications in the Packaging and Preservation of Food**. Compr. Rev. Food Sci.**

Food Saf. v. 11, p. 187–204, 2012. https://doi.org/10.1111/j.1541-4337.2011.00179.x

PLANT, L. D. et al. The production of amyloid beta peptide is a critical requirement for the viability of central neurons. **J. Neurosci**. v. 23, p. 5531–5535, 2003. https://doi.org/10.1523/JNEUROSCI.23-13-05531.2003

PROKOP, A. Bringing life into biology lessons: using the fruit fly *Drosophila* as a powerful modern teaching tool – Guest blog for "**Pedagoo.org**", 2015.

QUERFURTH, H. W.; LAFERLA, F. M. Alzheimer disease. **N. Engl. J. Med.** v. 362, n. 4, p. 329–344, 2010. https://doi.org/10.1056/NEJMra0909142

RASKIND, M. A. Alzheimer's disease: treatment of noncognitive behavioural abnormalities. In: Bloom FE, Kupper DJ. **Psychopharmacology: the fourth generation of progress.** New York: Raven Press; p. 1427-35, 1995.

RASMUSSEN, C.; CAMERON, S. A. Global stingless bee phylogeny supports ancient divergence, vicariance, and long distance dispersal. **Biol. J. Linn. Soc.** v. 99, p. 206–232, 2010. https://doi.org/10.1111/j.1095-8312.2009.01341.x

REITER, L. T. et al. A systematic analysis of human disease-associated gene sequences in *Drosophila melanogaster.* **Genome Research**, v. 11, n. 6, p. 1114–1125, 2001. https://doi.org/10.1101/gr.169101

REITZ, C.; BRAYNE, C.; MAYEUX, R. Epidemiology of Alzheimer disease. **Nat. Rev. Neurol.** v. 7, n. 3, p. 137–152, 2011. https://doi.org/10.1038/nrneurol.2011.2

REITZ, C.; MAYEUX, R. Alzheimer's disease: epidemiology, diagnostic criteria, risk factors and biomarkers. **Biochem. Pharmacol.** v. 88, n.4, p. 640–651, 2014. https://doi.org/10.1016/j.bcp.2013.12.024

ROBERDS, S. L. et al. BACE knockout mice are healthy despite lacking the primary beta-secretase activity in brain: implications for Alzheimer's disease therapeutics. **Hum. Mol. Genet.** v. 10, p. 1317–1324, 2001. https://doi.org/10.1093/hmg/10.12.1317

ROOTE, J.; PROKOP, A. How to design a genetic mating scheme: a basic training package for *Drosophila* genetics. **G3 (Bethesda, Md.)**, v. 3, n. 2, p. 353–8, 2013. https://doi.org/10.1534/g3.112.004820

ROUBIK, D.W. **Ecology and natural history of tropical bees**. Cambridge University Press, New York. 1989. https://doi.org/10.1017/CBO9780511574641

SÁNCHEZ, A.; VÁZQUEZ, A. Bioactive peptides: A review. **FQS** v. 1, p. 29–46, 2017. https://doi.org/10.1093/fqsafe/fyx006

SANG, T. K.; JACKON, G. R. *Drosophila* models of neurodegenerative disease. **Neuro. Rx.** v. 2, p. 438-446, 2005. https://doi.org/10.1602/neurorx.2.3.438

SANJUKTA, S. et al. Enhancement of antioxidant properties of two soybean varieties of Sikkim Himalayan region by proteolytic Bacillus subtilis fermentation. **J. Funct. Foods**. v. 14, p. 650–658, 2015. https://doi.org/10.1016/j.jff.2015.02.033

SARAH, C.; ROBERT, V. The Alzheimer's disease beta-secretase enzyme, BACE1. **Mol. Neurodegener**. v. 2, 2017.

SCHEUNER, D. et al. Secreted amyloid beta-protein similar to that in the senile plaques of Alzheimer's disease is increased in vivo by the presenilin 1 and 2 and APP mutations linked to familial Alzheimer's disease. **Nat. Med.** v. 2, p. 864–870, 1996. https://doi.org/10.1038/nm0896-864

SELKOE, D. Alzheimer's disease: genes, proteins, and therapy. **Physiol Rev**. v. 81, n. 2, p. 741- 66, 2001. https://doi.org/10.1152/physrev.2001.81.2.741

SELKOE, D. J. The cell biology of beta-amyloid precursor protein and presenilin in Alzheimer's disease. **Trends Cell Biol.** v. 8, p. 447–453, 1998. https://doi.org/10.1016/S0962-8924(98)01363-4

SELKOE, D. J. The molecular pathology of Alzheimer's disease**. Neuron.** v. 6, p. 487 – 498, 1991. https://doi.org/10.1016/0896-6273(91)90052-2

SELKOE, D. J.; HARDY, J. The amyloid hypothesis of Alzheimer's disease at 25 years. **EMBO Mol Med.** v. 8, n. 6, p. 595-608, 2016. https://doi.org/10.15252/emmm.201606210

SHANKAR, G. M.; WALSH, D. M. Alzheimer's disease: synaptic dysfunction and Abeta. **Mol. Neurodegener.** v. 4, p. 48, 2009. https://doi.org/10.1186/1750-1326-4-48

SHARON, M.; ROBINSON, C. V. The role of mass Spectrometry in structure elucidation of dynamic protein complexes. **Annual Review of Biochemistry**, v. 76, p. 167–193, 2007. https://doi.org/10.1146/annurev.biochem.76.061005.090816

SINHA, S. et al. Purification and cloning of amyloid precursor protein beta-secretase from human brain**. Nature.** v. 402, p. 537–540, 1999. https://doi.org/10.1038/990114

TANZI, R. E. et al. Amyloid beta protein gene: cDNA, mRNA distribution, and genetic linkage near the Alzheimer locus. **Science.** v. 235, p. 880–884, 1987. https://doi.org/10.1126/science.2949367

THOMPSON, D. B.; TREAT-CLEMONS, L.G.; DOANE, W. W. Tissue-specific and dietary control of alphaamylase gene expression in the adult midgut of *Drosophila melanogaster.* **J. Exp. Zool**. v. 262, p. 122–34, 1992. https://doi.org/10.1002/jez.1402620203

VASSAR, R. et al. Beta-secretase cleavage of Alzheimer's amyloid precursor protein by the transmembrane aspartic protease BACE. **Science.** v. 286, p. 735–741, 1999. https://doi.org/10.1126/science.286.5440.735

VENTURIERI, G.C. et al. Meliponiculture in Brazil: current situation and future perspectives for use in agricultural pollination. In: Pollinators in Brazil - contribution and perspectives for biodiversity, sustainable use, conservation and environmental services. São Paulo: EDUSP, p.213-236, 2012.

WASHBURN, M. P.; WOLTERS, D.; YATES, J. R. Large-scale analysis of the yeast proteome by multidimensional protein identification technology. **Nature Biotechnology**, v. 19, n. 3, p. 242–247, 2001. https://doi.org/10.1038/85686

WEINER, J. **Time, love, memory : a great biologist and his quest for the origins of behavior**. [s.l.] Vintage Books, 2000.

XIAO, Y. et al. Aβ (1-42) fibril structure illuminates self-recognition and replication of amyloid in Alzheimer's disease. **Nat. Struct. Mol. Biol.** v. 22, n. 6, p. 499-505, 2015. https://doi.org/10.1038/nsmb.2991

XU, Y. et al. Flexibility of the flap in the active site of BACE1 as revealed by crystal structures and molecular dynamics simulations. **Acta Crystallogr .D. Biol. Crystallogr.** v. 68, p. 13-25, 2012. https://doi.org/10.1107/S0907444911047251

YAN, R. et al. Membrane-anchored aspartyl protease with Alzheimer's disease beta-secretase activity. **Nature.** v. 402, p. 533–537, 1999. https://doi.org/10.1038/990107

YAN, R.; VASSAR, R. Targeting the b secretase BACE1 for Alzheimer's disease therapy. **Lancet Neurol.** v. 13, p. 319–329, 2014. https://doi.org/10.1016/S1474-4422(13)70276-X

YANG, L. B. et al. Elevated beta-secretase expression and enzymatic activity detected in sporadic Alzheimer disease. **Nat. Med.** v. 9, p. 3–4, 2003. https://doi.org/10.1038/nm0103-3

ZOU, K. et al. Amyloid beta-protein (Abeta)1–40 protects neurons from damage induced by Abeta1–42 in culture and in rat brain. **J. Neurochem**. v. 87, p. 609–619, 2003. https://doi.org/10.1046/j.1471-4159.2003.02018.x

Capítulo 2

Artigos Científicos

Scientific Reports:

Title: Anti-Alzheimer potential of bacterial secretome of stingless bees' larval food Brazilian natives

Tamiris Sabrina Rodrigues [1,*], Lucas Ian Veloso Correia [2], Ana Carolina Santos [1], Mário Machado Martins [2], Luiz Ricardo Goulart [2], Carlos Ueira-Vieira [1] and Ana Maria Bonetti [1]

[1] Laboratory of Genetics, Institute of Biotechnology, Federal University of Uberlândia, Uberlândia, MG, Brazil

[2] Laboratory of Nanobiotechnology, Institute of Biotechnology, Federal University of Uberlândia, Uberlândia, MG, Brazil

Corresponding author: Tamiris Sabrina Rodrigues and Carlos Ueira Vieira

Address: Laboratory of Genetics, Institute of Biotechnology, Federal University of Uberlândia, Uberlândia, Acre Street, 2E building, room 230, Uberlândia, MG, Brazil

tamiris.rodrigues@ufu.br and ueira@ufu.br

Abstract

Alzheimer's disease is a progressive neurodegenerative disorder characterized by the presence of amyloid plaques, neurofibrillary tangles, inflammation, oxidative damage, synapse loss, and selective neuron death. Inhibition of BACE1 expression has been considered a therapeutic target for the prevention and treatment of Alzheimer's disease. This study evaluated BACE1 inhibitory activity of bacterial secretome, isolated from stingless bees' larval food of native Brazilian species, *Melipona quadrifasciata* and *Tetragonisca angustula* using *Drosophila melanogaster* as model organism. We assessed the survival rate of transgenic fly with rough eye phenotype, generated by overexpression of human APP and BACE1 orthologs in the developing nervous system of the eye. Morphological modifications in the eyes of newly hatched *D. melanogaster* were examined by stereomicroscopy, scanning electron microscopy and histology. We carried out the proteomic analysis of the most efficient secretomes searching for bioactive peptides with inhibitory action on BACE1 and β-amyloid plaques. We verified reduction of morphological alterations in the eye, presenting compound eyes with smooth surface, difference in the fusion of the omatids and presence of a large number of bristles when compared to the control groups. Histological sections showed agreement with this improvement, exhibiting compound eyes with regular morphology and organized surface. The proteomic analysis of the secretomes with the best performance in the tests indicated, through *in silico* analysis, the presence of peptides that interact with BACE1 and β-amyloid plaques, potentially modifying the action of these proteins and decreasing the neurodegenerative process. Our analysis found two peptides that interact with BACE1 and β-amyloid plaques, respectively, with potential action in reducing the neurodegenerative process of Alzheimer's disease. We herein conclude that the bacterial secretome of the larval food of stingless bees proved to be a potential source of therapeutic molecules targeting neurodegenerative disorders, such as Alzheimer's disease.

Keywords: Alzheimer's disease; *Drosophila melanogaster*; stingless bees' larval food; secretome; neurodegeneration; β-amyloid

1. Introduction

Alzheimer's disease (AD) is the most common cause of presenile and senile dementia in developed and developing countries [1, 2]. The incidence of AD increases exponentially with age, and the number of affected people is increasing as a result of population aging. Worldwide prevalence is estimated at 135 million sick people by 2050 [3]. AD is a progressive neurodegenerative disease affecting the central nervous system, characterized by progressive loss of neurons in the hippocampus and cerebral cortex, thus compromising information processing and storage. Clinically, AD patients experience short-term memory, word search and language difficulties resulting in memory loss and slow progression of cognitive impairment [4-6]. The main histopathological features of AD are the neurofibrillary tangles, formed by hyperphosphorylated Tau protein filaments and β-amyloid (Aβ) deposits generating extracellular senile plaques, derived from sequential proteolytic processing of amyloid precursor protein (APP) [7-9].

Accumulation of amyloid plaques occurs due to inadequate cleavage of APP in the brain [10, 11]. Normally, APP is cleaved in both its extracellular and intracellular domains by the α- and γ-secretase enzymes, resulting in a 40-amino acid polypeptide, characterizing the non-amyloidogenic pathway and causing age-dependent learning deficits, but without neurodegeneration. When APP is cleaved by β-secretase (BACE1) and γ-secretase enzymes, a 42-amino acid polypeptide is generated ($A\beta_{42}$). The two extra amino acids in this peptide increase the hydrophobicity, promoting their aggregation and formation of amyloid plaques. These plaques are responsible for disrupting normal cell processes in the brain through oxidative stress, resulting in loss of synaptic activity and death of neurons [12-15].

Since Aβ protein is derived from APP and cleaved by two membrane-bound enzymes, β-secretase and γ-secretase complex, the modulation of these enzymes to inhibit Aβ production has been an important focus in the development of therapies for AD. Some compounds have been evaluated as BACE1 inhibitors, but none had succeeded in the early stages of clinical trials due to lack of efficacy or undesirable side effects [16-20]. Hence,

89 further studies are needed in the search of new molecules with pharmacological potential to
90 prevent and treat AD.
91 Honey, propolis and fermented pollen obtained from stingless bees have
92 immunomodulatory, antioxidant, anti-inflammatory, analgesic, sedative, expectorant and
93 hyposensitizing effects [21-25]. Interestingly, since larval food is a mixture of fermented
94 pollen, honey and mandibular secretion, it is possible that various microorganisms present
95 in it secrete biologically active molecules that may be beneficial to human health.
96 Thus, the aim of this study was to evaluate neuroprotective effects of different
97 bacterial secretomes, isolated from stingless bees' larval food (Brazilian native) *Melipona*
98 *quadrifasciata* and *Tetragonisca angustula*. These effects were evaluated on survival rate
99 of transgenic *Drosophila melanogaster* with rough eye phenotype, generated by
100 overexpressing human APP and BACE1 orthologs in the developing nervous system of the
101 eye. Morphological changes in compound eyes of newly hatched transgenic flies were also
102 examined by optical microscopy, scanning electron microscopy (SEM) and histological
103 sections. We carried out the proteomic analysis of bacterial secretomes in order to assess
104 the bioactive peptides with the potential to reduce the neurodegenerative process. Finally,
105 we performed *in silico* analyzes to predict three-dimensional conformations of the peptides
106 and their interaction with the target sites (BACE1 and β-amyloid plaques).
107
108 **2. Results**
109
110 **2.1 Bacteria isolated from stingless bees' larval food**
111
112 The colonies of the bacteria were numerically represented as 7, 9, 12, 14, 20, 27, 45
113 and 54. Table 1 lists the bee species whose larval food was collected, isolated colonies and
114 culture medium for isolation. The secretomes of these microorganisms were collected for
115 food supplementation of *GMR-GAL4 > UAS-BACE1, UAS-APP* transgenic flies, amyloid-
116 induced neurodegeneration model fly, and named as S7, S9, S12, S14, S20, S27, S45 and
117 S54, according to their respective microorganism.

2.2 Bacterial secretomes do not affect the survival and hatching rates of the *Drosophila melanogaster* rough eye phenotype

The larvae of amyloid-induced neurodegeneration model fly treated with different bacterial secretomes were examined in their metamorphosis process. Thirty flies were evaluated in each treatment group. The group treated with water, negative control (NC), showed transformation rates of 86.6% of larvae into pupae and 70% of pupae into adults (Figure 1A). Treatments with secretomes did not significantly change the survival rate of flies during their metamorphosis when compared to the negative control. There was no significant difference in hatching rates in the groups treated with bacterial secretomes, in comparison to the negative control (Figure 1B).

2.3 Effects of bacterial secretomes isolated from stingless bees' larval food on amyloid-induced neurodegeneration model flies

To evaluate the bacterial secretome isolated from stingless bees' larval food in the amyloid-induced neurodegeneration model fly, morphological changes in the eyes were assessed. Wild-type *Canton-S* strain, used as a control, showed normal, well-organized and smooth external ocular surface under stereomicroscope and scanning electron microscopy (Figures 2-A1, B1, C1 and D1).

External phenotypic changes were observed in all groups of *GMR-GAL4 > UAS-BACE1, UAS-APP* flies photographed in stereomicroscope (5x magnification). Distinction between treatment effects using different bacterial secretomes was only possible after observation by SEM. In this analysis, amyloid-induced neurodegeneration model transgenic flies treated with water showed altered ocular morphology, uneven surface and edges, rough appearance and fusion and/or absence of omatids (Figures 2-A2, B2, C2 and D2). Transgenic flies treated with S7 (Figures 2-A3, B3, C3 and D3), S12 (Figures 2-A5, B5, C5 and D5), S14 (Figures 2-A6, B6, C6 and D6), S20 (Figures 2-A8, B7, C7 and D7), S45 (Figures 2-A9, B9, C9 and D9) and S54 (Figures 2-A10, B10, C10 and D10) secretomes

showed improvement in eye morphology, but only in some regions of the ocular edges, keeping the rough appearance on the ocular surface and with a small or nonexistent number of bristles on the omatids. Transgenic flies treated with S9 (Figures 2-A4, B4, C4 and D4) and S27 (Figures 2-A8, B8, C8 and D8) secretomes showed less ocular morphological defects, presenting compound eyes with smooth surface, recovery of omatids in the central area and in the edges, differences in the size of omatids, without fusion between them and with presence of large number of bristles, characterizing putative anti-neurodegenerative effect.

2.4 Protective effect of bacterial secretomes of stingless bees' larval food in the histology of the fly's eye

Eye sections of the wild-type *Canton S* strain and w^{1118} mutant strain (used as control strains), as well as amyloid-induced neurodegeneration model flies treated with different bacterial secretomes of stingless bees' larval food or water (NC) were examined to verify the effects on the histology of the eye. For this analysis, we selected bacterial secretomes that showed the best effects when evaluated by light microscopy and SEM: S9, S27 and S54. For comparison, we included ocular sections of the bacterial secretome S14, which did not improve the phenotype of rough eye. Histological results demonstrated a high level of organization on the ocular surface and complete photoreceptor integrity in *Canton S* (Figure 3A) and w^{1118} (Figure 3B) control strains.

The *GMR-GAL4 > UAS-BACE1, UAS-APP* treated with water (NC) had an irregular ocular surface and photoreceptor neurodegeneration (Figure 3C). *GMR-GAL4 > UAS-BACE1, UAS-APP* transgenic flies treated with S9 (Figure 3D) and S27 (Figure 3E) supernatants showed ocular morphology with an organized and regular surface, despite the incomplete development of the omatid structure when compared to the Canton S and w1118 strains. There was no complete reduction of the photoreceptor degeneration. Eye section analysis of *GMR-GAL4 > UAS-BACE1* flies treated with S14 supernatant (Figure

3F), which showed no recovery of rough phenotype in stereomicroscope and SEM, exhibited an irregular ocular surface compared to those treated with the other supernatants.

2.5 Proteomic analysis of bacterial secretomes

The two best bacterial secretomes that recovered the rough eye phenotype, identified as S9 and S27, were analyzed by mass spectrometry. Twenty-eight peptides unique to the S9 secretome (Table S1, Figure S1), 16 unique to the S27 secretome (Table S2) and 58 peptides common to both secretomes were identified, the latter derived from 55 different proteins (Table 2).

2.6 Molecular Docking

The bioactivity prediction of the 58 peptides identified simultaneously in the S9 and S27 secretomes was calculated using the Peptide Ranker software. Of these, only the 4 sequences with at least 9 amino acids and a classification of at least 0.05 were considered in our analysis. The best 3D model for each of them was selected for molecular docking with β-secretase (BACE) and β-Amyloid (Table 3). Figure 4 shows the 3D images of the interaction of these peptides with their respective target site.

2.7 Toxicity and solubility predictions for potential peptides

After analysis using the ToxinPred software, the AEGAVPMTCPRGK peptide, selected for docking with BACE1, showed no toxicity and appeared to be highly soluble in water. The findings revealed a molecular weight of 1316.73g/mol, isoelectric point of 8.57 and a net charge of 0.9 at pH 7. The peptide TPPITYFLK, selected for docking with β-amyloid, showed no toxicity and appeared to have low water solubility. Its molecular weight was 1079.43g/mol, with isoelectric point of 8.94 and a net charge of 1.0 at pH 7 (Table 4).

3. Discussion

Alzheimer's disease is a progressive neurodegenerative disorder characterized by the presence of amyloid plaques, neurofibrillary tangles, inflammation, oxidative damage, synapse loss, and selective neuron death [26-30]. Remarkably, inhibition of BACE1 expression has been considered a therapeutic target for its prevention and treatment [31, 32].

Studies have selected peptides and heterocyclic compounds as potential inhibitors of BACE1, which failed in the final stages of clinical tests/trial because they did not perform well as AD treatment drugs. Thus, the search for new biologically active molecules that treat AD has aroused the interest of several researchers and pharmaceutical companies [33-35].

The stingless Brazilian bees' larval food is composed of a mixture of fermented pollen, honey and mandibular secretion of nurse bees. The brood cells in which this food is found are moist, dark, nutritionally rich microenvironments with acidic pH and temperature around 30ºC, favoring the growth of a wide range of microorganisms. This microbiota and its secretome vary according to bee species and local flora. Knowledge about this biodiversity of microorganisms and their secretomes is still scarce, especially regarding their function.

In stingless bee colonies, bacteria of the genera *Bacillus* and *Streptomyces* have been identified and appear to play important role in secreting enzymes that ferment and convert pollen constituents and secrete antibiotics, respectively [36-42]. Researchers have isolated *Bacillus* from pollen pots and larval food from *Melipona quadrifasciata* and found that these microorganisms are capable of secreting lipids, carbohydrates and protein cleavage enzymes [38, 43]. Beneficial effects of honey and propolis on human health have been identified [21-25], but there are no studies investigating the effects of bacterial secretomes isolated from stingless bees' larval food. Clearly, the present study is relevant, being the first to search for new molecules of biotechnological potential to prevent or treat neurological diseases using the bacterial secretomes of native Brazilian stingless bees.

For more than a century, *D. melanogaster* has been used as model organism in Life Sciences for development of scientific studies and was one of the first species to have its genome sequenced [44]. Upon completion of human genome sequencing, the homology observed between both genomes reinforced the role of this fly as a model organism for understanding human biology, as well as the mechanisms of certain diseases.

Approximately 75% of human disease-related genes are estimated to have functional orthologs in *D. melanogaster.* The homology between the sequences of these genes has about 40% identity, 80% - 90% in conserved functional domains [45]. Fruit fly studies have substantially altered estimates of the evolutionary relationship between vertebrate and invertebrate organisms. Over the past 50 years, the genetic study on *D. melanogaster* has been successfully applied to decipher the major mechanisms underlying many processes, including development [46], signaling [47], cell cycle [48], system development, function and behavior [49] and molecular aspects of human diseases [50].

The use of *D. melanogaster* as a model for the study of diseases is consolidated due to the high degree of biological conservation between the fruit fly and human genomes, the availability of manipulation techniques and the advantage of the short life cycle of flies [51]. Additionally, the use of *D. melanogaster* significantly reduces costs for studies aimed at understanding molecular and physiological mechanisms applicable to mammals, thereby being of help to identify new targets for therapy [52, 53] and to promote screening for treatment molecules.

The similarity of cell biology aspects between *Drosophila* and humans ranges from gene expression to synaptogenesis, neural connectivity, signaling, and cell death [54]. *D. melanogaster* presents a complex nervous system, being attractive for studying neuronal dysfunction and neurodegenerative diseases, with the ability to develop behaviors such as learning and memory [55].

The possibility of overexpressing proteins involved in the neurodegenerative process, mimicking human diseases, increases the potential of this model in the study of these pathologies [54]. The *GAL4/UAS* system was used for overexpression of interest genes in a specific fly tissue. In the *GAL4* system, the enhancer directs the expression of the

transcriptional yeast activator *GAL4* in specific cells and tissues and *GAL4* directs the transcription of the *GAL4-UAS* target genes in an identical pattern [56-57].

The analysis of secretomes of microorganisms isolated from larval food of stingless bees (Brazilian native) through treatment of disease model organisms may culminate in the isolation of molecules with pharmacological potential to treat neurodegenerative disorders. These pathologies have a high incidence in the world population, and alternative approaches to their treatment become relevant.

In this work, we isolated 2 bacteria of stingless bees' larval food from the species *Tetragonisca angustula* and 6 from the species *Melipona quadrifasciata*. The supernatants of these bacteria were collected and used to supplement food of the *GMR-GAL >UAS-BACE1, UAS-APP* transgenic flies, which overexpress the human APP and BACE1 orthologous genes in the eye, generating the rough eye phenotype and characterizing an amyloid-induced neurodegeneration model fly.

We reported that the treatment with the secretomes of stingless bees' larval food did not alter the survival rate of the flies nor did it affect the hatching rate of pupae in adults. These data showed that the treatment with the secretomes was not toxic to the flies and did not interfere with their metamorphosis process. These are the first evidences of the beneficial action of secretomes in the transgenic lineage of *D. melanogaster.*

The analysis of the phenotype of the rough eye of the model fly with amyloid-induced neurodegeneration revealed considerable antineurodegenerative effects in individuals treated with S9 and S27 secretomes, based on the optical microscopy, SEM and histological sections observations. The results obtained showed that both secretomes acted on the *D. melanogaster* transgenic lineage, modifying the rough eye phenotype and recovering the structure of the omatids. These findings indicate the presence of biologically active molecules in the content of the samples, which are responsible for the neuroprotective effect.

When we recall the amyloidogenic pathway involved in the Alzheimer's process, we hypothesized three possible sites of action for these bioactive peptides, namely: 1) Interaction between the peptide and BACE1 (β-secretase), preventing this enzyme from

erroneously cleaving the APP protein; 2) Interaction between the peptide and APP or Aβ42, making these proteins unavailable for erroneous cleavage of BACE1; and 3) Interaction between the peptide and β-amyloid plaques, so that, despite the existence of plaques, they are neutralized by binding to the peptide, avoiding its toxicity and deposition in the nervous system. The use of *in silico* methods based on bioinformatics has been shown to be efficient in predicting sequences of peptides with biological action for the prevention and treatment of diseases [58]. For this reason, we carried out the docking analysis of the potentially more bioactive peptides against BACE1, APP and amyloid plaques.

The sequences of the bioactive peptides are inactive when inside the protein that originated them and can be obtained, among other ways, by hydrolysis of these proteins using digestive enzymes. The studied bacterial secretomes were prepared with enzymatic action of trypsin, before their proteomic analysis [59]. Interestingly, this enzyme is also present in the digestive system of *D. melanogaster,* and we performed a simulated gastrointestinal digestion, mimicking the process in the fly and obtaining bioactive peptides from the bacterial proteins in the secretomes [60].

The prediction of peptide toxicity was in agreement with the beneficial effects observed in our tests, since none of them were toxic. We found that the AEGAVPMTCPRGK peptide exhibited good water solubility. Water solubility has a great influence on the degree of *in vivo* absorption of bioactive peptides, and water-soluble peptide sequences generally have high biological availability [61]. Although the prediction of water solubility of the TPPITYFLK peptide is low, this does not prevent its potential bioactivity. Future analyzes can be done by generating mutants of this sequence in order to improve its degree of solubility, optimizing its absorption in the gastrointestinal tract or its use for injection in organisms.

In order to assess the interaction between the potentially bioactive peptides and the BACE1 and beta-amyloid target sites, molecular docking procedures were performed. As shown in 3D images, although the peptide does not interact with the BACE1 active site (conserved catalytic dyad formed by Asp32 and Asp 228), there was interaction with Thr72, Pro70, Tyr71 and Val69 residues in the enzyme flap region. This hook loop located

in the N-terminal portion of the molecule (residues 67-75) is perpendicular to the active BACE1 site, partially covering it, being the most flexible region of β-secretase [62, 63]. Changes in the flap, through the binding of a peptide, for example, seem to control the access to the target site, correctly positioning the substrate for the catalysis to occur [64]. Thereby, the docking of the AEGAVPMTCPRGK peptide could modify the conformation of the flap, blocking the access of APP to the target site of BACE1. This would inhibit the action of this enzyme, preventing the erroneous cleavage of APP and the appearance of beta-amyloid plaques. Thus, a positive interaction would be maintained between the peptide and BACE1.

Hong and colleagues (2000) observed crystalline structures of complexes formed between BACE1 and peptides that brought up the flap into a closed conformation, moving closer to the Asp dyad [65, 66]. The structures of this study are similar to that of the peptide sequence AEGAVPMTCPRGK, containing residues of Ala and Glu, being yet another indication of the potential binding of this highly bioactive peptide with BACE1, culminating in its inhibition, and preventing the neurodegenerative process triggered by the amyloid pathway.

The non-amyloidogenic pathway of APP protein cleavage is characterized by its sequential cleavage by the enzymes α and γ-secretase, generating a peptide of 40 amino acids. The APP amyloidogenic pathway, involved in the AD neurodegenerative process, consists of the cleavage of this same protein by α and β-secretase, generating the 42-amino acid Aβ peptide [67]. Despite the small difference in the number of amino acids, Aβ42 is more toxic and has a high aggregating power, although Aβ40 is more abundant in plasma [68, 69, 70, 71]. Xiao et al. (2015) [72] identified a single β triple motif in the structure of Aβ42, formed by three β leaves that cover the residues 12-18 (β1), 24-33 (β2) and 36-40 (β3) . This tertiary fold is highly different from that observed in Aβ40 and seems to give Aβ42 the format responsible for its cytotoxicity and aggregation, resulting in the formation of β-amyloid plaques found in patients with neurodegenerative diseases.

When predicting the docking between TPPITYFLK and β-amyloid plaques, the 3D image generated from this interaction showed that the connection between the peptide and

the amyloid plaque was efficient and altered its conformation, causing the opening of one of its domains. Based on those reported above, we believe that the conformational change in the plaque, caused by the binding to the potentially active peptide TPPITYFLK, undoes its triple motif β. The change in this tertiary fold could neutralize β-amyloid plaques, reducing its cytotoxicity and preventing its neuronal accumulation. We hypothesize that the TPPITYFLK peptide could play an active role in preventing Alzheimer's disease.

Thus, our study was able to predict the docking of two peptides with potential bioactivity with BACE1 (AEGAVPMTCPRGK) and β-amyloid (TPPITYFLK), valuable sites for the search of therapies for the prevention and treatment of AD. In fact, the connection between them was efficient and brings good prospects for their clinical use.

We concluded that the bacterial secretomes of the larval food of Brazilian stingless bees proved to be a potential source of therapeutic molecules targeting neurodegenerative diseases. Furthermore, our group has explored the biotechnological potential of microorganisms isolated from the larval food of native Brazilian stingless bees, evaluating their antimicrobial and antitumor effects, as well as their therapeutic use in other pathological processes.

4. Material and Methods

4.1 Biological material

Were tested eight bacterial secretomes (S7, S9, S12, S14, S20, S27, S45 and S54) obtained from bacteria in the microorganism bank Collection of isolated stingless bee microorganisms LABGEN UFU (COMIALG) of Laboratory of Genetics - Federal University of Uberlândia.

The secretomes analyzed in this study were obtained from bacteria isolated from the Brazilian stingless bee hives *Melipona quadrifasciata* and *Tetragonisca angustula,* located at the UFU Meliponary (S 180 55 '/ W 450 17') of the Biotechnology Institute of the Federal University of Uberlandia, Uberlandia, Minas Gerais , Brazil.

4.2 Obtaining bacterial secretome

To obtain the supernatant of each bacteria isolated from larval food, 50 mL of Luria Bertani (LB) medium was prepared and autoclaved, followed by inoculation of 10 µL of bacteria. The medium was incubated in a bacteriological incubator at 37°C for 48 hours under 200 rpm agitation. Medium was transferred to a sterile 15 mL tube and centrifuged at 1000g. The supernatant was filtered through a sterile 0.22 µm syringe filter. The supernatants/secretomes were frozen in -20°C freezer until its use in flies' treatment.

4.3 Fly stock and Genetics

The strains under study were kept in stock at the Genetics Laboratory of the Institute of Biotechnology (IBTEC) of the Federal University of Uberlândia (UFU) in flasks containing ¼ of Bloomington culture medium (1500 mL of water, 27g of yeast, 15g soybean meal; 109.5g corn meal; 9g agar; 115.5g glucose syrup; acid and Nipagin solution) in BOD incubator (Biochemical Oxygen Demand, SOLAB) at 25°C, 70% relative humidity and 12:12 hours light-dark cycle.

GMR-GAL4 (stock number 1104), *UAS-BACE1, UAS-APP* (29877), w^{1118} (3605) and *Canton S* (9514) strains were purchased from Bloomington Stock Center at the University of Indiana. The *GAL4/UAS* system was used for overexpression of human APP and BACE1 orthologs in the fly eyes [56-57]. In our study, *GMR-GAL4* (driver strain) directs the expression of the human APP and BACE1 orthologs (*UAS-BACE1*, responder strain) to fly compound eyes. From crossing *GMR-GAL4* females and *UAS-BACE1* males, we obtained the overexpression of the human APP and BACE1 orthologs in the fly eyes, generating the rough eye phenotype in *D. melanogaster*, an amyloid-induced neurodegeneration model fly.

405 **4.4 Experimental groups**

406

407 Eight bacterial secretomes isolated from the stingless bees' larval food, 6 isolated
408 from *Melipona quadrifasciata* and 2 from *Tetragonisca angustula*, were tested in *GMR-*
409 *GAL4 > UAS-BACE1*, *UAS-APP* transgenic flies of *D. melanogaster.* Morphological and
410 structural changes in the compound eyes of newly hatched adult flies after supplementation
411 with the secretomes were evaluated. Eggs from the progeny of *GMR-GAL4 > UAS-BACE1,*
412 *UAS-APP* were collected in oviposition flasks containing agar-based culture medium (4%)
413 and sucrose-supplemented yeast. The collected eggs were placed in transparent polystyrene
414 vials (94 x 25 mm) containing Yoki® mashed potato medium (1g) supplemented with
415 supernatant (2.5 mL), ensuring that flies were fed with the secretomes since the first larval
416 stage. Negative control was composed of larvae treated with mashed potato medium
417 prepared with water.

418

419 **4.5 Survival test and hatching rate of flies**

420

421 For the survival test and hatching rate of flies, thirty third instar larvae were treated,
422 through food supplementation with each secretome. For the survival test, the number of
423 larvae that became pupae and the number of pupae that hatched in adults were recorded.
424 The hatching rate of the flies was calculated by adopting the number of pupae as 100% in
425 relation to the number of hatched adults. Treated flies and negative control (NC, water)
426 were handled under the same conditions.

427

428 **4.6 Stereomicroscopy and scanning electron microscopy of flies' eyes**

429

430 From the egg stage, *GMR-GAL4 > UAS-BACE1, UAS-APP* flies were kept in
431 polystyrene vials containing mashed potato medium (1g Yoki® mashed potato)
432 supplemented with 2.5 mL bacterial supernatant isolated from stingless bees' larval food
433 (secretome). The control group received 1g of Yoki® Mashed Potato with 2.5 mL of water

434 or LB medium. The newly hatched adult flies were anesthetized with ethyl ether and placed
435 in a Petri dish at room temperature. The morphology of compound eyes was observed and
436 photographed at 5x magnification using a stereomicroscope (Nikon SMZ745) equipped
437 with a 2.3 megapixel DFK 23UX236 (Sony) camera.
438 For SEM, newly hatched adult flies were collected, anesthetized with ethyl ether
439 and kept in 70% ethanol. For analysis, the flies were dried at room temperature and
440 metallized with gold. The outer surface morphology of the compound eye was visualized
441 using the scanning electron microscope (Zeiss EVO MA10) operated at 5 kV.
442
443 **4.7 Histological analysis**
444
445 For histological analysis, newly hatched adult flies were collected, anesthetized with
446 ethyl ether and fixed in Carnoy solution (6: 3: 1, 99% ethanol, chloroform and glacial acetic
447 acid) for 24 hours and processed in 70% ethyl alcohol (2x), 80% ethyl alcohol (2x), 90%
448 ethyl alcohol (2x), absolute ethyl alcohol (2x), xylol (2x), 60% liquid paraffin (2x) for 15
449 minutes in each repetition. The flies' heads were aligned in an apparatus [73] and
450 embedded in paraffin. The blocks were sectioned at 3 μm thick using a semi-automatic
451 microtome (SLEE CUT5062). The sections were dehydrated, stained with hematoxylin and
452 eosin and mounted. The images were captured under light microscope (Leica) at 40x
453 magnification, through a coupled image capture system (LAS EZ software).
454
455 **4.8 Proteomic analysis**
456
457 For the proteomic analysis, the proteins were reduced with 100 mM dithiothreitol
458 (DTT), alkylated with 0.5 M iodoacetamide and digested with trypsin (0.01 μg/μL). The
459 desalination step was performed with ZipTips C18 (Millipore, Billerica, MA, United
460 States).
461 The proteomic analysis was performed on the Liquid Chromatography-Electrospray
462 Ionization – Quadrupole - Time of Flight-Mass Spectrometry (6520B LC-ESI-Q-TOF-MS)

from Agilent. The chromatographic parameters were AdvanceBio Peptide Mapping column (Agilent) with 2.1 mm internal diameter, 10 cm of length and 2.7 µm particles. The mobile phase was composed by water (A) and acetonitrile (B), both acidified with formic acid (0.1% vv), with the gradient: 2% B (0 min), 2% B (10 min), 15% B (40 min), 50% B (150 min), 70% B (200 min), 98% B (220 min), 98% B (300 min), 100% B (301 min) and 100% B (400 min), in a flow of 400 µL/min. The ionization parameters were nebulizer pressure of 45 psi, drying gas at 8L / min at a temperature of 325 °C and 4KV energy was applied to the capillary.

The analysis of the raw data was performed in the Spectrum Mill software (Agilent) using the Swiss-Prot database (337654 results in November 2020). Carbamidomethylation was set as fixed modification. Maximum missed cleavages were selected in two for trypsin. The search parameters were as follows: precursor mass error and the fragments: 20 ppm; product mass tolerance: 50 ppm; and maximum ambiguous precursor charge: 3.

4.9 Screening of bioactive peptides

The proteins were digested with trypsin in proteomic protocols, which can mimic the digestive process in *D. melanogaster* gut and create bioactive peptides from bacterial proteins. Only peptides present in both samples (S9 and S27) were used for bioactivity prediction using the Peptide Ranker (http://distilldeep.ucd.ie/PeptideRanker/) tool. The peptides with rank above 0.5 were considered as potential bioactivity.

4.10 Peptides tertiary structure prediction

The 3D structures of peptides were created using PEP-FOLD 2.0 (https://mobyle.rpbs.univ-paris-diderot.fr/cgi-bin/portal.py#forms::PEP-FOLD). Analysis of the global energy and the contribution of the atomic contact energy (ACE) were carried to determinate the best 3D models of each peptide.

4.11 Molecular Docking

The PDB file from BACE (3TPJ) and 42-Residue Beta Amyloid Fibril (2MXU) were retrieved from Protein Data Bank (https://www.rcsb.org/). The online docking was performed by using Path Docking (https://bioinfo3d.cs.tau.ac.il/PatchDock/) and refined by Fire Doock (http://bioinfo3d.cs.tau.ac.il/PatchDock/php.php) with the best sequence chosen for docking with BACE1 and for docking with 42-B-amyloid Fibril Residue.

To estimate the possible targets of the selected peptides, we use the website Swiss Target Prediction (http://www.swisstargetprediction.ch/).

4.12 Toxicity and solubility predictions for potential peptides

The Toxin Pred tool (http://crdd.osdd.net/raghava/toxinpred/) was utilized to predict the toxicity of potential peptides based on their important physicochemical properties. The peptide property calculator Innovagen (http://www.innovagen.com/proteomicstools) was used to calculate the solubility of peptides. The results were calculated based on the isoelectric point and the peptide length.

4.13 Statistic analysis

Statistical comparisons regarding survival rates and hatching rates of flies were performed using the Chi-square test for reasons of independent samples.

Author Contributions: T.S.R. Conception, design, development of the methodology, analysis and interpretation of data, writing and revision of the manuscript. A.C.C.S. Development of the methodology. M. M. M. Proteomic analysis. L.I.V.C. Proteomic and bioinformatics analysis L.R.G. Proteopeptidomic analysis. C.U.V. Conception, design, writing and revision of the manuscript, technical and material support. A.M.B. Conception, design, writing and revision of the manuscript, technical and material support.

Funding: This research was funded by the Conselho Nacional Científico e Tecnológico do Brasil (CNPq), the Fundação de Amparo à Pesquisa do Estado de Minas Gerais (FAPEMIG APQ-02766-17) and the Coordenadoria de Aperfeiçoamento de Pessoal de Nível Superior (CAPES). Federal University of Uberlândia provided physical conditions for experimental procedures.

Acknowledgments: We are thankful to the Institute of Cell Biology for providing access to the Light Microscope and Software LAS EZ, to the Scanning Electron Microscopy Laboratory of the Faculty of Chemical Engineering of the Federal University of Uberlândia for the SEM analysis, and to the Pathology Laboratory of the Faculty of Odontology for the microscope sections.

Conflicts of Interest: The authors declare no conflict of interest.

Abbreviations

AD	Alzheimer's disease
APP	amyloid precursor protein
BACE1	β-secretase enzyme
$A\beta_{42}$	β-amyloid protein
MRS Agar	Man Rogosa Sharpe
TSA Agar	Tryptic Soy Agar
BHI Agar	Brain Heart Infusion
LB	Luria Bertani
D. melanogaster	*Drosophila melanogaster*
mL	milliliter
µm	micrometer
°C	degrees Celsius
rpm	rotations per minute
µL	microliter

mm	millimeter
IBTEC	Institute of Biotechnology
UFU	Federal University of Uberlândia
BOD	Biochemical Oxygen Demand
NC	negative control
SEM	scanning electron microscopy
CNPq	Conselho Nacional Científico e Tecnológico
FAPEMIG	Fundação de Amparo à Pesquisa do Estado de Minas Gerais
CAPES	Coordenadoria de Aperfeiçoamento de Pessoal de Nível Superior

References

1. Ferri, C.; Prince, M.; Brayne, C. et al. Global prevalence of dementia: a Delphi consensus study. *Lancet.* **2005**, *366*, 2112–2117. doi: 10.1016/S0140-6736(05)67889-0
2. Kalaria, R.; Maestre, G. E.; Arizaga, R. et al. Alzheimer's disease and vascular dementia in developing countries: prevalence, management, and risk factors. *Lancet Neurol.* **2008**, *7*, 812–826. doi: 10.1016/S1474-4422(08)70169-8
3. Alzheimer's Association. Alzheimer's disease facts and figures. *Alzheimers Dement.* **2018**, *14*, 367–429.
4. Singh, A.; Tare, M.; Puli, O. R. et al. A glimpse into dorso-ventral patterning of the Drosophila eye. *Dev Dyn*. **2012**, *24*, 69–84. doi: 10.1002/dvdy.22764
5. O'Brien, R. J.; Wong, P. C. Amyloid precursor protein processing and Alzheimer's disease. *Annu Ver Neurosci.* **2011**, *34*, 185-204. doi: 10.1146/annurev-neuro-061010-113613
6. Albert, M. S.; DeKosky, S. T.; Dickson, D. et al. The diagnosis of mild cognitive impairment due to Alzheimer's disease: recommendations from the National Institute on Aging-Alzheimer's Association workgroups on diagnostic guidestrains for Alzheimer's disease. *Alzheimers Dement.* **2011**, *7*, 270–279. doi: 10.1016/j.jalz.2011.03.008
7. Hardy, J.; Selkoe, D. J. The amyloid hypothesis of Alzheimer's disease: progress and problems on the road to therapeutics. *Science.* **2002**, *297,* 353–356.
8. Suh, Y. H.; Checler, F. Amyloid precursor protein, presenilins, and alpha-synuclein: molecular pathogenesis and pharmacological applications in Alzheimer's disease. *Pharmacol.* **2002**, *54*, 469–525.
9. Baptista, F. I.; Henriques, A. G.; Silva, A. M. S. et al. Flavonoids as therapeutic compounds targeting key protein involved in Alzheimer's disease. *ACS Chem Neurosci.* **2014**, *5*, 83–92.
10. Aguzzi, A.; O'Connor, T. Protein aggregation diseases: pathogenicity and therapeutic perspectives. *Nat Rev Drug Discov*. **2010**, *9*, 237-248. doi: 10.1038/nrd3050
11. Fernandez-Funez, P.; Sanchez-Garcia, J.; Ribncon-Limas, D.E. *Unraveling the basis of neurodegeneration using the developing eye.* New York: Springer; 2013.
12. Selkoe, D. J.; Hardy, J. The amyloid hypothesis of Alzheimer's disease at 25 years. *EMBO Mol Med.* **2016**, *8*, 595–608. doi: 10.15252/emmm.201606210
13. Goldman, D. P.; Fillit, H.; Neumann, P. Accelerating Alzheimer's disease drug innovations from the research pipestrain to patients. *Alzheimers Dement.* **2018**, *14*, 833-836. doi: 10.1016/j.jalz.2018.02.007
14. Sierra-Fonseca, J. A.; Gosselink, K. L. Tauopathy and neurodegeneration: A role for stress. *Neurobiol Stress.* **2018**, *9*, 105–112. doi: 10.1016/j.ynstr.2018.08.009

15. Kandalepas, P. C.; Vassar, R. Identification and biology of β-secretase. *J. Neurochem.* **2012**, *120*, 55–61. doi: 10.1111 / j.1471-4159.2011.07512.x
16. Kennedy, M. E.; Stamford, A.W.; Chen, X. et al. The BACE1 inhibitor verubecestat (MK-8931) reduces CNS β-amyloid in animal models and in Alzheimer's disease patients. *Sci Transl Med.* **2016**, *8*, 363-150. doi: 10.1126 / scitranslmed.aad9704
17. May, P. C.; Willis, B. A.; Lowe, S. L. et al. The Potent BACE1 Inhibitor LY2886721 Elicits Robust Central Aβ Pharmacodynamic Responses in Mice, Dogs, and Humans. *J. Neurosci.* **2015**, *35*, 1199–1210. doi: 10.1523 / JNEUROSCI.4129-14.2015
18. May, P. C.; Dean, R. A.; Lowe, S. L. et al. Robust Central Reduction of Amyloid-β in Humans with an Orally Available, Non-Peptidic β-Secretase Inhibitor. *J. Neurosci.* **2011**, *31*, 16507-16516. doi: 10.1523 / JNEUROSCI.3647-11.2011
19. Hung, S. Y.; Fu, W. M. Drug candidates in clinical trials for Alzheimer's disease. *J Biomed Sci.* **2017**, *24*, 47. doi: 10.1186 / s12929-017-0355-7
20. Moussa, C. E. Beta-secretase inhibitors in phase I and phase II clinical trials for Alzheimer's disease. *Expert Opin Investig Drugs.* **2017**, *26*, 1131-1136. doi: 10.1080 / 13543784.2017.1369527
21. Almaraz-Abarca, N. et al. Antioxidant activity of polyphenolic extract of monofloral honeybee-collected pollen from mesquite (*Prosopisjuliflora, Leguminosae). J Food Comp*. **2007**, *20(2)*, 119-124.
22. Naito, Y. et al. Anti-inflammatory effect of topically applied propolis extract in carrageenan-induced rat hind paw edema. *Photother. Res.* **2007**, *21(5)*, 452-456.
23. Orsatti, C. L.; Missima, F.; Pagliarone, A. C. Propolis immunomodulatory action in vivo on Toll like receptors 2 and 4 expressions and on pro-inflammatory cytokines production in mice. *Phytother Res.* **2010,** *24(8)*, 1141-1146.
24. Sforcin, J. M.; Bankova, V. Propolis: Is there a potential for the development of new drugs. *J Ethnopharmacol.* **2011**, *133(2)*, 253-260.
25. Wiese, H. *New Beekeeping.* 7 ed. Porto Alegre: Agropecuária. 493pp.1986.
26. Selkoe, D. J. Alzheimer's disease is a synaptic failure. *Science.* **2002**, *298*, 789–791.doi: 10.1126/science.1074069
27. Walsh, D. M.; Selkoe, D. J. Deciphering the molecular basis of memory failure in Alzheimer's disease. *Neuron*. **2004**, *44,* 181–193. doi: 10.1016/j.neuron.2004.09.010
28. Serrano-Pozo, A.; Frosch, M. P.; Masliah, E. et al. Neuropathological alterations in Alzheimer disease. *Cold Spring HarbPerspect Med.* **2011**, *1*, 6189. doi: 10.1101/cshperspect.a006189
29. Hardy, J.; Selkoe, D. J. The Amyloid Hypothesis of Alzheimer's Disease: Progress and Problems on the Road to Therapeutics. *Science.* **2002**, *297*, 353–356. doi: 10.1126 / science.1072994
30. Suh, Y. H.; Checler, F. Amyloid Precursor Protein, Presenilins, and α-Synuclein: Molecular Pathogenesis and Pharmacological Applications in Alzheimer's Disease. *Pharmacol Rev.* **2002**, *54*, 469-525. doi: 10.1124 / pr.54.3.469
31. Ghosh, A. K.; Gemma, S.; Tang, J. beta-Secretase as a therapeutic target for Alzheimer's disease. *Neurotherapeutics.* **2008**, *5*, 399-408. doi: 10.1016 / j.nurt.2008.05.007
32. Mancini, F.; De Simone, A.; Andrisano, V. Beta-secretase as a target for Alzheimer's disease drug discovery: an overview of in vitro methods for characterization of inhibitors. *Anal Bioanal Chem.* **2011**, *400*, 1979-1996. doi: 10.1007 / s00216-011-4963-x
33. Thompson, L. A.; Bronson, J. J.; Zusi, F. C. Progress in the Discovery of BACE Inhibitors. *Curr Pharm Des.* **2005**, *11*, 3383-3404. doi: 10.2174 / 138161205774370825

34. John, V. Human beta-secretase (BACE) and BACE inhibitors: progress report. *Curr Top Med Chem*. **2006**, *6*, 569-578. doi: 10.2174 / 156802606776743084
35. Orhan, I. E. Current concepts on selected plant secondary metabolites with promising inhibitory effects against enzymes linked to Alzheimer's disease. *Curr Med Chem.* **2012**, *19*, 2252- 2261.
36. Gilliam, M.; Buchmann, S. L.; Lorenz, B. J. et al. Microbiology of the larval provisions of the stingless bee, *Trigona hypogea*, an obligate necrophage. *Biotropica.* **1985**, *71*, 28–31.
37. Gilliam, M.; Prest, D. B.; Lorenz, B. J. Microbiology of pollen and bee bread: taxonomy and enzymology of molds. *Apidologie.* **1989**, *20*, 53–68.
38. Gilliam, M.; Roubik, D. W.; Lorenz, B. J. Microorganisms associated with pollen, honey, and brood provisions in the nest of a stingless bee, *Meliponafasciata. Apidologie.* **1990**, *21*, 89–97.
39. Can, R. J.; Borucki, M. K.; Higby-Schweitzer, M. et al. *Bacillus* DNA in fossil bees: an ancient symbiosis? *Appl Environ Microbiol.* **1994**, *60*, 2164–2167.
40. Camargo, J. M. F.; Grimaldi, D.; Pedro, S. R. M. The extinct fauna of stingless bees (*Hymenoptera: Apidae: Meliponini*) in Dominican amber: two new species and redescription of the male of *Proplebeiadominicana* (Wille and Chandler). *American Museum Novitates.* **2000,** *3293*, 1–24.
41. Yoshiyama, M.; Kimura, K. Bacteria in the gut of Japanese honeybee, *Apiscerana japonica*, and their antagonistic effect against *Paenibacillus* larvae , the causal agent of American foulbrood. *J Invertebr Pathol.* **2009**, *102,* 91–96.
42. Kroiss, J.; Kaltenpoth, M.; Schneider, B. et al. Symbiotic streptomycetes provide antibiotic combination prophylaxis for wasp offspring. *Nat Chem Biol.* **2010**, *6*, 261–263.
43. Machado, J. O. Symbiosis among Brazilian social bees (*Meliponinae, Apidae*) and a species of bactéria. *Science and Cult.* **1971**, *23*, 625–633.
44. Adams, M. D. et al. The genome sequence of *Drosophila melanogaster*. Science. **2000**, *287*, 2185–95.
45. Zettervall, C. J.; Anderl, I.; Williams, M. J. et al. A directed screen for genes involved in *Drosophila* blood cell activation. *Proc of the Natl AcadSc USA*. **2004**, *101*, 14192–14197.
46. Lawrence, P. A. *The making of a fly: the genetics of animal design.* 1992.
47. Cadigan, K. M.; Peifer, M. Wnt signaling from development to disease: Insights from model systems. *Cold Spring Harb Perspect Biol.* **2009**, *1*, 2881–2881.
48. Lee, L. A.; Orr-Weaver, T. L. Regulation of cell cycles in *Drosophila* development: intrinsic and extrinsic cues. *Annu Revi Genet.* **2003**, *37*, 545–578.
49. Bellen, H. J.; Tong, C.; Tsuda, H. 100 years of *Drosophila* research and its impact on vertebrate neuroscience: a history lesson for the future. *Nat Rev Neurosci.* **2010**, *11*, 514–522. doi: 10.1038/nrn2839.
50. Bier, E. *Drosophila*, the golden bug, emerges as a tool for human genetics. *Nat Revi Genet.* **2005**, *6*, 9–23.
51. Bilen, J.; Bonini, N. M. *Drosophila* as a Model for Human Neurodegenerative Disease. *Annu Revi Genet.* **2005**, *39*, 153-171.
52. Lloyd, T. E.; Taylor, J. P. Flightless flies: *Drosophila* models of neuromuscular disease. *Ann N Y Acad of Sci.* **2010**, *1184*, 1-20.
53. Reiter, L. T.; Potocki, L.; Chien, S. et al. A systematic analysis of human disease-associated gene sequences in *Drosophila melanogaster. Genome Res.* **2001**, *11*, 1114–1125.
54. Sang, T. K.; Jackon, G. R. *Drosophila* models of neurodegenerative disease. Neuro Rx. **2005**, *2*, 438-446. doi: 10.1602/neurorx.2.3.438

55. Chan, H. Y.; Bonini, M. N. *Drosophila* models of human neurodegenerative disease. *Cell death differ.* **2000**, *7*, 1075-1080.
56. Elliott, D. A.; Brand, A. H. The GAL4 System. In: Dahmann C, editor. *Drosophila.* Methods in molecular biology. *Human Press*. **2008**, *420*, 79–95. doi:
57. Roote, J.; Prokop, A. How to design a genetic mating scheme: a basic training package for *Drosophila* genetics. *G3* (Bethesda, Md.). **2013**, *3*, 353–358.
58. Gu, Y.; Majumder, K.; Wu, J. QSAR-aided in silico approach in evaluation of food proteins as precursors of ACE inhibitory peptides. *Food Res*. Int. **2011**, 44, 2465–2474.
59. Korhonen, H.; Pihlanto, A. Bioactive peptides: Production and functionality. Int. *Dairy J*. **2006**, 16, 945–960.
60. Buchon, N., Osman, D., David, F. et al. Morphological and molecular characterization of adult midgut compartmentalization in *Drosophila*. *Cell Rep.***2013**, 3:1725–38.
61. Hanke, A.T.; Ottens, M. Purifying biopharmaceuticals: Knowledge-based chromatographic process development. *Trends Biotechnol.* **2014**, 32, 210–220.
62. Hong, L. & Tang, J. *Biochemistry*. **2004**, 43, 4689–4695.
63. James, M. N., Sielecki, A., Salituro, F. et al. *Proc. Natl Acad.* Sci. **1982.** 79, 6137–6141.
64. Shimizu, H., Tosaki, A., Kaneko, K. et al. *Mol. Cell. Biol*. **2008**, 28, 3663–3671.
65. Hong, L., Koelsch, G., Lin, X. et al. *Science.* **2000**, 290, 150–153.
66. Turner, R., Hong, L., Koelsch, G. et al. *Biochemistry*. **2005**, 44, 105–112.
67. Ray B, Maloney B, Sambamurti K, et al. Rivastigmine modifies the α-secretase pathway and potentially early Alzheimer's disease [published correction appears in Transl Psychiatry.*Transl Psychiatry*. **2020**, 10(1):47.
68. Davis, J., Van Nostrand, W. Enhanced pathologic properties of Dutch-type mutant amyloid beta-protein. *Proc Natl Acad Sci.* **1996,** 93:2996–3000.
69. Luheshi L. et al. Systematic in vivo analysis of the intrinsic determinants of amyloid beta pathogenicity. *Plos Biology.* **2007,** 5:2493–2500.
70. Gravina S. et al. Amyloid β protein (Aβ) in Alzheimer's disease brain. Biochemical and immunocytochemical analysis with antibodies specific for forms ending at Aβ40 or Aβ42(43) *J Biol Chem.* **1995,** 270:7013–7016.
71. Iwatsubo T, et al. Visualization of A-beta-42(43) and A-beta-40 in senile plaques with end-specific A-beta monoclonals – evidence that an initially deposited species is A-beta-42(43) *Neuron.* **1994**, 13:45–53.
72. Xiao, Y., Ma, B., McElheny, D. et al. Aβ(1-42) fibril structure illuminates self-recognition and replication of amyloid in Alzheimer's disease. *Nat Struct Mol Biol***. 2015,** 22(6):499-505. doi:10.1038/nsmb.2991
73. Sunderhaus, E. R.; Kretzschmar, D. Mass Histology to Quantify Neurodegeneration in *Drosophila. J Vis Exp.* **2016**, *118*.

Table legends:

Table 1. Bacteria isolated from stingless bees' larval food.

Table 2. List of peptides identified in both secretomes (S9 and S27) and the respective proteins that are derived from.

Table 3. Characteristics of the best 3D models of peptides with potentially bioactive properties.

Table 4. Characteristics of the best 3D models of peptides considered to be potentially bioactive for molecular docking.

Table S1. List of peptides identified exclusively in the S9 secretome and the respective proteins that are derived from.

Table S2. List of peptides identified exclusively in the S27 secretome and the respective proteins that are derived from.

Figure legends

Figure 1. Effect of bacterial secretome isolated from stingless bees' larval food on survival and hatching rates of adult flies in amyloid-induced neurodegeneration model fly. A. Survival rates of amyloid-induced neurodegeneration model fly (GMR-GAL4 > UAS-BACE1, UAS-APP) treated with different bacterial secretomes isolated from stingless bees' larval food of the species *Melipona quadrifasciata* and *Tetragonisca angustula*. Transgenic flies from the third larvae stage (n = 30, considered as 100%) were maintained in polystyrene vials containing mashed potato medium supplemented with bacterial secretome (experimental group) or water (control group). The number of pupae and adults was recorded in order to evaluate the effect of treatment on fly metamorphosis. **B.** Hatching rates of GMR-GAL4 > UAS-BACE1, UAS-APP flies. The number of pupae was considered as 100% in relation to the number of hatched adults. NC = negative control (water). Treatment supplemented with 2.5 mL of each secretome or water and 1g of mashed potato. * Statistically significant difference ($P \leq 0.05$) according to the Chi-square test for independent sample ratios.

Figure 2. Effect of bacterial secretomes isolated from stingless bees' larval food on the rough eye phenotype on amyloid-induced neurodegeneration model fly. (A1-A10) Optical microscopy (5x magnification): (NC) transgenic flies treated with water, (A3-A10) *GMR-GAL4 > UAS-BACE1*, *UAS-APP* transgenic flies treated with secretomes. Scanning Electron Micrograph (300x, 550x, and 1230x magnifications): the images show in details the ocular structure with organized omatids and regular sizes.

NC presented deformed eyes with altered ocular morphology, rough surface and irregular edges and fusions and/or absence of omatids. Transgenic flies treated with S7, S12, S14, S20, S45 and S54 secretomes showed slight improvement in the morphology of the eye, but retained the rough appearance on the ocular surface and exhibited reduced or no bristles in the omatids. Transgenic flies treated with S9 and S27 secretomes had their ocular morphological defects considerably suppressed, presenting eyes with smooth surface, slight differences in the size of omatids (without fusion between them) and presence of a large number of bristles, characterizing the positive effect of these secretomes in the amyloid-induced neurodegeneration model fly.

Figure 3. Effect of bacterial secretomes isolated from stingless bees' larval food on the histology of the eye of amyloid-induced neurodegeneration model fly. (A) Control: *Canton S* wild flies and (B) Control: w^{1118} mutant flies, both presenting normal eyes. (C) Negative control: *GMR-GAL4 > UAS-BACE1, UAS-APP* treated with water, with irregular ocular surface. *GMR-GAL4 > UAS-BACE1, UAS-APP* transgenic flies treated with S9 (D) and S27 (E) secretomes, which showed the best effect on eye phenotype when analyzed by stereomicroscope and electron microscopy. (F) *GMR-GAL 4 > UAS-BACE1, UAS-APP* flies treated with S14 secretome, which showed no recovery of rough phenotype by stereomicroscope and SEM analyzes. The histological sections were examined in 40x magnification.

Figure 4. Three-dimensional analysis of the AEGAVPMTCPRGK and TPPITYFLK peptides and their interaction with the BACE1 and β-amyloid target sites. A. 3D Image of the interaction between the peptide AEGAVPMTCPRGK with the active sites of BACE1. **B.** Zoom of the image A, showing 3D molecular interactions of the peptide AEGAVPMTCPRGK with the active sites of BACE1. **C.** 3D Image (Cartoon type) of the interaction between TPPITYFLK and β-amyloid plaque. **D.** 3D Image (Surface type) of the interaction between TPPITYFLK and β-amyloid plaque.

Figure S1. Venn diagram representing the proteins identified in the S9 (blue circle) and S27 (yellow circle) secretomes, according to the peptides found.

Tables:

Table 1.

Stingless bee larval food		
Bacteria (colony)	**Culture medium**	**Specie**
7	MacConkey	*Melipona quadrifasciata*
9	MRS	*Melipona quadrifasciata*
12	TSA	*Melipona quadrifasciata*
14	TSA	*Tetragonisca angustula*
20	BHI	*Melipona quadrifasciata*
27	Oatmeal	*Melipona quadrifasciata*
45	Nutrient	*Tetragonisca angustula*
54	Nutrient	*Melipona quadrifasciata*

Bee species whose larval food was collected, isolated colonies and culture medium for isolation.

Table 2. List of peptides identified in both secretomas (S9 and S27) and the respective proteins that are derived.

S9 - S27	Function	Organism	Sequence	Spectrum Intensity	Database Accession
UPF0421 protein SSP0904	Multi-pass membrane protein; integral component of membrane	*Staphylococcus saprophyticus subsp. saprophyticus (strain ATCC 15305 / DSM 20229 / NCIMB 8711 / NCTC 7292 / S-41)*	(K)VETLLSYQK(D); (K)VETLLSYQK(D); (K)VETLLSYQK(D)	7.74e+005 3.96e+005 2.28e+005	Q49YT4
tRNA-2-methylthio-N(6)-dimethylallyladenosine synthase	Catalyzes the methylthiolation of N6-(dimethylallyl)adenosine (i_6A), leading to the formation of 2-methylthio-N6-(dimethylallyl)adenosine (ms_2i_6A) at position 37 in tRNAs that read codons beginning with uridine.	*Protochlamydia amoebophila (strain UWE25)*	(K)ELMEAIR(D)	6.19e+005	Q6MAB7
Leucine--tRNA ligase	x	*Acholeplasma laidlawii (strain PG-8A); Saccharopolyspora erythraea (strain ATCC 11635 / DSM 40517 / JCM 4748 / NBRC 13426 / NCIMB 8594 / NRRL 2338)*	(K)SKTGVFTGAFAK(H); (R)IVVPASAGQDEVK(A); (K)SKTGVFTGAFAK(H;) (K)SKTGVFTGAFAK(H)	9.58e+005 1.20e+004 3.34e+005 2.21e+005	A9NET8; A4FR54
UvrABC system protein A	The UvrABC repair system catalyzes the recognition and processing of DNA lesions. UvrA is an ATPase and a DNA-binding protein. A damage recognition complex composed of 2 UvrA and 2 UvrB subunits scans DNA for abnormalities. When the presence of a lesion has been verified by UvrB, the UvrA molecules dissociate (By similarity)	*Chlamydia pneumoniae (Chlamydophila pneumoniae)*	(K)NLTYKVWR(G); (R)TVFENTIEAK(A); (K)NLTYKVWR(G)	1.23e+006 6.07e+005 2.36e+005	Q9Z985
4-hydroxy-3-methylbut-2-enyl diphosphate reductase	Catalyzes the conversion of 1-hydroxy-2-methyl-2-(E)-butenyl 4-diphosphate (HMBPP) into a mixture of isopentenyl diphosphate (IPP) and dimethylallyl diphosphate (DMAPP). Acts in the terminal step of the DOXP/MEP pathway for isoprenoid precursor biosynthesis.	*Acidothermus cellulolyticus (strain ATCC 43068 / 11B); Bacillus halodurans (strain ATCC BAA-125 / DSM 18197 / FERM 7344 / JCM 9153 / C-125)*	(K)ALELYGPPVYVRK(Q); (R)QEAVAEQAR(E)	2.82e+005 1.67e+006	A0LW20
Beta-hexosaminidase	Plays a role in peptidoglycan recycling by cleaving the terminal beta-1,4-linked N-acetylglucosamine (GlcNAc) from peptide-linked peptidoglycan fragments, giving rise to free GlcNAc, anhydro-N-acetylmuramic acid and anhydro-N-acetylmuramic acid-linked peptides.	*Neisseria meningitidis serogroup C / serotype 2a (strain ATCC 700532 / DSM 15464 / FAM18); Neisseria meningitidis serogroup C (strain 053442); Neisseria gonorrhoeae (strain NCCP11945); Neisseria meningitidis serogroup A / serotype 4A (strain DSM 15465 / Z2491); Neisseria meningitidis serogroup B (strain MC58)*	(R)LTEEEK(Q)	9.02e+004	A1KSD9; A9M1Z4; B4RQ67; Q5FA94; Q9JVT3; Q9K0Q4
Protein translocase subunit SecA	Part of the Sec protein translocase complex. Interacts with the SecYEG preprotein conducting channel. Has a central role in coupling the hydrolysis of ATP to the transfer of proteins into and across the cell membrane, serving as an ATP-driven molecular motor driving the stepwise translocation of polypeptide chains across the membrane.	*Aquifex aeolicus (strain VF5)*	(R)LTEEEK(Q)	9.02e+004	O67718
4-hydroxy-3-methylbut-2-en-1-yl diphosphate synthase (flavodoxin)	Converts 2C-methyl-D-erythritol 2,4-cyclodiphosphate (ME-2,4cPP) into 1-hydroxy-2-methyl-2-(E)-butenyl 4-diphosphate.	*Treponema denticola (strain ATCC 35405 / CIP 103919 / DSM 14222)*	(R)LTEEEK(Q)	9.02e+004	Q73N90
Porphobilinogen deaminase	Tetrapolymerization of the monopyrrole PBG into the hydroxymethylbilane pre-uroporphyrinogen in several discrete steps.	*Sulfurimonas denitrificans (strain ATCC 33889 / DSM 1251) (Thiomicrospira denitrificans (strain ATCC 33889 / DSM 1251))*	(R)IETTIER(S)	6.19e+005	Q30S90
Homoserine kinase	Catalyzes the ATP-dependent phosphorylation of L-homoserine to L-homoserine phosphate.	*Bacillus cereus (strain ATCC 10987 / NRS 248)*	(K)EERIEL(-)	1.71e+005 1.01e+005	Q48QX8
UPF0298 protein YdgE	Citoplasmatic protein, homoserine quinase	*Lactococcus lactis subsp. lactis (strain IL1403) (Streptococcus lactis)*	(K)EERIEL(-)	1.71e+005 1.01e+005	Q739T5; Q9CIJ9
Protein RnfH	x	*Pseudomonas fluorescens (strain Pf0-1)*	(K)VIADPDAR(R)	7.11e+005	Q3KIA5
50S ribosomal protein L29	Ribonucleoprotein, Ribosomal protein	*Trichodesmium erythraeum (strain IMS101)*	(-)MPFPK(I)	2.56e+005	Q110B5
Uncharacterized protein YjaZ	x	*Bacillus subtilis (strain 168)*	(R)LEFGSKSGLAFQDK(M)	1.37e+005	O31596

Gamma-glutamyl phosphate reductase	Catalyzes the NADPH-dependent reduction of L-glutamate 5-phosphate into L-glutamate 5-semialdehyde and phosphate. The product spontaneously undergoes cyclization to form 1-pyrroline-5-carboxylate.	*Neisseria meningitidis serogroup B (strain MC58)*	(R)IEAGLPPIR(F)	8.55e+005	Q9JZG3
4-diphosphocytidyl-2-C-methyl-D-erythritol kinase	Catalyzes the phosphorylation of the position 2 hydroxy group of 4-diphosphocytidyl-2C-methyl-D-erythritol.	*Desulfotalea psychrophila (strain LSv54 / DSM 12343)*	(R)AALAYLARSSRVGQR(G)	7.74e+005	Q6AJL6
Exodeoxyribonuclease 7 large subunit	Bidirectionally degrades single-stranded DNA into large acid-insoluble oligonucleotides, which are then degraded further into small acid-soluble oligonucleotides. 2) Bidirectionally degrades single-stranded DNA into large acid-insoluble oligonucleotides, which are then degraded further into small acid-soluble oligonucleotides.	*Lactobacillus reuteri (strain DSM 20016); Lactobacillus reuteri (strain JCM 1112)*	(R)LTAASPLHR(V)	1.63e+006	A5VKR6; B2G849
Transcriptional regulator ZurR	Probably required for the zinc-specific repression of the operon zuRMA implicated in zinc uptake.	*Listeria monocytogenes serovar 1/2a (strain ATCC BAA-679 / EGD-e)*	(R)KNKYLTAK(D)	1.66e+006	P0A3E6
Trigger factor	Involved in protein export. Acts as a chaperone by maintaining the newly synthesized protein in an open conformation. Functions as a peptidyl-prolyl cis-trans isomerase	*Nitrosococcus oceani (strain ATCC 19707 / BCRC 17464 / NCIMB 11848 / C-107)*	(K)VISVTAPR(L)	6.98e+005	Q3JAJ7
50S ribosomal protein L11	Forms part of the ribosomal stalk which helps the ribosome interact with GTP-bound translation factors.	*Rhodospirillum centenum (strain ATCC 51521 / SW)*	(K)TPPITYFLK(K)	4.21e+006	B6IRP2
Shikimate dehydrogenase (NADP(+))	Involved in the biosynthesis of the chorismate, which leads to the biosynthesis of aromatic amino acids. Catalyzes the reversible NADPH linked reduction of 3-dehydroshikimate (DHSA) to yield shikimate (SA).	*Pelagibacter ubique (strain HTCC1062)*	(K)NAKKYGGITK(N)	1.74e+006	Q4FNS5
DNA-directed RNA polymerase subunit beta'	DNA-dependent RNA polymerase catalyzes the transcription of DNA into RNA using the four ribonucleoside triphosphates as substrates.	*Sorangium cellulosum (strain So ce56) (Polyangium cellulosum (strain So ce56); Ehrlichia ruminantium (strain Gardel)*	(R)GYVNTIKSAK(K); (R)LYVNDGQLVKITEK(I)	2.48e+005 2.97e+005	A9GRB4; Q5HC04
Thiazole synthase	Catalyzes the rearrangement of 1-deoxy-D-xylulose 5-phosphate (DXP) to produce the thiazole phosphate moiety of thiamine. Sulfur is provided by the thiocarboxylate moiety of the carrier protein ThiS. In vitro, sulfur can be provided by H_2S.	*Psychrobacter cryohalolentis (strain ATCC BAA-1226 / DSM 17306 / VKM B-2378 / K5)*	(R)ELLGGHNLVK(L)	9.67e+005	Q1QE71; Q4FV61
Probable cadmium-transporting ATPase	Couples the hydrolysis of ATP with the export of cadmium.	*Listeria monocytogenes serovar 1/2a (strain ATCC BAA-679 / EGD-e)*	(K)LPFIVNLSRK(T)	5.73e+004	P58414
Tryptophan synthase alpha chain	The alpha subunit is responsible for the aldol cleavage of indoleglycerol phosphate to indole and glyceraldehyde 3-phosphate.	*Thermotoga maritima (strain ATCC 43589 / MSB8 / DSM 3109 / JCM 10099)*	(R)IMEENPK(D)	7.27e+004	P50908
5'-nucleotidase SurE	Nucleotidase that shows phosphatase activity on nucleoside 5'-monophosphates.	*Marinobacter hydrocarbonoclasticus (strain ATCC 700491 / DSM 11845 / VT8)*	(R)AEGAVPMTCPRGK(Q)	4.11e+004	A1TZ53
Phenylalanine--tRNA ligase beta subunit	x	*Dehalococcoides mccartyi (strain CBDB1)*	(R)TSLRPSLYASLAANR(R)	8.87e+004 3.59e+005 3.80e+005	Q3ZZD2
50S ribosomal protein L3	One of the primary rRNA binding proteins, it binds directly near the 3'-end of the 23S rRNA, where it nucleates assembly of the 50S subunit.	*Rhodobacter sphaeroides (strain ATCC 17023 / 2.4.1 / NCIB 8253 / DSM 158)*	(R)VSAAQRGHFAK(A)	2.54e+005	Q3J5S2
Maltodextrin transport system permease protein MdxG	Part of the ABC transporter complex involved in maltodextrin import. Probably responsible for the translocation of the substrate across the membrane (Probable).	*Bacillus subtilis (strain 168)*	(K)NFVSGLTAGGTK(G)	2.36e+005	O06991
Oxalate decarboxylase OxdD	Converts oxalate to formate and CO_2.	*Bacillus subtilis (strain 168)*	(K)LDHGGWSR(E)	8.59e+004	O34767
Recombination protein RecR	May play a role in DNA repair. It seems to be involved in an RecBC-independent recombinational process of DNA repair. It may act with RecF and RecO.	*Anaplasma marginale (strain St. Maries)*	(R)AALSSRYVIT(-)	1.51e+005	Q5PB75

3-methyl-2-oxobutanoate hydroxymethyltransferase	Catalyzes the reversible reaction in which hydroxymethyl group from 5,10-methylenetetrahydrofolate is transferred onto alpha-ketoisovalerate to form ketopantoate.	*Bacillus velezensis (strain DSM 23117 / BGSC 10A6 / FZB42) (Bacillus amyloliquefaciens subsp. plantarum)*	(R)VFPEEK(H)	9.02e+004	A7Z5Z4
Monomeric sarcosine oxidase	Catalyzes the oxidative demethylation of sarcosine.	*Streptomyces sp. (strain KB210-8SY)*	(R)LTAPAARGVQP(-)	1.23e+005	P40854
50S ribosomal protein L4	One of the primary rRNA binding proteins, this protein initially binds near the 5'-end of the 23S rRNA. It is important during the early stages of 50S assembly. It makes multiple contacts with different domains of the 23S rRNA in the assembled 50S subunit and ribosome.	*Nocardia farcinica (strain IFM 10152)*	(K)FLVVVGREDVTAWK(S)	4.15e+005	Q5Z1W2
Transcription antitermination protein NusB	Involved in transcription antitermination. Required for transcription of ribosomal RNA (rRNA) genes. Binds specifically to the boxA antiterminator sequence of the ribosomal RNA (rrn) operons.	*Arcobacter butzleri (strain RM4018)*	(R)LASDGAPK(F)	2.78e+005	A8EVW4
Diaminopimelate epimerase	Catalyzes the stereoinversion of LL-2,6-diaminoheptanedioate (L,L-DAP) to meso-diaminoheptanedioate (meso-DAP), a precursor of L-lysine and an essential component of the bacterial peptidoglycan.	*Xanthomonas axonopodis pv. citri (strain 306)*	(R)FIIDSPATAHAVER(L)	1.34e+005	Q8PPQ1
ECF RNA polymerase sigma-E factor	Sigma factors are initiation factors that promote the attachment of RNA polymerase (RNAP) to specific initiation sites and are then released. Extracytoplasmic function (ECF) sigma-E controls the envelope stress response, responding to periplasmic protein stress, increased levels of periplasmic lipopolysaccharide (LPS) as well as heat shock and oxidative stress; it controls protein processing in the extracytoplasmic compartment (By similarity).	*Haemophilus influenzae (strain ATCC 51907 / DSM 11121 / KW20 / Rd)*	(R)IAVNTAKNYLTAQGR(R)	8.87e+004	P44790
Phosphoglucomutase	Catalyzes the interconversion between glucose-6-phosphate and alpha-glucose-1-phosphate. This is the first step in the biosynthesis of diglucosyl-diacylglycerol (Glc2-DAG), i.e. the predominant glycolipid found in B.subtilis membrane, which is also used as a membrane anchor for lipoteichoic acid (LTA). Has a role in the biosynthesis of all phosphate-containing envelope polymers, since glucose-1-phosphate is the precursor of UDP-glucose, which serves as a glucosyl donor not only for the biosynthesis of LTA but also for wall teichoic acids (WTAs). Is required for biofilm formation. This is likely due to another role of UDP-glucose, which might also act as a metabolic signal regulating biofilm formation or may be involved in some unknown biosynthetic pathway essential for biofilm formation, e.g. the synthesis of an exopolysaccharide.	*Bacillus subtilis (strain 168)*	(R)KASAGFAAYISK(Q)	3.87e+005	P18159
Methylthioribose-1-phosphate isomerase	Catalyzes the interconversion of methylthioribose-1-phosphate (MTR-1-P) into methylthioribulose-1-phosphate (MTRu-1-P)	*Exiguobacterium sibiricum (strain DSM 17290 / CIP 109462 / JCM 13490 / 255-15)*	(K)ALELYQTDAK(T)	6.75e+005	B1YIY4
Bifunctional enzyme IspD/IspF	Bifunctional enzyme that catalyzes the formation of 4-diphosphocytidyl-2-C-methyl-D-erythritol from CTP and 2-C-methyl-D-erythritol 4-phosphate (MEP) (IspD), and catalyzes the conversion of 4-diphosphocytidyl-2-C-methyl-D-erythritol 2-phosphate (CDP-ME2P) to 2-C-methyl-D-erythritol 2,4-cyclodiphosphate (ME-CPP) with a corresponding release of cytidine 5-monophosphate (CMP) (IspF).	*Wolbachia sp. subsp. Brugia malayi (strain TRS)*	(R)VDTKLLSPVYGGKSR(Q)	8.02e+004	Q5GSM7
DNA polymerase III PolC-type	Required for replicative DNA synthesis. This DNA polymerase also exhibits 3' to 5' exonuclease activity	*Lactobacillus paracasei (strain ATCC 334 / BCRC 17002 / CIP 107868 / KCTC 3260 / NRRL B-441)*	(K)LDTLAKQYK(V)	6.44e+005	Q038M0
Serine hydroxymethyltransferase	Catalyzes the reversible interconversion of serine and glycine with tetrahydrofolate (THF) serving as the one-carbon carrier. This reaction serves as the major source of one-carbon groups required for the biosynthesis of purines, thymidylate, methionine, and other important biomolecules. Also exhibits THF-independent aldolase activity toward beta-hydroxyamino acids, producing glycine and aldehydes, via a retro-aldol mechanism.	*Natranaerobius thermophilus (strain ATCC BAA-1301 / DSM 18059 / JW/NM-WN-LF); Geobacter uraniireducens (strain Rf4) (Geobacter uraniumreducens)*	(R)ELAKEHKPK(M); (R)ELAKEHKPK(M); (R)LTLEHKPK(M)	5.43e+006 2.77e+005 2.43e+005	B2A3H6; A5GF66
Biphenyl dioxygenase subunit alpha	x	*Pseudomonas furukawaii; Pseudomonas sp. (strain KKS102)*	(K)KEGDCGFDK(A)	1.16e+005	Q52028; Q52438

Phosphoglycerate kinase	This protein is involved in step 2 of the subpathway that synthesizes pyruvate from D-glyceraldehyde 3-phosphate. This subpathway is part of the pathway glycolysis, which is itself part of Carbohydrate degradation.	*Borrelia burgdorferi (strain ZS7)*	(K)KNSKYSLKPVANR(L)	2.99e+005	B7J0Z2
Glycine--tRNA ligase beta subunit	x	*Ruegeria sp. (strain TM1040) (Silicibacter sp.), Bacillus halodurans (strain ATCC BAA-125 / DSM 18197 / FERM 7344 / JCM 9153 / C-125)*	(K)TGRIEKFITVANR(E); (R)VLYEAYVQTK(D)	2.55e+005; 4.79e+005	Q1GE74; Q9KD48
D-alanine--D-alanine ligase	Cell wall formation.	*Streptococcus pneumoniae serotype 19F (strain G54); Streptococcus pneumoniae (strain ATCC 700669 / Spain 23F-1); Streptococcus pneumoniae (strain JJA); Streptococcus pneumoniae (strain Taiwan19F-14); Streptococcus pneumoniae serotype 4 (strain ATCC BAA-334 / TIGR4); Synechococcus sp. (strain CC9605); Streptococcus pneumoniae (strain ATCC BAA-255 / R6)*	(R)VLVEQGVNAR(E)	2.38e+005	B5E721; B8ZM66; C1CFP2; C1CST6; P0CB57; Q3ALB5; Q8DNV5
Outer-membrane lipoprotein LolB	Plays a critical role in the incorporation of lipoproteins in the outer membrane after they are released by the LolA protein.	*Shewanella sediminis (strain HAW-EB3)*	(K)VYQDKDAQR(L)	2.69e+005	A8FYZ2
Probable GTP-binding protein EngB	Necessary for normal cell division and for the maintenance of normal septation.	*Thermotoga neapolitana (strain ATCC 49049 / DSM 4359 / NS-E); Thermotoga maritima (strain ATCC 43589 / MSB8 / DSM 3109 / JCM 10099)*	(R)SNVGKSSLLNALFNR(K)	2.70e+004	B9K8C0; Q9X1H7
Valine--tRNA ligase	Catalyzes the attachment of valine to tRNA(Val). As ValRS can inadvertently accommodate and process structurally similar amino acids such as threonine, to avoid such errors, it has a 'posttransfer' editing activity that hydrolyzes mischarged Thr-tRNA(Val) in a tRNA-dependent manner.	*Streptococcus thermophilus (strain CNRZ 1066); Streptococcus thermophilus (strain ATCC BAA-250 / LMG 18311)*	(K)NVLIHGLIRDEQGR(K)	6.35e+004	Q5M111; Q5M5J8
50S ribosomal protein L5	This is 1 of the proteins that binds and probably mediates the attachment of the 5S RNA into the large ribosomal subunit, where it forms part of the central protuberance. In the 70S ribosome it contacts protein S13 of the 30S subunit (bridge B1b), connecting the 2 subunits; this bridge is implicated in subunit movement. Contacts the P site tRNA; the 5S rRNA and some of its associated proteins might help stabilize positioning of ribosome-bound tRNAs.	*Pseudomonas putida (strain ATCC 700007 / DSM 6899 / BCRC 17059 / F1); Pseudomonas putida (strain GB-1); Pseudomonas aeruginosa (strain LESB58); Pseudomonas fluorescens (strain SBW25); Pseudomonas aeruginosa (strain UCBPP-PA14); Pseudomonas entomophila (strain L48); Pseudomonas savastanoi pv. phaseolicola (strain 1448A / Race 6) (Pseudomonas syringae pv. phaseolicola (strain 1448A / Race 6)); Pseudomonas fluorescens (strain ATCC BAA-477 / NRRL B-23932 / Pf-5); Pseudomonas syringae pv. syringae (strain B728a); Pseudomonas syringae pv. tomato (strain ATCC BAA-871 / DC3000); Pseudomonas aeruginosa (strain ATCC 15692 / DSM 22644 / CIP 104116 / JCM 14847 / LMG 12228 / 1C / PRS 101 / PAO1)*	(R)AFKFPFRN(-)	1.13e+005	A5VXQ9; B0KK79; B7V656; C3K2W4; Q02T68; Q1IFV4; Q48D48; Q4K545; Q4ZMQ6; Q889V9; Q9HWE7
30S ribosomal protein S18	Binds as a heterodimer with protein S6 to the central domain of the 16S rRNA, where it helps stabilize the platform of the 30S subunit.	*Gramella forsetii (strain KT0803)*	(R)YLTPLNIETTKAKK(Y)	8.87e+004 3.57e+005	A0M0D8
Methionine--tRNA ligase	Is required not only for elongation of protein synthesis but also for the initiation of all mRNA translation through initiator tRNA(fMet) aminoacylation.	*Enterobacter sp. (strain 638); Salmonella arizonae (strain ATCC BAA-731 / CDC346-86 / RSK2980); Salmonella heidelberg (strain SL476); Salmonella schwarzengrund (strain CVM19633); Salmonella paratyphi A (strain AKU_12601); Salmonella agona (strain SL483); Salmonella dublin (strain CT_02021853); Salmonella enteritidis PT4 (strain P125109); Salmonella gallinarum (strain 287/91 / NCTC 13346); Salmonella paratyphi C (strain RKS4594); Salmonella choleraesuis (strain SC-B67); Salmonella paratyphi A (strain ATCC 9150 / SARB42); Salmonella typhi; Salmonella typhimurium (strain LT2 / SGSC1412 / ATCC 700720)*	(R)QTVMVANLAPR(K)	3.10e+005	A4WCF6; A9MKV0; B4T9X0; B4TNL2; B5BE81; B5EXZ5; B5FMX1; B5R0E7; B5RBZ5; C0Q0Y1; Q57MI5; Q5PJ43; Q8Z5C3; Q8ZNN4
Isoleucine--tRNA ligase	Catalyzes the attachment of isoleucine to tRNA(Ile). As IleRS can inadvertently accommodate and process structurally similar amino acids such as valine, to avoid such errors it has two additional distinct tRNA(Ile)-dependent editing activities. One activity is designated as 'pretransfer' editing and involves the hydrolysis of activated Val-AMP. The other activity is designated 'posttransfer' editing and involves deacylation of mischarged Val-tRNA(Ile).	*Cupriavidus taiwanensis (strain DSM 17343 / BCRC 17206 / CIP 107171 / LMG 19424 / R1) (Ralstonia taiwanensis (strain LMG 19424)); Cupriavidus necator (strain ATCC 17699 / H16 / DSM 428 / Stanier 337) (Ralstonia eutropha);Cupriavidus metallidurans (strain ATCC 43123 / DSM 2839 / NBRC 102507 / CH34) (Ralstonia metalliduran)*	(K)VLKDMIIKAR(G)	9.25e+004	B3R6E8; Q0K7A0

Selenocysteine-specific elongation factor	Translation factor necessary for the incorporation of selenocysteine into proteins. It probably replaces EF-Tu for the insertion of selenocysteine directed by the UGA codon. SelB binds GTP and GDP.	*Escherichia coli (strain K12)*	x	x	P14081
Ribonuclease PH	Phosphorolytic 3'-5' exoribonuclease that plays an important role in tRNA 3'-end maturation. Removes nucleotide residues following the 3'-CCA terminus of tRNAs; can also add nucleotides to the ends of RNA molecules by using nucleoside diphosphates as substrates, but this may not be physiologically important. Probably plays a role in initiation of 16S rRNA degradation (leading to ribosome degradation) during starvation.	*Synechococcus sp. (strain WH8102)*	(R)SQGVLTQDPIR(Q)	4.79e+005	Q7U9I1

Table 3.

Peptide	Rank	Docking (Kcal/mol)			
		β-secretase (BACE)		β-Amyloid	
		Global energy	ACE	Global energy	ACE
AEGAVPMTCPRGK	0.64	-42.88	-10.66	-59.66	-14.98
TPPITYFLK	0.64	-13.15	-0.92	-63.10	-20.30
SNVGKSSLLNALFNR	0.57	-19.48	-1.65	-70.89	-13.62
IEAGLPPIR	0.53	-26.55	-0.51	-54.04	-14.37

Table 4.

Peptide Sequence	Toxicity	Net charge at pH 7	pI	Water Solubility	Molecular weight (g/mol)
AEGAVPMTCPRGK	Non-Toxic	0.9	8.57	High	1316.73
TPPITYFLK	Non-Toxic	1.00	8.94	Low	1079.43

* pI = isoelectric point.

Table S1. List of peptides identified exclusively in the S9 secretome and the respective proteins that are derived.

S9	Function	Organism	Peptide	Spectrum Intensity	Database Accession
30S ribosomal protein S21	Structural constituent of ribosome.	*Nitratiruptor sp. (strain SB155-2)*	(K)QVDRNLIVTEARAR(R)	2.36e+004	A6Q194
Probable cytosol aminopeptidase	Presumably involved in the processing and regular turnover of intracellular proteins. Catalyzes the removal of unsubstituted N-terminal amino acids from various peptides.	*Rhizobium leguminosarum bv. trifolii (strain WSM2304)*	(K)AGGTAAAR(I)	1.45e+005	B5ZWY7
Putative cytochrome P450 135A1	x	*Mycobacterium tuberculosis (strain CDC 1551 / Oshkosh); Mycobacterium tuberculosis (strain ATCC 25618 / H37Rv)*	(R)LGGLGDSDPP(-); (R)LGGLGDSDPP(-)	6.55e+004; 7.09e+004	P9WPN0; P9WPN1
Argininosuccinate synthase	x	*Rhodopseudomonas palustris (strain TIE-1); Rhodopseudomonas palustris (strain ATCC BAA-98 / CGA009)*	(R)INGMKLGRLLYQGR(W)	4.21e+005	B3Q9D3; Q6NCS7
Lipid-A-disaccharide synthase 2	Condensation of UDP-2,3-diacylglucosamine and 2,3-diacylglucosamine-1-phosphate to form lipid A disaccharide, a precursor of lipid A, a phosphorylated glycolipid that anchors the lipopolysaccharide to the outer membrane of the cell.	*Legionella pneumophila (strain Lens)*	(R)YSHLKIQIIQGNAR(E)	2.36e+004	Q5WSK6
Lipoyl synthase	Catalyzes the radical-mediated insertion of two sulfur atoms into the C-6 and C-8 positions of the octanoyl moiety bound to the lipoyl domains of lipoate-dependent enzymes, thereby converting the octanoylated domains into lipoylated derivatives.	*Pseudoalteromonas atlantica (strain T6c / ATCC BAA-1087)*	(K)SGLMMGMGENK(E); (K)SGLMMGMGENK(E)	4.61e+005; 7.75e+005	Q15VL3
30S ribosomal protein S17	One of the primary rRNA binding proteins, it binds specifically to the 5'-end of 16S ribosomal RNA.	*Pelobacter carbinolicus (strain DSM 2380 / NBRC 103641 / GraBd1)*	(K)MDKTVVVKVDQMVK(H); (K)MDKTVVVKVDQMVK(H)	3.35e+005; 2.02e+005	Q3A6N8
UPF0346 protein lwe1876	x	*Listeria welshimeri serovar 6b (strain ATCC 35897 / DSM 20650 / CIP 8149 / NCTC 11857 / SLCC 5334 / V8)*	(R)DHSFPK(Q)	3.29e+005	A0AJW2
UPF0346 protein LMHCC_0699	x	*Listeria monocytogenes serotype 4a (strain HCC23)*	(R)DHSFPK(Q)	3.29e+005	B8DDP5
UPF0346 protein Lm4b_01873	x	*Listeria monocytogenes serotype 4b (strain CLIP80459)*	(R)DHSFPK(Q)	3.29e+005	C1KWF6
UPF0346 protein LMOf2365_1885	x	*Listeria monocytogenes serotype 4b (strain F2365)*	(R)DHSFPK(Q)	3.29e+005	Q71YF9
UPF0346 protein lmo1857	x	*Listeria monocytogenes serovar 1/2a (strain ATCC BAA-679 / EGD-e)*	(R)DHSFPK(Q)	3.29e+005	Q8Y643
UPF0346 protein lin1971	x	*Listeria innocua serovar 6a (strain ATCC BAA-680 / CLIP 11262)*	(R)DHSFPK(Q)	3.29e+005	Q92AF1
Tryptophanase	x	*Aeromonas hydrophila subsp. hydrophila (strain ATCC 7966 / DSM 30187 / JCM 1027 / KCTC 2358 / NCIMB 9240); Yersinia enterocolitica serotype O:8 / biotype 1B (strain NCTC 13174 / 8081); Desulfovibrio vulgaris subsp. vulgaris (strain DP4); Aeromonas salmonicida (strain A449); Citrobacter koseri (strain ATCC BAA-895 / CDC 4225-83 / SGSC4696); Shewanella sediminis (strain HAW-EB3); Klebsiella aerogenes (Enterobacter aerogenes); Desulfovibrio vulgaris (strain Hildenborough / ATCC 29579 / DSM 644 / NCIMB 8303); Photorhabdus laumondii subsp. laumondii (strain DSM 15139 / CIP 105565 / TT01); Chromobacterium violaceum (strain ATCC 12472 / DSM 30191 / JCM 1249 / NBRC 12614 / NCIMB 9131 / NCTC 9757); Vibrio parahaemolyticus serotype O3:K6 (strain RIMD 2210633)*	(R)IPEPFR(I)	1.11e+006	A0KJP3; A1JJH3; A1VC86; A4SNA7; A8AKE2; A8G097; Q59342; Q729Z3; Q7N8C9; Q7NYV9; Q87JQ6

Transposase InsG for insertion sequence element IS4	Involved in the transposition of the insertion sequence IS4.	*Escherichia coli (strain K12)*	(R)IPEPFR(I)	1.11e+006	P03835
Proline-rich antimicrobial peptide 2	Antimicrobial protein. Has antibacterial activity against the Gram-positive bacterium M.luteus (MIC=8.6 µM). Lacks antibacterial activity against the Gram-positive bacteria B.circulans, L.monocytogenes, S.aureus, and S.lutea, and the Gram-negative bacteria E.coli D31, E.coli ATCC 25922, and S.typhimurium. Lacks antifungal activity against S.cerevisiae, P.pastoris, Z.marxianus, C.albicans, C.fructus, C.wickerhamii, A.niger, F.oxysporum, and T.harizianum.	*Galleria mellonella (Greater wax moth)*	(R)IPEPFR(I)	1.11e+006	P85212
23S rRNA (uracil(1939)-C(5))-methyltransferase RlmD	Catalyzes the formation of 5-methyl-uridine at position 1939 (m5U1939) in 23S rRNA.	*Shewanella sp. (strain W3-18-1); Shewanella baltica (strain OS155 / ATCC BAA-1091); Shewanella putrefaciens (strain CN-32 / ATCC BAA-453); Shewanella baltica (strain OS185); Shewanella baltica (strain OS195); Shewanella baltica (strain OS223)*	(K)ANNLDK(L)	1.36e+005	A1RHE4; A3D7B5; A4Y952; A6WR37; A9KYI1; B8E8S1
UPF0306 protein CKO_04548	x	*Citrobacter koseri (strain ATCC BAA-895 / CDC 4225-83 / SGSC4696)*	(R)MLPAPVWEIR(L)	8.51e+004	A8AQ39
Dihydrofolate synthase/folylpolyglutamate synthase	Functions in two distinct reactions of the de novo folate biosynthetic pathway. Catalyzes the addition of a glutamate residue to dihydropteroate (7,8-dihydropteroate or H2Pte) to form dihydrofolate (7,8-dihydrofolate monoglutamate or H2Pte-Glu). Also catalyzes successive additions of L-glutamate to tetrahydrofolate, leading to folylpolyglutamate derivatives.	*Bacillus subtilis (strain 168)*	(R)AFHVAGTNGK(G)	1.44e+006	Q05865
Medium/long-chain-fatty-acid--[acyl-carrier-protein] ligase MbtM	Activates lipidic moieties required for mycobactin biosynthesis (PubMed:23935107). Converts medium- to long-chain aliphatic fatty acids into acyl adenylate, which is further transferred on to the phosphopantetheine arm of the carrier protein MbtL (PubMed:23935107). Shows a strong preference for palmitic acid (C16) and cannot use short-chain fatty acids (PubMed:23935107). Proceeds via a Bi Uni Uni Bi ping-pong mechanism. During the first half-reaction (adenylation), fatty acid binds first to the free enzyme, followed by ATP and the release of pyrophosphate to form the adenylate intermediate. During the second half-reaction (ligation), holo-MbtL binds to the enzyme followed by the release of products AMP and acylated MbtL (PubMed:23935107).	*Mycolicibacterium smegmatis (strain ATCC 700084 / mc(2)155) (Mycobacterium smegmatis)*	(R)VASECGVVPADVVFLAPGSLPR TSSGK(L)	1.99e+005	A0QUA1
Elongation factor G	Catalyzes the GTP-dependent ribosomal translocation step during translation elongation. During this step, the ribosome changes from the pre-translocational (PRE) to the post-translocational (POST) state as the newly formed A-site-bound peptidyl-tRNA and P-site-bound deacylated tRNA move to the P and E sites, respectively. Catalyzes the coordinated movement of the two tRNA molecules, the mRNA and conformational changes in the ribosome.	*Wolbachia pipientis subsp. Culex pipiens (strain wPip); Wolbachia sp. subsp. Drosophila simulans (strain wRi); Wolbachia pipientis wMel*	(K)MLEPIMK(V)	1.06e+006	B3CLA3; C0R543; Q73IX7
Ribose import ATP-binding protein RbsA	Part of the ABC transporter complex RbsABC involved in ribose import. Responsible for energy coupling to the transport system.	*Lactococcus lactis subsp. lactis (strain IL1403) (Streptococcus lactis)*	(K)MVGRSITDYYPPK(N)	2.58e+005	Q9CF44

Outer membrane transporter CdiB-2	Potential outer membrane protein component of a toxin-immunity protein module, which functions as a cellular contact-dependent growth inhibition (CDI) system. CDI modules allow bacteria to communicate with and inhibit the growth of closely related neighboring bacteria in a contact-dependent fashion. This protein may be required for secretion and assembly of the CdiA toxin protein.	*Burkholderia pseudomallei (strain 1026b)*	(K)GLSQAILARGYITTR(V)	1.77e+005	P0DMJ8
C4-dicarboxylate transport protein	Responsible for the transport of dicarboxylates such as succinate, fumarate, and malate from the periplasm across the membrane.	*Escherichia coli O157:H7 (strain EC4115 / EHEC)*	(K)KLDDALNNRAPDGK(T)	2.50e+005	B5YVH5
Putative S-adenosyl-L-methionine-dependent methyltransferase MAP_3777	Exhibits S-adenosyl-L-methionine-dependent methyltransferase activity.	*Mycolicibacterium paratuberculosis (strain ATCC BAA-968 / K-10) (Mycobacterium paratuberculosis)*	(R)YFDNYFAR(T)	3.14e+005	Q73TE1
Uncharacterized protein BB_0038	x	*Borrelia burgdorferi (strain ATCC 35210 / B31 / CIP 102532 / DSM 4680)*	(R)IDNPNSNVLEVNK(M)	3.80e+004	O51067
Uncharacterized HTH-type transcriptional regulator FruR	DNA binding.	*Bacillus subtilis (strain 168)*	(K)HAYVLADPSK(F)	1.38e+005	O31713
Alanine racemase	Catalyzes the interconversion of L-alanine and D-alanine. May also act on other amino acids.	*Streptococcus pyogenes serotype M4; Streptococcus pyogenes serotype M6 (strain ATCC BAA-946 / MGAS10394); Streptococcus pyogenes serotype M18 (strain MGAS8232)*	(K)QEWPDLKGLK(V)	2.61e+005	Q1J545; Q5XAA4; Q8NZK4
Protoheme IX farnesyltransferase	Converts heme B (protoheme IX) to heme O by substitution of the vinyl group on carbon 2 of heme B porphyrin ring with a hydroxyethyl farnesyl side group.	*Bradyrhizobium sp. (strain ORS 278)*	(R)DRIPSLRANR(K)	6.46e+005	A4Z2D2
PTS system arbutin-, cellobiose-, and salicin-specific EIIBC component	The phosphoenolpyruvate-dependent sugar phosphotransferase system (sugar PTS), a major carbohydrate active -transport system, catalyzes the phosphorylation of incoming sugar substrates concomitantly with their translocation across the cell membrane. This system is involved in arbutin, cellobiose, and salicin transport.	*Escherichia coli (strain K12)*	(R)VFTPTIIQTIAETGK(E)	1.67e+005	P24241
ATP synthase subunit b 1	F_1F_0 ATP synthase produces ATP from ADP in the presence of a proton or sodium gradient. F-type ATPases consist of two structural domains, F_1 containing the extramembraneous catalytic core and F_0 containing the membrane proton channel, linked together by a central stalk and a peripheral stalk. During catalysis, ATP synthesis in the catalytic domain of F_1 is coupled via a rotary mechanism of the central stalk subunits to proton translocation.	*Methylococcus capsulatus (strain ATCC 33009 / NCIMB 11132 / Bath)*	(K)EAAKIEGERILANAR(S)	2.36e+004	Q60CR8
Threonine--tRNA ligase	Catalyzes the attachment of threonine to tRNA(Thr) in a two-step reaction: L-threonine is first activated by ATP to form Thr-AMP and then transferred to the acceptor end of tRNA(Thr). Also edits incorrectly charged L-seryl-tRNA(Thr).	*Clostridium acetobutylicum (strain ATCC 824 / DSM 792 / JCM 1419 / LMG 5710 / VKM B-1787)*	(K)VPYMIVIGDKEIK(E)	3.31e+005	Q97GK4
ATP-dependent helicase/nuclease subunit A	The heterodimer acts as both an ATP-dependent DNA helicase and an ATP-dependent, dual-direction single-stranded exonuclease. Recognizes the chi site generating a DNA molecule suitable for the initiation of homologous recombination. The AddA nuclease domain is required for chi fragment generation; this subunit has the helicase and 3' -> 5' nuclease activities.	*Moorella thermoacetica (strain ATCC 39073 / JCM 9320)*	(R)AGYPENPAAATPAVEVYLQEGK(V)	2.57e+005	Q2RL77

UvrABC system protein C	The UvrABC repair system catalyzes the recognition and processing of DNA lesions. UvrC both incises the 5' and 3' sides of the lesion. The N-terminal half is responsible for the 3' incision and the C-terminal half is responsible for the 5' incision.	*Pseudomonas putida (strain ATCC 700007 / DSM 6899 / BCRC 17059 / F1); Pseudomonas putida (strain W619); Pseudomonas putida (strain ATCC 47054 / DSM 6125 / NCIMB 11950 / KT2440)*	(K)ARRVSSLEDVAGVGPK(R)	4.01e+004	A5W1B2; B1JB85; Q88FJ7
Uracil phosphoribosyltransferase	Catalyzes the conversion of uracil and 5-phospho-alpha-D-ribose 1-diphosphate (PRPP) to UMP and diphosphate.	*Mesoplasma florum (strain ATCC 33453 / NBRC 100688 / NCTC 11704 / L1) (Acholeplasma florum)*	(K)HPLIIDKLSR(M)	1.27e+005	Q6F210
Chaperone protein dnaK1	Acts as a chaperone.	*Thermosynechococcus elongatus (strain BP-1)*	(K)HPLIIDKLSR(M)	1.61e+005	Q8DKR6

Table S2. List of peptides identified exclusively in the S27 secretome and the respective proteins that are derived.

S27	Function	Organism	Sequence	Spectrum Intensity	Database Accession
tRNA 5-methylaminomethyl-2-thiouridine biosynthesis bifunctional protein MnmC	Catalyzes the last two steps in the biosynthesis of 5-methylaminomethyl-2-thiouridine (mnm_5s_2U) at the wobble position (U34) in tRNA. Catalyzes the FAD-dependent demodification of $cmnm_5s_2U34$ to nm_5s_2U34, followed by the transfer of a methyl group from S-adenosyl-L-methionine to nm_5s_2U34, to form mnm_5s_2U34.	*Salmonella choleraesuis (strain SC-B67); Salmonella paratyphi A (strain ATCC 9150 / SARB42)*	(K)TSAAPAPVYPGLFVLGAL GSR(G)	1.89e+005	Q57LX5; Q5PCW7
Aspartate 1-decarboxylase	Catalyzes the pyruvoyl-dependent decarboxylation of aspartate to produce beta-alanine.	*Campylobacter curvus (strain 525.92); Wolinella succinogenes (strain ATCC 29543 / DSM 1740 / LMG 7466 / NCTC 11488 / FDC 602W) (Vibrio succinogenes)*	(K)VEILDVNNGER(F)	5.10e+004	A7H0Y2; O34246
Phosphopantetheine adenylyltransferase	Reversibly transfers an adenylyl group from ATP to 4'-phosphopantetheine, yielding dephospho-CoA (dPCoA) and pyrophosphate.	*Streptococcus agalactiae serotype Ia (strain ATCC 27591 / A909 / CDC SS700); Streptococcus agalactiae serotype V (strain ATCC BAA-611 / 2603 V/R)*	(K)MLEEAIR(Q)	7.59e+004	Q3K2R6; Q8E1A6
Ribose 1,5-bisphosphate phosphokinase PhnN	Catalyzes the phosphorylation of ribose 1,5-bisphosphate to 5-phospho-D-ribosyl alpha-1-diphosphate (PRPP).	*Thiobacillus denitrificans (strain ATCC 25259)*	(R)ETEDQISR(R)	5.55e+004	Q3SGK8
tRNA-specific 2-thiouridylase MnmA	Catalyzes the 2-thiolation of uridine at the wobble position (U34) of tRNA, leading to the formation of s_2U34.	*Helicobacter pylori (strain Shi470); Helicobacter pylori (strain HPAG1); Helicobacter pylori (strain J99 / ATCC 700824) (Campylobacter pylori J99)*	(K)NKSLTKDFK(N)	7.59e+005	B2UV99; Q1CRS3; Q9ZJQ0
Histidinol-phosphate aminotransferase	x	*Listeria welshimeri serovar 6b (strain ATCC 35897 / DSM 20650 / CIP 8149 / NCTC 11857 / SLCC 5334 / V8)*	(K)NVIITRTFSK(I)	1.03e+005	A0AK37
Translation initiation factor IF-3	IF-3 binds to the 30S ribosomal subunit and shifts the equilibrum between 70S ribosomes and their 50S and 30S subunits in favor of the free subunits, thus enhancing the availability of 30S subunits on which protein synthesis initiation begins.	*Rickettsia felis (strain ATCC VR-1525 / URRWXCal2) (Rickettsia azadi); Rickettsia conorii (strain ATCC VR-613 / Malish 7)*	(-)MPFPK(I)	2.56e+005	Q4ULG2; Q92HK6
tRNA-cytidine(32) 2-sulfurtransferase 1	Catalyzes the ATP-dependent 2-thiolation of cytidine in position 32 of tRNA, to form 2-thiocytidine (s_2C32). The sulfur atoms are provided by the cysteine/cysteine desulfurase (IscS) system.	*Francisella tularensis subsp. novicida (strain U112); Francisella tularensis subsp. tularensis (strain WY96-3418); Francisella tularensis subsp. tularensis (strain FSC 198); Francisella tularensis subsp. tularensis (strain SCHU S4 / Schu 4)*	(K)LLSDDK(R)	8.36e+004	A0Q6E3; A4IXY7; Q14HG9; Q5NG17
tRNA-cytidine(32) 2-sulfurtransferase	Catalyzes the ATP-dependent 2-thiolation of cytidine in position 32 of tRNA, to form 2-thiocytidine (s_2C32). The sulfur atoms are provided by the cysteine/cysteine desulfurase (IscS) system;	*Psychrobacter sp. (strain PRwf-1); Francisella tularensis subsp. mediasiatica (strain FSC147); Psychrobacter cryohalolentis (strain ATCC BAA-1226 / DSM 17306 / VKM B-2378 / K5); Francisella tularensis subsp. mediasiatica (strain FSC147); Dechloromonas aromatica (strain RCB); Psychrobacter arcticus (strain DSM 17307 / VKM B-2377 / 273-4)*	(K)LLSDDK(R)	8.36e+004	A5WG99; B2SGI4; B3PID5; Q1QCP2; Q477W2; Q4FTN3
tRNA-cytidine(32) 2-sulfurtransferase 2	Catalyzes the ATP-dependent 2-thiolation of cytidine in position 32 of tRNA, to form 2-thiocytidine (s_2C32). The sulfur atoms are provided by the cysteine/cysteine desulfurase (IscS) system;	*Francisella tularensis subsp. holarctica (strain FTNF002-00 / FTA); Francisella philomiragia subsp. philomiragia (strain ATCC 25017 / FSC 153 / O#319-036); Francisella tularensis subsp. holarctica (strain OSU18); Francisella tularensis subsp. holarctica (strain LVS)*	(K)LLSDDK(R)	8.36e+004	A7NC76; B0U092; Q0BLX1; Q2A3F9
Macrodomain Ter protein	Required for spatial organization of the terminus region of the chromosome (Ter macrodomain) during the cell cycle. Prevents early segregation of duplicated Ter macrodomains during cell division. Binds specifically to matS, which is a 13 bp signature motif repeated within the Ter macrodomain.	*Vibrio atlanticus (strain LGP32) (Vibrio splendidus (strain Mel32))*	(K)LLSDDK(R)	8.36e+004	B7VNL8

ATP-dependent protease ATPase subunit HslU	ATPase subunit of a proteasome-like degradation complex; this subunit has chaperone activity. The binding of ATP and its subsequent hydrolysis by HslU are essential for unfolding of protein substrates subsequently hydrolyzed by HslV. HslU recognizes the N-terminal part of its protein substrates and unfolds these before they are guided to HslV for hydrolysis.	*Rickettsia bellii (strain RML369-C)*	(K)LLSDDK(R)	8.36e+004	Q1RIB7
Chaperone protein DnaK	Acts as a chaperone.	*Blochmannia floridanus*	(K)LLSDDK(R)	8.36e+004	Q7VQL4
UPF0246 protein Spy49_1742	x	*Streptococcus pyogenes serotype M49 (strain NZ131)*	(K)EMMIPK(E)	1.12e+006	B5XIZ3
UPF0246 protein MGAS10270_Spy1856	x	*Streptococcus pyogenes serotype M2 (strain MGAS10270)*	(K)EMMIPK(E)	1.12e+006	Q1JEI8
UPF0246 protein M28_Spy1772	x	*Streptococcus pyogenes serotype M28 (strain MGAS6180)*	(K)EMMIPK(E)	1.12e+006	Q48QX8
50S ribosomal protein L24	One of two assembly initiator proteins, it binds directly to the 5'-end of the 23S rRNA, where it nucleates assembly of the 50S subunit.	*Pseudothermotoga lettingae (strain ATCC BAA-301 / DSM 14385 / NBRC 107922 / TMO) (Thermotoga lettingae)*	(R)FLDDGAKVRFCK(K)	6.34e+004	A8F4S2
ATP-dependent Clp protease ATP-binding subunit ClpX	ATP-dependent specificity component of the Clp protease. It directs the protease to specific substrates. Can perform chaperone functions in the absence of ClpP.	*Mycolicibacterium gilvum (strain PYR-GCK) (Mycobacterium gilvum (strain PYR-GCK))*	(R)GLGFGAEVHSK(A)	1.41e+004	A4T2N8
N-acetyl-gamma-glutamyl-phosphate reductase	Catalyzes the NADPH-dependent reduction of N-acetyl-5-glutamyl phosphate to yield N-acetyl-L-glutamate 5-semialdehyde.	*Mycobacterium bovis (strain ATCC BAA-935 / AF2122/97); Mycobacterium tuberculosis (strain CDC 1551 / Oshkosh); Mycobacterium tuberculosis (strain ATCC 25618 / H37Rv)*	(R)TRSPLSQLRAAYEK(A)	8.87e+004	P63563; P9WPZ8; P9WPZ9
Cytidylate kinase	x	*Xanthobacter autotrophicus (strain ATCC BAA-1158 / Py2); Methylobacterium sp. (strain 4-46)*	(-)MVIAIDGPAASGK(G)	2.41e+005	A7IEB7; B0UC53
Phenylalanine--tRNA ligase alpha subunit	x	*Marinobacter hydrocarbonoclasticus (strain ATCC 700491 / DSM 11845 / VT8); Mycobacterium leprae (strain TN)*	(K)INEAKGQVEQAINA(R) ; (R)ELPVYVISIGRAFR(T)	1.68e+005; 7.46e+005	A1U2B9; Q9CC17
ATP-dependent dethiobiotin synthetase BioD	Catalyzes a mechanistically unusual reaction, the ATP-dependent insertion of CO2 between the N7 and N8 nitrogen atoms of 7,8-diaminopelargonic acid (DAPA, also called 7,8-diammoniononanoate) to form a ureido ring.	*Xylella fastidiosa (strain M12)*	(K)TFVSCILLHMLRGRGQR(A)	1.38e+005	B0U3W7

Figures:

Figure 1.

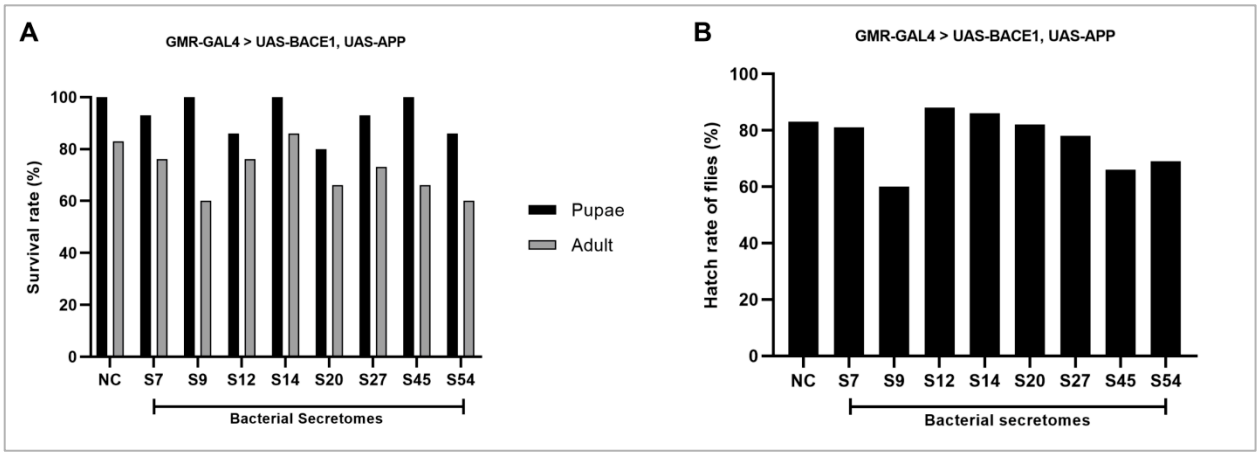

Figure 2.

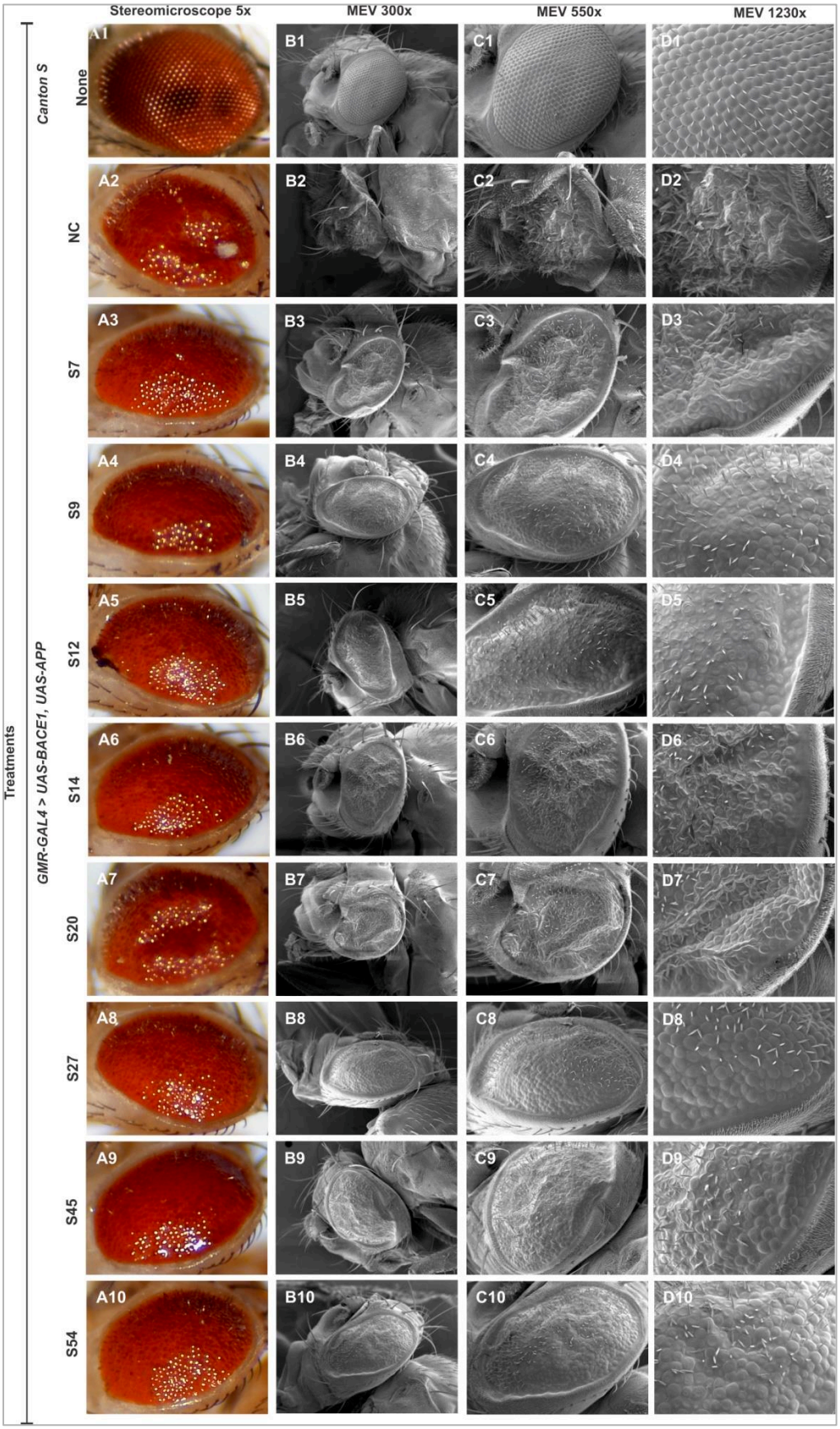
Stereomicroscope 5x
MEV 300x
MEV 550x
MEV 1230x
Treatments
Canton S
None
GMR-GAL4 > UAS-BACE1, UAS-APP
NC
S7
S9
S12
S14
S20
S27
S45
S54
A1
B1
C1
D1
A2
B2
C2
D2
A3
B3
C3
D3
A4
B4
C4
D4
A5
B5
C5
D5
A6
B6
C6
D6
A7
B7
C7
D7
A8
B8
C8
D8
A9
B9
C9
D9
A10
B10
C10
D10

Figure 3.

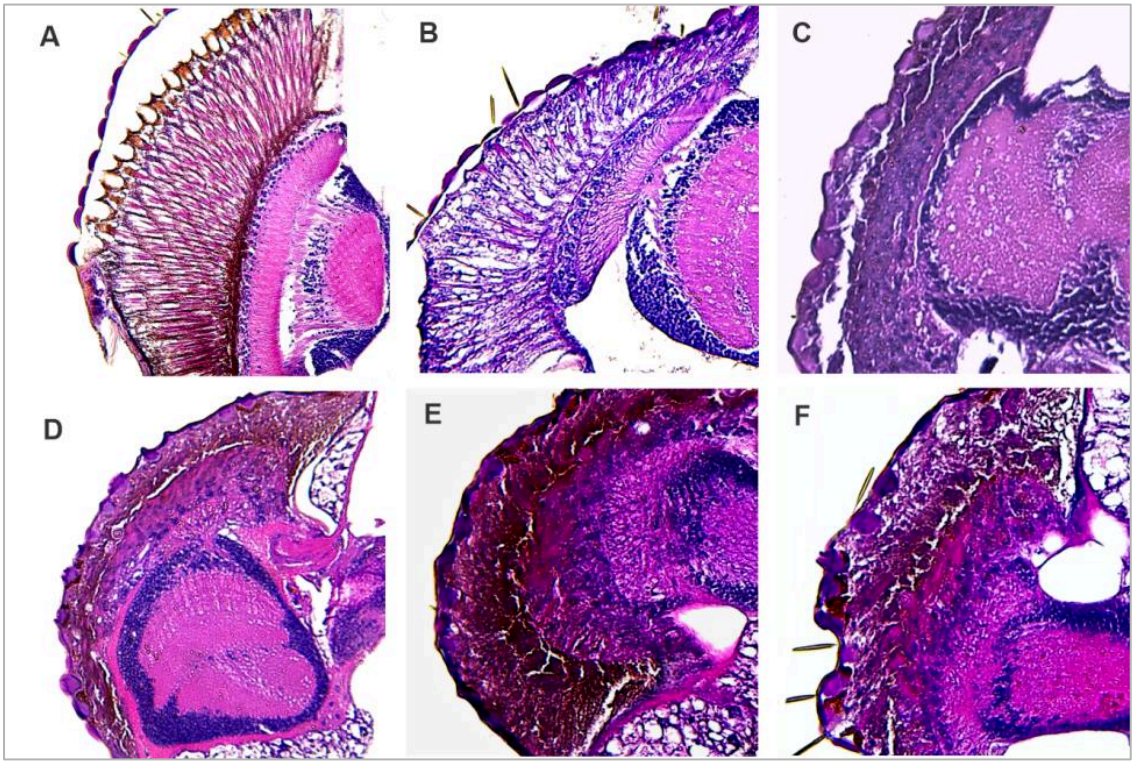

Figure 4.

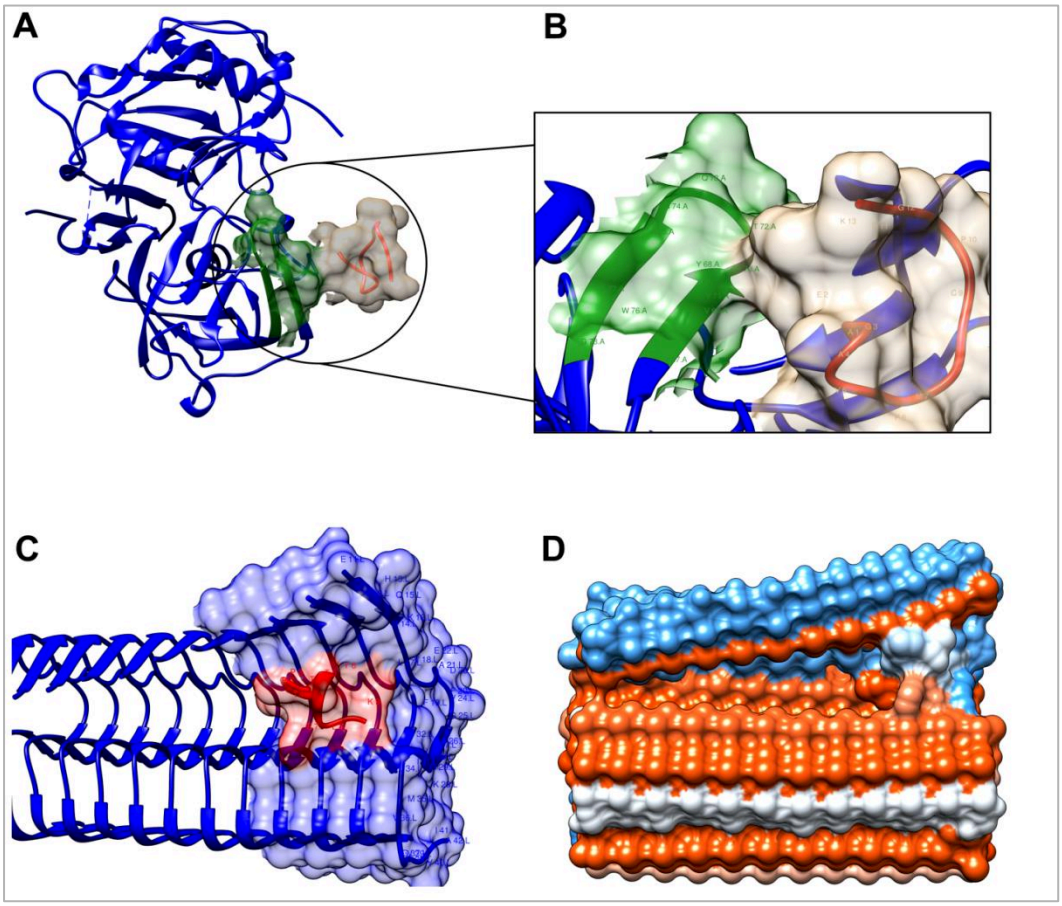

Figure S1.

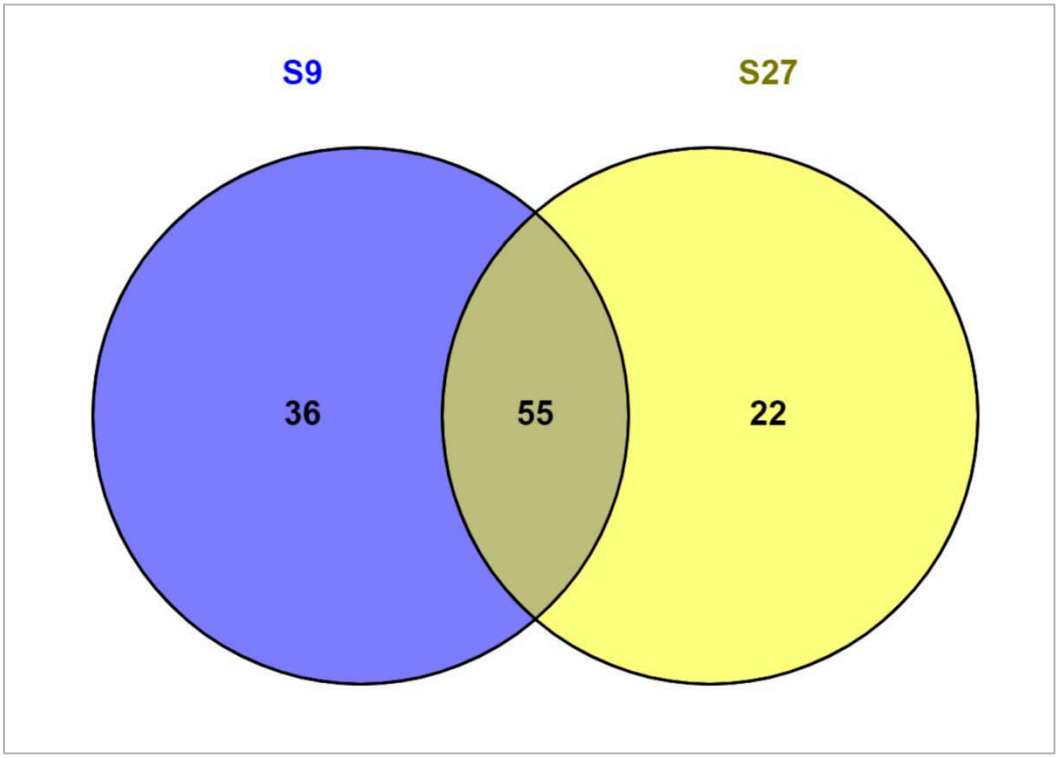

Scientific Reports:

Title: Bacterial secretomes of Brazilian stingless bees' larval food: Implications in Alzheimer Disease

Tamiris Sabrina Rodrigues[1,*], Serena Mares Malta[1], Lucas Ian Veloso Correia[2], Anderson Santos[3], Ana Carolina Santos[1], Mário Machado Martins[2], Luiz Ricardo Goulart[2], Carlos Ueira-Vieira[1] and Ana Maria Bonetti[1]

[1] Laboratory of Genetics, Institute of Biotechnology, Federal University of Uberlândia, Uberlândia, MG, Brazil

[2] Laboratory of Nanobiotechnology, Institute of Biotechnology, Federal University of Uberlândia, Uberlândia, MG, Brazil

[3] Faculty of Computer Science, Federal University of Uberlândia, Uberlândia, MG, Brazil

Corresponding author: Tamiris Sabrina Rodrigues and Carlos Ueira Vieira

Address: Laboratory of Genetics, Institute of Biotechnology, Federal University of Uberlândia, Uberlândia, Acre Street, 2E building, room 230, Uberlândia, MG, Brazil

tamiris.rodrigues@ufu.br and ueira@ufu.br

Abstract

Alzheimer disease is a progressive neurodegenerative disorder that affects the central nervous system, characterized by progressive loss of neurons in the hippocampus and cerebral cortex, thus compromising information processing and storage. The inhibition of amyloid precursor protein cleavage enzyme (BACE1) associated with Alzheimer's disease has been the main target for the development of drugs that can treat or prevent this disease. The objective of our investigation was to identify anti-AD peptides in bacterial secretomes from larval food of native Brazilian stingless bees *Melipona quadrifasciata.* For this purpose, the screening of secretomes in the *Drosophila melanogaster* strain model AD-like was performed, followed by *in silico* analysis. The anti-AD model of *D. melanogaster* was treated with several bacterial secretomes for 15 days after hatching. The flies treated with the S1 secretome showed an improvement in the climbing rate when compared to the negative control and vehicle groups. Additionally, the groups treated with the S1 and S27 secretomes showed a decline in beta-amyloid levels after 15 days of treatment. The histology analysis of the brain revealed a decrease in neurodegeneration in flies treated with S1 visualized through the reduction of vacuolar lesions, when compared to the NC and vehicle groups. After these tests, the S1 secretome was considered the one with the best action, and its content was assessed by proteomic analysis and whole-genome sequencing. The *in silico* analysis selected the most potentially bioactive peptides to interact with BACE1 and beta-amyloid. Finally, 3D images of the interaction of the peptides with their respective targets were generated, predicting the docking between them. The HLINLFFDSGTIK and PLLTAGFFSK peptides were able to interact with BACE1 and β-amyloid, respectively, and exhibited a potential effect for the prevention and treatment of Alzheimer Disease.

Keywords: Alzheimer’s disease; *Drosophila melanogaster*; stingless bees’ larval food; bioactive peptide; β-amyloid; BACE1

1 Introduction

Neurodegenerative diseases are a heterogeneous group of disorders that usually strike in mid-life, causing progressive loss of motor and cognitive function [1]. Current estimates indicate that by 2030, there will be 74.7 million people with dementia, and the cost of caring for these individuals could reach US$2 trillion [2].

Dementia is a progressive degenerative process that affects memory, locomotion, thinking and behavior. With the rise in life expectancy, diseases such as Alzheimer's disease (AD) have become increasingly common, characterizing a worldwide public health problem [3]. Its number is about 20 million cases, that is, almost 4% of the world population and these data tend to increase with time [4, 5]. The World Bank and the World Health Organization declare that neurological disorders are one of the greatest burdens on public health [6].

AD has several etiologies and is pathologically characterized by the presence of β-amyloid plaques and neurofibrillary tangles in the brain [7]. The accumulation of amyloid plaques occurs due to inadequate cleavage of β-amyloid precursor protein (APP) in the brain [8-10]. Normally, APP is cleaved both in its extracellular domain and in its intracellular domain by α and γ-secretase enzymes, respectively, generating a polypeptide of 40 amino acids. This non-amyloidogenic pathway causes learning defects, without neurodegeneration. When an APP is cleaved by β-secretase (BACE1) and γ-secretase enzymes, a 42-amino acid polypeptide is generated (Aβ42). The two extra amino acids in this peptide increase hydrophobicity, thus promoting its aggregation and generation of amyloid plaques. These plaques cause disruption of normal cellular processes in the brain through oxidative stress, loss of synaptic activity and death of neurons [11-14].

Although Aβ42 is less abundant, it is more prone to form Aβ oligomers, and is viewed as a highly toxic component [15-20]. Other pathological factors, including inflammatory response, ion homeostasis disruption, oxidative stress, and decreased levels of neurotransmitters have also been identified and are considered to be sequential events of Aβ aggregation. These factors will contribute to AD synaptic dysfunction and pathogenesis [21-24].

As many researchers support the amyloid hypothesis, attempts to prevent or treat AD are actively turned toward to reducing Aβ levels to improve or reverse the synaptic failures presented by patients. Thus, the inhibition of β-site amyloid precursor protein cleavage enzyme 1 (BACE1) remains a potential pathway for the treatment of this disease [25, 26].

A range of compounds, such as organophosphorus homodimers, losartan and N-propargylpiperidines with naphthalene-2-carboxamide or naphthalene-2-sulfonamide that have cholinesterase or BACE 1 inhibitory activity have been studied in recent years. However, none of them were very efficient for the treatment of AD [27-29]. These data reinforce the need of new studies looking for biologically active molecules with the potential to prevent or treat AD.

Honey, propolis and fermented pollen obtained from Brazilian stingless bees have immunomodulatory, antioxidant, anti-inflammatory, analgesic and sedative effects [30-34]. The larval food is a mixture of fermented pollen, honey and mandibular secretion and it is possible that the microorganisms present in it secrete biologically active compounds that can be beneficial for human health and that exhibit anti-AD effects.

Drosophila melanogaster, popularly known as the fruit fly, is a model organism used in several studies to evaluate neurological and neurodegenerative diseases, not only gaining an understanding of the biological pathways impaired in the disease, but also as basis for intervention in mammalian systems [35].

The use of this model organism for the study of diseases offers various advantages for elucidating the molecular and cellular mechanisms underlying human diseases [36, 37]. Short shelf life, large number of offspring, easy maintenance, well-marked anatomical and cellular characteristics, presence of several orthologous genes involved in human diseases and a wide variety of transgenic strains are characteristics that justify the use of the fruit fly in the studies [38, 39, 40]. Comparisons between the fly and human genomes indicate a high degree of conservation in fundamental biological pathways [41]. Importantly, it is estimated that 75% of the genes involved in human diseases have a functional ortholog in *D. melanogaster* [42].

Thus, the objective of this work was to identify anti-AD peptides in bacterial secretomes from larval food of Brazilian stingless bees *Melipona quadrifasciata.* We performed the screening of bacterial secretomes in *D. melanogaster* AD-like model and the results were evaluated by climbing test, beta-amyloid quantification and histological analysis of the fly's brain.

In order to identify the microorganism that produced the secretome with the best anti-AD effect in the tests with *D. melanogaster* AD-like model, we carried out the new generation sequencing (NGS). Proteomic analysis was performed to identify the peptides present in the secretome and to guide the search for the sequences with bioactive potential to act on the BACE1 targets and β-amyloid plaques and reduce the neurodegenerative process. The selection of the most bioactive peptides was made by *in silico* analysis. We performed *in silico* analysis to predict three-dimensional conformations of the peptides and their interaction with the target sites (BACE1 and β-amyloid plaques).

2. Results

2.1 Bacteria isolated from stingless bees' larval food

The colonies of the bacteria were numerically represented as 1, 9, 27 and 54. Table 1 depicts bacterial colonies and culture media for isolation. The secretomes of these microorganisms were collected and used for food supplementation of *elav-GAL4>UAS-BACE1, UAS-APP* transgenic flies, amyloid-induced neurodegeneration model.

The bacterial colonies were named as 1, 9, 27, 54 and their respective secretomes as S1, S9, S27 and S54.

2.2 Bacterial secretomes affect the fly climbing ability of the *D. melanogaster* AD-like phenotype

The Rapid Iterative Negative Geotaxis (RING) assay was used as a measurement for motor reflex decline related to neurodegeneration, observed as the fly climbing ability. Untreated AD-like model flies had their motor reflex tested and compared to a control genotype (elav-GAL4) 15 days post-eclosion and presented a reduction in climbing capacity (Figure 1A, $P < 0.05$), when compared to elav-GAL4 flies.

Fifteen (15) days after treatment, the flies treated with the S1 secretome increased the greater climbing capacity ($P < 0.01$) when compared to the untreated group (NC) (Figure 1B). There was also a significative difference between the vehicle and S1 groups ($P < 0.05$).

2.3 S1 and S27 secretomes reduce beta-amyloid levels in the brain of AD-like flies

The AD-like flies with 15 days of hatching that did not receive treatment showed high rates of beta-amyloid (Figure 2). The groups treated with the S1 and S27 secretomes showed a significative reduction of beta-amyloid ($P < 0.05$), when compared to the untreated group (NC) (Figure 2).

2.4 S1 secretome reduces neurodegeneration in the AD-like fly brain, after 15 days of treatment

In order to verify the action of secretomes in reducing neurodegeneration, we performed a histopathological analysis of the brain of AD-like flies treated for 15 days after hatching (Figure 3). The occurrence of neurodegeneration is manifested by the appearance of vacuolar lesions in the central region of the brain. The flies treated with S1 (Fig. E) showed histological characteristics similar to the elav-GAL4 control group (Fig. A, B), free of vacuoles. In the histological sections of the NC, vehicle and treated groups with S9, S27 and S54 (Fig. C-G, respectively), we visualize the brain with numerous vacuolar lesions.

2.5. Whole-genome sequencing of Bacteria 1

After DNA sequencing, the raw reads were filtered to remove adaptor sequences, contamination and low-quality reads. The clean data generated 9,996,950 reads with 1,499,542,500 bases. After genome assembly, it was discovered that the DNA from bacterial 1 belongs to two different bacterial species, *Proteus mirabilis* and *Enterococcus faecalis*. Their genomes were previously sequenced, and were used for resequencing genome assembly. The genomes of new strains isolated from *M. quadrifasciata* stingless bee were named as IsAbel.Pmir and IsAbel.Efae and same features annotated are shown in Table 2.

2.5 Proteomic analysis of bacterial secretomes

The bacterial secretome S1 showed the best results in tests performed with the AD-like fly and, therefore, was analyzed by mass spectrometry. The proteomic analysis was guided by the annotation of the genomes. Thirty-six peptides were identified, being 20 of them derived from proteins produced by both *Enterococcus faecalis* and *Proteus mirabilis*; 13 protein derivatives produced exclusively by *Proteus mirabilis*; and 3 protein derivatives produced exclusively by *Enterococcus faecalis* (Table 3) (Figure S1).

2.6 Molecular Docking

The bioactivity prediction of the 36 peptides present in the S1 secretome was calculated using the Peptide Ranker software. Of these, only 4 sequences with at least 9 amino acids and a classification of at least 0.04 were considered in our analysis. The best 3D model for each of them was selected for docking with β-secretase (BACE) and β-amyloid (Table 4). Figure 4 shows the 3D images of the interaction of these peptides with their respective target site. After submitting the two peptides to Swiss Target Prediction, both presented BACE1 as a target.

205 **2.7 *In silico* predictions of toxicity and solubility for potential peptides**

206

207 After analysis in the software, the HLINLFFDSGTIK peptide, selected for docking with
208 BACE1, showed no toxicity and presented low water solubility. Its molecular weight was
209 1080.43 g/mol, with an isoelectric point of 9.11 and a net charge of 1.00 at pH 7. The peptide
210 PLLTAGFFSK, selected for docking with β-amyloid, showed no toxicity and presented low
211 water solubility. Its molecular weight was 1504.95 g/mol, with an isoelectric point of 7.09
212 and a net charge of 0.10 at pH 7 (Table 5).

213

214 **2.8 New bacterial strains (IsAbel.Pmir and IsAbel.Efae) with biotechnological potential**

215

216 The whole-genome sequencing and proteomic analysis showed that the peptide
217 HLINLFFDSGTIK is part of the protein MobC from *E. faecalis* and is encoded by one gene
218 localized in plasmid. The PLLTAGFFSK is part of the protein NADH-ubiquinone reductase
219 encoded by the *nuo* operon in the *P. mirabilis* IsAbel.Pmir genome (Figure 5). Remarkably,
220 the knowledge of genomic structure and function is important for genomic manipulation and
221 to improve the overexpression of proteins of biotechnological interest.

222

223 **3 Discussion**

224

225 Several strains of *D. melanogaster* have been used to study neurodegenerative diseases.
226 This is possible due to the complexity of their nervous system, including eyes, olfactory
227 organs, taste organs, auditory organs, ventral nerve cord (analogous to the spinal cord),
228 peripheral sensory neurons for nociception and brain [43]. Furthermore, the development of
229 the GAL4/UAS system allowed the creation of transgenic lines with overexpression of genes
230 for specific tissues of the fly, adapting it to target of study [44]. Currently, there are
231 well-validated tests to assess neurodegeneration in *Drosophila*, such as the assessment of
232 central brain vacuolization using histological staining and locomotor performance
233 measurements using the climbing test [45, 46].

In our study, elav-GAL4 (driver strain) directs the expression of the human APP and BACE1 orthologs (UAS-BACE1, UAS-APP, responder strain) to the brain of the fly. From crossing elav-GAL4 females and UAS-BACE1, UAS-APP males, we obtained the overexpression of the human APP and BACE1 orthologs in the brain, generating the Alzheimer disease phenotype (AD-like) in *D. melanogaster*, an amyloid-induced neurodegeneration model fly.

In the last few decades, various studies have developed BACE1 inhibitors that are bioavailable by the oral route and able to permeate cells and penetrate into the brain, being approved for clinical tests. [47-49]. Verubecestate (MK-8931), for example, was the first low molecular weight BACE1 inhibitor with oral availability and blood-brain barrier permeability [50]. Despite its anti-AD potential, trial participants reported adverse effects, in addition to worsening of cognitive symptoms [51]. Moreover, several BACE1 inhibitors, such as LY2886721, impaired the liver function of patients [52]. These data support the need to identify new molecules to prevent or treat AD.

Products derived from stingless bees are promising sources of biologically active compounds [53]. It is estimated that in Brazil there are about 400 species of stingless bees [54, 55].

Studies have already identified several potentially therapeutic effects of bee products (honey, propolis, pollen), highlighting the effects on wound healing, diabetes, eye diseases, hypertension, cancer and microbial infections [56-59]. The honey produced by stingless bees has antioxidant, anti-inflammatory, antimicrobial, anti-cancer and anti-obesity effects [60-68]. Another product of beneficial effect to human health is propolis, owing to the antioxidant, anti-inflammatory, antimicrobial and healing properties. Still, studies on stingless bees are scarce.

Another promising source of biologically active peptides is the larval food of bees, a mixture of glandular secretion of the bee, honey and pollen. In stingless bees, the workers build and fill the brood cells with the food on which the larva will feed. This food is deposited just before the egg is laid. As soon as the queen lays an egg per brood cell, the cell is closed

by the workers. The brood cells are dark, hot and humid environments, ideal conditions for the growth of microorganisms.

Some studies have already isolated and identified bacteria present in honey and propolis from stingless bees, being *Bacillus* the predominant genus, showing antimicrobial effects against Gram-positive and Gram-negative bacteria [69, 70]. Despite this, there are no studies evaluating the microorganisms in the larval food of stingless bees in search of peptides with beneficial effects on human health. Thus, identifying these microorganisms and the content of their secretomes is the key to find new molecules with bioactive potential to prevent or treat AD.

The S1 secretome assessed in this work showed efficient anti-AD performance in the tests performed in *D. melanogaster* AD-like model. The S1 secretome improved the fly's climbing ability, reducing the decline of the motor reflex related to neurodegeneration, when compared to the untreated fly and treated with vehicle. The hypothesis is that the improvement could be related to a reduction in the levels of beta-amyloid in the treated group. This reduction was seen in the amyloid quantification test by Thioflavin T. The histological analysis of the fly's brain showed a decrease in the signs of neurodegeneration in the group treated with S1, with a reduction in vacuolar lesions and an aspect similar to normal brain (elav-GAL4). These results led to the selection of the S1 secretome to continue the search. In order to identify the microorganisms responsible for the production of the S1 secretome, their respective bacterial sample was analyzed by new generation DNA sequencing. Two microorganisms were found in the sample: *Enterococcus faecalis* and *Proteus mirabilis.* These data guided the proteomic analysis, performed to identify which peptides would be present in the S1 secretome.

The sequences of the bioactive peptides are inactive when inside the protein that originated them and can be obtained, among other ways, by the hydrolysis of these proteins by means of digestive enzymes (trypsin in this case). As the treatment of AD-like flies was carried out through feeding (medium of mashed potatoes and secretome), the proteins present in the secretome underwent enzymatic action during digestion and only then did the generated peptides act on their target sites. For this reason, before the analysis of the S1

291 secretome by mass spectrometry, it was prepared through enzymatic digestion steps with
292 trypsin. As this enzyme is also present in the digestive system of *D. melanogaster*, we
293 performed a simulated gastrointestinal digestion, mimicking this process in the fly and
294 obtaining bioactive peptides from the bacterial proteins present in the secretomes [71].
295 Of the 36 peptides identified in the S1 secretome through peptide-protein analysis, 2
296 were selected by bioinformatics tools as the most potentially bioactive molecules to interact
297 with the target sites under study. The peptide HLINLFFDSGTIK has its origin in a protein
298 secreted by the bacterium *Enterococcus faecalis* and its potential target is the enzyme
299 BACE1. Previous study conducted in Malaysia with a stingless bee also identified the
300 presence of *Enterococcus faecalis,* however in bee bread of the stingless bee *Heterotrigona*
301 *itama* [72]. The peptide PLLTAGFFSK is the result of the enzymatic action of a protein
302 secreted by the bacterium *Proteus mirabilis* and has a potential target for beta-amyloid.
303 The Swiss Target Prediction allows estimating the most likely macromolecular targets
304 for a small molecule, considered to be bioactive. The forecast is based on a combination of
305 2D and 3D similarity with a library of 370,000 known assets in more than 3,000 proteins
306 from three different species [73]. After submitting the two peptides to this prediction, both
307 presented BACE1 as target.
308 The toxicity of the peptides selected as potentially bioactive molecules confirmed the
309 effects observed in the tests performed. The results revealed that none of them were toxic.
310 Water solubility has a great influence on the degree of *in vivo* absorption of bioactive
311 peptides, and water-soluble peptide sequences generally have high biological availability
312 [74]. Although the prediction of water solubility of the HLINLFFDSGTIK and
313 PLLTAGFFSK peptides is low, this does not invalidate their bioactive potential. The
314 generation of mutants of these sequences to improve the degree of solubility, optimizing the
315 absorption in the gastrointestinal tract, must be done. The molecular docking of the peptides
316 with BACE1 and beta-amyloid was carried out in order to verify if and how the predicted
317 anti-AD effect occurs.
318 The BACE1 enzyme has three domains: an N-terminal extracellular domain, a
319 transmembrane domain and a cytosolic C-terminal domain. Its extracellular domain has the

correct orientation for APP cleavage. Between the N- and C-terminal regions, there is a gap with the conserved catalytic Asp dyad (Asp32 and Asp228), being the active site of action for this enzyme [75]. Next to this region, there is a loop that, depending on the conformation, can obstruct access to the active site [76].

The 3D images of the docking between HLINLFFDSGTIK and BACE1 showed that, despite the interaction between these molecules, the peptide does not interact directly with the active site, not even with the loop. However, it is possible to notice that the peptide is located exactly in the gap between the N- and C-terminal regions, just above the active BACE1 site. Thus, the peptide could block access to the active site, preventing the enzyme from cleaving its substrate. Therefore, we believe that the interaction of the HLINLFFDSGTIK peptide with BACE1 can inhibit the action of this enzyme, preventing the cleavage of APP and the production of Aβ.

Studies show that APP cleavage by BACE1 generates Aβ proteins of various sizes. Although Aβ40 is the most abundant protein in plasma, Aβ42 is the most toxic and has a high aggregating power [77, 78]. According to the researchers, the toxicity of Aβ42 is justified by its molecular conformation that comprises a single triple motif β in its structure, formed by three β leaves that cover the residues 12-18 (β1), 24-33 (β2) and 36-40 (β3). This tertiary fold would be responsible for its cytotoxicity and aggregation, resulting in the formation of β-amyloid plaques in patients with AD [79, 80].

When analyzing the 3D images of the docking between PLLTAGFFSK and the β-amyloid plaque, we noticed that there is a positive interaction between them. Docking altered the conformation of the plaque, causing an opening in its structure and, consequently, altering its triple motif β. Thus, it is possible that the bioactive anti-AD potential of the PLLTAGFFSK peptide occurs through the conformational change of Aβ42, neutralizing its cytotoxicity and aggregation and avoiding the damage caused by its accumulation and deposition in neurons.

Our investigation validates the biotechnological potential of secretomes isolated from larval food of native Brazilian stingless bees as a source of bioactive peptides with therapeutic potential to treat human diseases. Our analyses were able to identify and predict

the docking of two peptides with potential bioactivity to interact with BACE1 (HLINLFFDSGTIK) and β-amyloid (PLLTAGFFSK), sites that have been extensively explored for the development of new therapies for AD.

4. Material and Methods

4.1 Biological material

Four bacterial secretomes (S1, S9, S27 and S54) obtained from bacteria in the microorganism bank Collection of isolated stingless bee microorganisms LABGEN UFU (COMIALG) of Laboratory of Genetics - Federal University of Uberlândia were tested.

All of the secretomes analyzed in this study were obtained from bacteria isolated from the stingless bee hive *Melipona quadrifasciata*, located at the UFU Meliponary (S 180 55 '/ W 450 17') of the Institute of Biotechnology of the Federal University of Uberlândia, Uberlândia, Minas Gerais, Brazil.

4.2 Obtaining bacterial secretome

To obtain the supernatant of each bacteria isolated from larval food, 50 mL of Luria Bertani (LB) medium was prepared and autoclaved, followed by inoculation of 10 µL of bacteria. The medium was incubated in a bacteriological incubator at 37°C for 48 hours under 200 rpm agitation. Medium was transferred to a sterile 15 mL tube and centrifuged at 1000g. The supernatant was filtered through a sterile 0.22 µm syringe filter. The supernatants/secretomes were frozen in -80°C freezer until their use in flies' treatment.

4.3 Flies stock and Genetics

The strains under study were kept in stock in flasks containing ¼ of Bloomington culture medium (1500 mL of water, 27g of yeast, 15g soybean meal; 109.5g corn meal; 9g agar;

115.5g glucose syrup; acid and Nipagin solution) in BOD incubator (Biochemical Oxygen Demand, SOLAB) at 25°C, 70% relative humidity and 12:12 hours light-dark cycle.

P{GawB}elavC155,P{UAS-mCD8::GFP.L}LL4,P{hsFLP}1,w* (named as *elav-GAL4*; stock number BL#5146); P(UASBACE,UAS-APP1.L) (named as *UAS-BACE1, UAS-APP;* BL#29877) and w^{1118} (BL#3605) strains were obtained from Bloomington Stock Center of the University of Indiana.

4.4 Obtaining Alzheimer's model flies

The *GAL4/UAS* system was used for overexpression of human APP and BACE1 orthologs in the fly brain. The *elav-GAL4* (driver strain) directs the expression of the human APP and BACE1 orthologs (*UAS-BACE1, UAS-APP*, responder strain) to the fly brain. From crossing *elav-GAL4* females and *UAS-BACE1, UAS-APP* males, we obtained the overexpression of the human APP and BACE1 orthologs in the fly brain, producing the Alzheimer disease phenotype (AD-like) in *D. melanogaster*, an amyloid-induced neurodegeneration model fly.

For such, the parental strains were previously expanded and placed in glass flasks containing standard Bloomington culture medium. The expansion crosses of each strain were maintained for 10 days. On the 7th day, adults of the *elav-GAL4* strain were discarded for the collection of virgin females, later crossed with males of the UAS-BACE, UAS-APP strain.

After the crossing, the pupal stage of the F1 generation was awaited. Only 50% of these descendants had the genotype of interest (AD-like), being selected through the elongated shape of the pupae. The other individuals were discarded while still in the pupal stage, presenting the flattened phenotype due to the presence of the tubby balancer in their genotype. The remaining pupae, genotype w *, elav-GAL-4; UAS-BACE, UAS-APP / +, gave rise to the AD-like adult flies that were analyzed.

4.5 Experimental groups

Four bacterial secretomes, named as S1, S9, S27 and S54, isolated from the *Melipona quadrifasciata* stingless bees larval food were tested in *elav-GAL4 > UAS-BACE1, UAS-APP* transgenic flies of *D. melanogaster.* Behavior and morphology/structural changes in the brain of adult flies after supplementation with the secretomes (without dilutions) were evaluated. The water-treated group was the negative control (NC).

4.6 Behavioral assessment

The RING test (Rapid Iterative Negative Geotaxis), originally described by Gargano et al (2005) [81], consists of assessing the locomotor performance of *Drosophila melanogaster* using the climbing ability. This evaluation explores the natural characteristic of these flies to climb upwards, after sufficient mechanical stimulus to take them to the bottom of the container in which they are. The RING test indicates if there is a reduction in locomotor activity associated with age or factors such as neurodegeneration [81].

Adult flies subjected to treatments with bacterial secretomes, as well as controls, had their climb evaluated at 10 and 15 days of life. For the test, transparent tubes of 9.5 cm in height and 2.3 cm in diameter were placed in a rack-type apparatus with a capacity of 12 tubes. For each replicate, about 20 flies from each treatment / control group were transferred to the tubes and, after being positioned in the rack, were kept for 30 minutes at rest in a quiet environment at room temperature. During the setting, the racket was positioned 40 cm away from a light source (fluorescent lamp, white color - specifications: 18W, 220V, 6500K and 122mA). No anesthetic was used to allocate the flies in the tubes. Only elav-GAL4 > UAS-BACE1, UAS-APP male flies were analyzed in this test.

After acclimatization, the rack containing the tubes with flies was subjected to three consecutive strokes on sponges positioned on the surface of the experimental bench and replaced on it, starting the time counting. The tests were recorded through filming. The number of flies that arrived / exceeded the 5 cm line delimited in the rack was counted, after

4 seconds of the third hit. Three biological replicates and three technical replicates were performed, with an interval of 1 minute between the tests.

All procedures were filmed with a 13 megapixel camera and the initial analyses of the RING test were performed using the Quicktime® program, with a standardization of 4 full seconds corresponding to 120 frames of video reading. The counting of the frames was started at the moment the racket returned to the surface of the bench after the strikes.

4.7 Amyloid quantification by Thioflavin T

For quantification of β-amyloid in AD-like flies, we used the amyloid quantification protocol by Thioflavin T according to Westfall et al (2019) [82], with adaptations. The trial was carried out in biological triplicate, in the control /treatment groups.

For protein extraction, twenty fly heads were macerated in 200µL of protein extraction buffer (50mM Tris-HCl buffer pH 8.0 containing 1mM EDTA and 1% Triton X-100), together with protease inhibitors (cOmplete™, Mini, EDTA-free Protease Inhibitor Cocktail diluted in 10ml of the cold buffer) in a 2 mL tube, followed by centrifugation at 10,000 rpm for 2 min, to separate the debris. The supernatant was transferred to a new microtube and placed on ice for quantification of β-amyloid by Thioflavin T and total proteins by Bradford.

For the quantification of amyloid by Thioflavin T, a stock solution (5X) was prepared by dissolving 8 mg of Thioflavin T in 10 mL of PBS pH 7.0. The 1:5 working solution was prepared from the stock solution (diluted in PBS 1X). Finally, 198 µL of the working solution and 2 µL of the homogenate (supernatant of the extracted protein) were added in a 96-well plate, incubated for 20 minutes while shaking 260 rpm for quantification.

The fluorescence reading was performed at an excitation/emission wavelength of 450/482 nm. For data analysis, the value of the blank (Thioflavin T) was subtracted and the amyloid levels were normalized with total proteins measured by Bradford. After this stage, the quantification was normalized by the fluorescence found in the control group (*elav-GAL4*).

4.8 Histological analysis

For histological analysis, 10 adult flies of the elav-GAL4 > UAS-BACE1, UAS-APP strain of 15 days old were collected from each control/treatment group, anesthetized with ethyl ether and fixed in Carnoy solution (6: 3: 1, 99% ethanol, chloroform and glacial acetic acid) for 24 hours and processed in 70% ethyl alcohol (2x), 80% ethyl alcohol (2x), 90% ethyl alcohol (2x), absolute ethyl alcohol (2x), xylol (2x), 60% liquid paraffin (2x) for 15 minutes in each repetition. The flies' heads were aligned in an apparatus [58] and embedded in paraffin. The blocks were sectioned at 3 μm thickness using a semi-automatic microtome (SLEE CUT5062). The sections were dehydrated, stained with hematoxylin and eosin and mounted.

4.9 Proteomic analysis

For proteomic analysis, 10 mL of each supernatant was filtered through a 0.22 μm syringe filter and lyophilized. We used 1 mL of ultrapure water to resuspend and we performed the total protein quantification in a BioDrop® Nano Spectrophotometer (reading at 280 nm). The proteins were reduced with 100 mM dithiothreitol (DTT), alkylated with 0.5 M iodoacetamide and digested with trypsin (0.01 μg/μL). The desalination step was performed with ZipTips C18 (Millipore, Billerica, MA, United States).

The proteomic analysis was performed on the Liquid Chromatography-Electrospray Ionization – Quadrupole - Time of Flight-Mass Spectrometry (6520B LC-ESI-Q-TOF-MS) from Agilent. The chromatographic parameters were AdvanceBio Peptide Mapping column (Agilent) with 2.1 mm internal diameter, 10 cm of length and 2.7 μm particles. The mobile phase was composed by water (A) and acetonitrile (B), both acidified with formic acid (0.1% vv), with the gradient: 2% B (0 min), 2% B (10 min), 15% B (40 min), 50% B (150 min), 70% B (200 min), 98% B (220 min), 98% B (300 min), 100% B (301 min) and 100% B (400 min), in a flow of 400 μL/min. The ionization parameters were nebulizer pressure of 45 psi,

493 drying gas at 8L / min at a temperature of 325 °C, and 4KV energy was applied to the
494 capillary.
495 The analysis of the raw data was performed in the Spectrum Mill software (Agilent)
496 using the Uniprot (40,428 results for *Proteus mirabilis* and 187,915 results for *Enterococcus*
497 *faecalis* in March 2021). Carbamidomethylation was set as fixed modification. Maximum
498 missed cleavages were selected in two for trypsin. The precursor mass error and the
499 fragments were set at 20 ppm, product mass tolerance at 50 ppm and maximum ambiguous
500 precursor charge at 3.
501
502 **4.10 Screening of bioactive peptides**
503
504 The proteins were digested with trypsin in proteomic protocols, which mimic the
505 digestive process in *D. melanogaster* gut and create bioactive peptides from bacterial
506 proteins. The peptides present in S1 secretome were used for bioactivity prediction using the
507 Peptide Ranker (http://distilldeep.ucd.ie/PeptideRanker/) tool. The peptides with rank above
508 0.4 were considered as potential bioactive compounds.
509
510 **4.11 Tertiary structure prediction of peptides**
511
512 The 3D structures of peptides were created using PEP-FOLD 2.0
513 (https://mobyle.rpbs.univ-paris-diderot.fr/cgi-bin/portal.py#forms::PEP-FOLD). Analysis of
514 the global energy and the contribution of the atomic contact energy (ACE) were carried out to
515 determinate the best 3D models of each peptide.
516
517 **4.12 Molecular Docking**
518
519 The PDB file from BACE (3TPJ) and 42-Residue Beta Amyloid Fibril (2MXU) were
520 retrieved from Protein Data Bank (https://www.rcsb.org/). The online docking was
521 performed by using PathDocking (https://bioinfo3d.cs.tau.ac.il/PatchDock/) and refined by

FireDoock (http://bioinfo3d.cs.tau.ac.il/PatchDock/php.php) with the best sequence chosen for docking with BACE1 and for docking with 42-B-amyloid Fibril Residue.

To estimate the possible targets of the selected peptides, we used the Swiss Target Prediction (http://www.swisstargetprediction.ch/) website.

4.13 Toxicity and solubility predictions for potential peptides

The ToxinPred (http://crdd.osdd.net/raghava/toxinpred/) tool was utilized to predict the toxicity of potential peptides based on their important physicochemical properties. The peptide property calculator Innovagen (http://www.innovagen.com/proteomicstools) was used to calculate the solubility of peptides. The results were calculated based on the isoelectric point and the peptide length.

4.14 Whole-genome sequencing and genome assembly

The DNA from bacteria S1 was extracted and used to do a DNA library of 150 bp paired-end. The library was sequenced by using DNBseq technology in Beijing Genome Institute (BGI) Facility. The raw data with adapter sequences or low-quality sequences were filtered with a series of data processing to remove contamination and to obtain valid data by SOAPnuke software developed by BGI. The bacterial genomes were assembled using SPAdes assembler.

4.15 Statistical analysis

The results of behavioral test performed only with males were evaluated using t-test with significance set at $P \leq 0.05$. For the analysis of the β-amyloid quantification, D'Agostino & Pearson test was applied to check for normality, followed by Kruskal-Wallis test with a post-hoc Dunn's multiple comparisons test with significance set at $P \leq 0.05$.

Author Contributions: T.S.R. Conception, design, development of the methodology, analysis and interpretation of data, writing and revision of the manuscript. A.C.C.S. Development of the methodology. M. M. M. Proteomic analysis. L.I.V.C. Proteomic and bioinformatics analysis L.R.G. Proteomic analysis. A. S. Genome Assembly. C.U.V. and A.M.B. Conception, design, writing and revision of the manuscript, technical and material support.

Funding: This research was funded by the Conselho Nacional Científico e Tecnológico do Brasil (CNPq), the Fundação de Amparo à Pesquisa do Estado de Minas Gerais (FAPEMIG APQ-02766-17) and the Coordenadoria de Aperfeiçoamento de Pessoal de Nível Superior (CAPES). The Federal University of Uberlândia provided physical conditions for experimental procedures.

Acknowledgments: We are thankful to the Institute of Cell Biology of UFU for use of Light Microscope and Software LAS EZ and the Pathology Laboratory of the Faculty of Odontology of UFU for the sections microscopes.

Conflicts of Interest: The authors declare no conflict of interest.

Abbreviations

AD	Alzheimer's Disease
APP	Amyloid Precursor Protein
BACE1	β-secretase enzyme
Aβ	β-amyloid protein
M. quadrifasciata	*Melipona quadrifasciata*
MRS	Man Rogosa Sharpe
LB	Luria Bertani
NC	Negative control
ACE	Contribution of the atomic contact energy
pH	Hydrogen potential
pI	Isoelectric point
D. melanogaster	*Drosophila melanogaster*
mL	milliliter
µm	micrometer

°C	degrees Celsius
rpm	rotations per minute
µL	microliter
mm	millimeter
W	Watts
V	Volts
mA	Milliampere
RING	Rapid Iterative Negative Geotaxis
P. mirabilis	*Proteus mirabilis*
E. faecalis	*Enterococcus faecalis*
CDS	Coding Sequence
COMIALG	Collection of isolated stingless bee microorganisms LABGEN UFU
LABGEN	Laboratório de Genética
IBTEC	Institute of Biotechnology
UFU	Federal University of Uberlândia
BOD	Biochemical Oxygen Demand
CNPq	Conselho Nacional Científico e Tecnológico
FAPEMIG	Fundação de Amparo à Pesquisa do Estado de Minas Gerais
CAPES	Coordenadoria de Aperfeiçoamento de Pessoal de Nível Superior

References

1. Huda Y., Zoghbi, J. *Mouse and fly models of neurodegeneration,* **2002,** 18(9), 463–471.
2. Hung, S., Fu, W. Drug candidates in clinical trials for Alzheimer's disease. *J Biomed Sci*. **2017**; 24(1):47.
3. Couteur, D., Doust, J., Creasey, H. et al. Political drive to screen for pre-dementia: not evidence based and ignores the harms of diagnosis. *Br. Med.J.* **2013,** 347, f5125.
4. Aliabadi A., Foroumadi A., Mohammadi-Farani A. et al. Synthesis and evaluation of anti-acetylcholinesterase activity of 2-(2-(4-(2-Oxo-2-phenylethyl)piperazin-1-yl) ethyl)Isoindoline-1,3-dione derivatives with potential anti-alzheimer effects. *Basic Med Sci.,* **2013**, 16, 1049–1054.
5. Guzior N., Wieckowska A., Panek D. et al. Recent development of multifunctional agents as potential drug candidates for the treatment of alzheimer's disease. *Curr. Med. Chem*., **2015**, 22, 373–404.
6. Aarli J., Dua T., Janca A. et al. Neurological Disorders. *Public Health Challenges*, World Health Organization, Geneva. **2006.**
7. Selkoe, D. J. The molecular pathology of Alzheimer's disease. *Neuron.* **1991;** 6(4):487-98.
8. Esler, W., Wolfe, M. A portrait of Alzheimer secretases-new features and familiar faces. *Science*. **2001;** 293(5534):1449-1454.
9. Aguzzi, A.; O'Connor, T. Protein aggregation diseases: pathogenicity and therapeutic perspectives. *Nat Rev Drug Discov*. **2010**, *9*, 237-248.

10. Fernandez-Funez, P.; Sanchez-Garcia, J.; Ribncon-Limas, D. *Unraveling the basis of neurodegeneration using the developing eye*. New York: Springer; **2013.**
11. Selkoe, D. J.; Hardy, J. The amyloid hypothesis of Alzheimer's disease at 25 years. *EMBO Mol Med.* **2016**, *8*, 595–608.
12. Goldman, D. P.; Fillit, H.; Neumann, P. Accelerating Alzheimer's disease drug innovations from the research pipestrain to patients. *Alzheimers Dement.* **2018**, *14*, 833-836.
13. Sierra-Fonseca, J. A.; Gosselink, K. L. Tauopathy and neurodegeneration: A role for stress. *Neurobiol Stress.* **2018**, *9*, 105–112.
14. Kandalepas, P. C.; Vassar, R. Identification and biology of β-secretase. *J. Neurochem.* **2012**, *120*, 55–61.
15. Selkoe, D. Cell biology of protein misfolding: the examples of Alzheimer's and Parkinson's diseases. *Nat. Cell. Biol.* **2004,** 6:1054–61.
16. Driscoll. M., Gerstbrein, B. Dying for a cause: Invertebrate genetics takes on human neurodegeneration. *Nat. Rev. Genet*. **2003,** 4:181–94.
17. Hardy J, Selkoe DJ. 2002. The amyloid hypothesis of Alzheimer's disease: progress and problems on the road to therapeutics. Science 297:353–56.
18. Yang T, Dang Y, Ostaszewski B. et al. Target engagement in an Alzheimer trial: Crenezumab lowers amyloid β oligomers in cerebrospinal fluid. *Ann. Neurol.* **2019**, 86 (2): 215–224.
19. Busche MA, Wegmann S, Dujardin S, et al. Tau impairs neural circuits, dominating amyloid-β effects, in Alzheimer models in vivo. *Nat Neurosci.* **2019**, 22(1):57-64.
20. Storey, E., Cappai, R. The amyloid precursor protein of Alzheimer's disease and the Abeta peptide. *Neuropathol Appl Neurobiol*. **1999;** 25(2):81–97.
21. Su, B. et al. Oxidative stress signaling in Alzheimer's disease. *Curr Alzheimer Res*. **2008**; 5(6):525–32.
22. Green, K., LaFerla, F. Linking calcium to Abeta and Alzheimer's disease. *Neuron*. **2008**; 59(2):190–4.
23. Hardy, J., Allsop, D. Amyloid deposition as the central event in the aetiology of Alzheimer's disease. *Trends Pharmacol Sci*. **1991**; 12(10):383–8.
24. Babic, T .The cholinergic hypothesis of Alzheimer's disease: a review of progress. *J Neurol Neurosurg Psychiatry*. **1999**; 67(4):558.
25. Ohno, M. et al. A deleção do gene BACE1 previne a perda de neurônios e déficits de memória em camundongos transgênicos 5XFAD APP / PS1 . *Neurobiol Dis* . **2007**; 26 (1): 134–45.
26. McConlogue, L. et al. A redução parcial de BACE1 tem efeitos dramáticos na placa de Alzheimer e na patologia sináptica em camundongos transgênicos APP . *J Biol Chem* . **2007;** 282 (36): 26326–34.
27. Xie, R., Zhao, Q., Zhang, T et al. Design, synthesis and biological evaluation of organophosphorous-homodimers as dual binding site acetylcholinesterase inhibitors, *Bioorg. Med. Chem.,* **2013**, 21, 278–282.

28. Papadopoulos, K, Tong, H. et al. Losartan improves cerebrovascular function in a mouse model of alzheimer's disease with combined overproduction of amyloid- and transforming growth factor-1, J. *Cereb. Blood Flow Metab*., **2017**, 37, 1959–1970.
29. Kosak U, Knez D, Coquelle N. et al. N-propargylpiperidines with naphthalene-2-carboxamide or naphthalene-2-sulfonamide moieties: potential multifunctional anti-alzheimer's agents, *Bioorg. Med. Chem.,* **2017,** 25, 633–645.
30. Almaraz-Abarca, N. et al. Antioxidant activity of polyphenolic extract of monofloral honeybee-collected pollen from mesquite (*Prosopisjuliflora, Leguminosae). J Food Comp*. **2007**, 20(2), 119-124.
31. Naito, Y. et al. Anti-inflammatory effect of topically applied propolis extract in carrageenan-induced rat hind paw edema. *Photother. Res.* **2007**, 21(5), 452-456.
32. Orsatti, C. L.; Missima, F.; Pagliarone, A. C. Propolis immunomodulatory action in vivo on Toll like receptors 2 and 4 expressions and on pro-inflammatory cytokines production in mice. *Phytother Res.* **2010,** 24(8), 1141-1146.
33. Sforcin, J. M.; Bankova, V. Propolis: Is there a potential for the development of new drugs. *J Ethnopharmacol.* **2011**, 133(2), 253-260.
34. Wiese, H. *New Beekeeping.* 7 ed. Porto Alegre: Agropecuária. 493pp.**1986.**
35. Chan, H. Y.; Bonini, M. N. *Drosophila* models of human neurodegenerative disease. *Cell death differ.* **2000**, *7*, 1075-1080.
36. Matthews, K.; Kaufman, T.; Gelbart, W. Research resources for *Drosophila:* The expanding universe. *Nat. Rev. Genet.* **2005**, 6 (3), 179-193.
37. Venken, K.; Bellen, H. Emerging technologies for gene manipulation in Drosophila melanogaster. *Nat. Rev. Genet.* **2005**, 6 (3), 167-178.
38. Dietzl, G.; Chen, D.; Schnorrer, F. et al. A genome-wide transgenic RNAi library for conditional gene inactivation in *Drosophila. Nature* **2007**, 448 (7150), 151-156.
39. McGurk, L., Berson, A., Bonini, N. *Drosophila* as an In Vivo Model for Human Neurodegenerative Disease. *Genetics*. **2015**; 201(2):377-402.
40. Mohr, S., Perrimon, N. *Drosophila melanogaster:* A simple system for understanding complexity. *Dis. Model. Mech.* **2019**; 12 doi: 10.1242/dmm.041871.
41. Rubin, G., Yandell, M., Wortman, J. et al. Comparative genomics of the eukaryotes. *Science,* **2000,** 287:2204–15.
42. Adams, M. et al. The genome sequence of *Drosophila melanogaster*. *Science*, **2000**; 287: 2185–95.
43. Hirth, F. On the origin and evolution of the tripartite brain. *Brain. Behav. Evol.* **2010;** 76:3–10.
44. Roote, J.; Prokop, A. How to design a genetic mating scheme: a basic training package for Drosophila genetics. *G3 (Bethesda, Md.),* **2013;** 3: 353–8.
45. McGurk, L., Berson A., Bonini, N. Drosophila as an In Vivo Model for Human Neurodegenerative Disease. *Geneticis*. **2015;** 201:377-402.
46. Gevedon, O., Bolus, H., Lye, S. et al. In Vivo Forward Genetic Screen to Identify Novel Neuroprotective Genes in Drosophila melanogaster. *J. Vis. Exp.* **2019**; 149.
47. Ghosh, A., Osswald, H. BACE1 (beta-secretase) inhibitors for the treatment of Alzheimer's disease. *Chem Soc Rev*. **2014**; 43(19):6765–813.

48. Yan, R., Vassar R. Targeting the beta secretase BACE1 for Alzheimer's disease therapy. *Lancet Neurol*. **2014**;13(3):319–29.
49. Zhu, K., et al. Consequences of pharmacological BACE inhibition on synaptic structure and function. *Biol Psychiatry*. **2018**; 84(7):478–87.
50. Scott, J. et al. Discovery of the 3-imino-1,2,4-thiadiazinane 1,1-dioxide derivative verubecestat (MK-8931)–a β-site amyloid precursor protein cleaving enzyme 1 inhibitor for the treatment of Alzheimer's disease. *J Med Chem*. **2016;** 59(23):10435–50.
51. Shimshek, D. et al. Pharmacological BACE1 and BACE2 inhibition induces hair depigmentation by inhibiting PMEL17 processing in mice. *Sci Rep*. **2016**; 6:21917.
52. Lahiri D. et al. Lessons from a BACE1 inhibitor trial: off-site but not off base. *Alzheimers Dement*. **2014;** 10(5 Suppl):S411–9.
53. Abd Jalil, M., Kasmuri, A., Hadi, H. Stingless Bee Honey, the Natural Wound Healer: A Review. *Skin Pharmacol. Physiol.* **2017**; 30:66–75.
54. Michener, C. Pot-Honey. In: *Pot-Honey: A Legacy of Stingless Bees*. **2013.**
55. Silva, C., Aleixo, K., Nunes-Silva, B. et al. *Guia Ilustrado de Abelhas Polinizadoras no Brasil*. Instituto de Estudos Avançados; **2015.**
56. Zulkhairi Amin, F., Sabri, S., Mohammad, S. et al. Therapeutic Properties of Stingless Bee Honey in Comparison with European Bee Honey. *Adv. Pharmacol. Sci.* **2018.**
57. Kustiawan, P., Puthong, S., Arung, E. et al. In vitro cytotoxicity of Indonesian stingless bee products against human cancer cell lines. *Asian Pac. J. Trop. Biomed.* **2014;** 4:549–556.
58. Nugitrangson, P., Puthong, S., Iempridee, T. et al. In vitro and in vivo characterization of the anticancer activity of Thai stingless bee *(Tetragonula laeviceps*) cerumen. *Exp. Biol. Med.* **2016**; 241:166–176.
59. Ismail, W., Hussin, N., Mazlan, S. et al. Physicochemical Analysis, Antioxidant and Anti Proliferation Activities of Honey, Propolis and Beebread Harvested from Stingless Bee; Proceedings of the IOP Conference Series: *Materials Science and Engineering*; Vanderbijlpark, South Africa. **2018**; p. 012048.
60. Biluca, F., da Silva, B., Caon, T. et al. Investigation of phenolic compounds, antioxidant and anti-inflammatory activities in stingless bee honey *(Meliponinae*) *Food Res. Int.* **2020;** 129:108756.
61. Hazirah, H., Yasmin, A., Norwahidah, A. Antioxidant Properties of Stingless Bee Honey and Its Effect on the Viability of Lymphoblastoid Cell Line. *Med. Health.* **2019;** 14:91–105.
62. Avila S., Hornung P., Teixeira G. et al. Bioactive compounds and biological properties of Brazilian stingless bee honey have a strong relationship with the pollen floral origin. *Food Res. Int.* **2019**; 123:1–10.
63. Budin, S., Jubaidi, F., Azam, S., et al. Kelulut honey supplementation prevents sperm and testicular oxidative damage in streptozotocin-induced diabetic rats. *J. Teknol.* **2017**; 79.
64. Arulselvan P., Fard M.T., Tan W.S., Gothai S., Fakurazi S., Norhaizan M.E., Kumar S.S. Role of Antioxidants and Natural Products in Inflammation. *Oxid. Med. Cell. Longev.* **2016.**

65. Patricia V. Effect of stingless bee honey in selenite induced cataracts. *Apiacta.* **2002**; 3:1–2.
66. Syam, Y., Natsir, R., Rahardjo, S. et al. Effect of Trigona honey to mRNA expression of interleukin-6 on *Salmonella Typhi* induced of BALB/c mice. *Am. J. Microbiol. Res.* **2016;** 4:77–80.
67. Saiful Yazan L., Muhamad Zali, M., Mohd, Ali R. et al. Gopalsamy B., Voon F.L., et al. Chemopreventive Properties and Toxicity of Kelulut Honey in Sprague Dawley Rats Induced with Azoxymethane. *Biomed. Res. Int.* **2016**; 2016:4036926.
68. Garedew, A., Schmolz, E., Lamprecht, I. Microcalorimetric investigation on the antimicrobial activity of honey of the stingless bee *Trigona spp*. and comparison of some parameters with those obtained with standard methods. *Thermochim. Acta.* **2004;** 415:99–106.
69. Lopes, A., Vasconcelos, C., Pereira F. et al. Anti-Inflammatory and Antinociceptive Activity of Pollen Extract Collected by Stingless Bee *Melipona fasciculata*. *Int. J. Mol. Sci.* **2019;** 20:4512.
70. Ngalimat, M., Raja Abd Rahman, R., Yusof, M. et al. Characterisation of bacteria isolated from the stingless bee, *Heterotrigona itama,* honey, bee bread and propolis. *PeerJ.* **2019;** 7:e7478.
71. Buchon, N., Osman, D., David, F. et al. Morphological and molecular characterization of adult midgut compartmentalization in *Drosophila*. *Cell Rep.***2013**, 3:1725–38.
72. Zulkhairi Amin, F.; Sabri, S.; Ismail, M. et al. Properties of *Bacillus* Strains Isolated from Stingless Bee (*Heterotrigona itama*) Honey Collected across Malaysia. *Int. J. Environ. Res. Public Health* **2020**, *17*, 278.
73. SwissTargetPrediction: updated data and new features for efficient prediction of protein targets of small molecules, *Nucl. Acids Res.* **2019.**
74. Hanke, A.T.; Ottens, M. Purifying biopharmaceuticals: Knowledge-based chromatographic process development. *Trends Biotechnol.* **2014**, 32, 210–220.
75. Lin, X., Koelsch, G., Wu, S. et al. Human aspartic protease memapsin 2 cleaves the β-secretase site of β-amyloid precursor protein. *Proc Natl* Acad Sci USA. **2000;** 97: 1456–1460.
76. Hong, L., Tang, J. Flap position of free memapsin 2 (beta-secretase), a model for flap opening in aspartic protease catalytics. *Biochem*. **2004**, 43, 4689–4695.
77. Davis, J., Van Nostrand, W. Enhanced pathologic properties of Dutch-type mutant amyloid beta-protein. *Proc Natl Acad Sci.* **1996,** 93:2996–3000.
78. Luheshi L. et al. Systematic in vivo analysis of the intrinsic determinants of amyloid beta pathogenicity. *Plos Biology.* **2007,** 5:2493–2500.
79. Gravina S. et al. Amyloid β protein (Aβ) in Alzheimer's disease brain. Biochemical and immunocytochemical analysis with antibodies specific for forms ending at Aβ40 or Aβ42(43) *J Biol Chem.* **1995,** 270:7013–7016.
80. Iwatsubo T, et al. Visualization of A-beta-42(43) and A-beta-40 in senile plaques with end-specific A-beta monoclonals – evidence that an initially deposited species is A-beta-42(43) *Neuron.* **1994**, 13:45–53.

81. Gargano, J., Martin, I., Bhandari, P. et al. Rapid iterative negative geotaxis (RING): a new method for assessing age-related locomotor decline in Drosophila. *Exp Gerontol.* **2005**; 40(5):386-95.
82. Westfall, S.; Lomis, N.; Prakash, S. A novel synbiotic delays Alzheimer's disease onset via combinatorial gut-brain-axis signaling in Drosophila melanogaster. *Plos One*, **2019;** 14:e0214985.

Table legends:

Table 1. Culture media used to isolate the bacteria from the larval food of the stingless bee *Melipona quadrifasciata.*

Table 2. Features annotated of the genome of the new strains of *Proteus mirabilis* and *Enterococcus faecalis* isolated from the larval food of the stingless bee *Melipona quadrifasciata.*

Table 3. List of peptides identified in the S1 secretome and the respective proteins that are possibly derived.

Table 4. Characteristics of the best 3D models of peptides considered to be potentially bioactive molecules.

Table 5. Characteristics of the best 3D models of potentially bioactive peptides.

Figure legends:

Figure 1. Effect of bacterial secretomes on the fly climbing ability of AD-like flies. A. AD-like flies showed a lower climbing capacity than the control genotype 15 days after hatching. **B.** AD-like flies treated with S1, S9, S27 and S54. S1 secretomes showed increased climbing capacity when compared to untreated flies and to vehicle (culture medium LB). Data are presented as the mean ± S.E.M. Statistical significance is indicated as * for $P < 0.05$ and ** for $P < 0.01$ according to t-test. NC = Negative Control.

Figure 2. Amyloid quantification by thioflavin T, normalized according to fluorescence, in the brain of flies treated and not treated with bacterial secretomes. Data are presented as the mean ± S.E.M. Statistical significance is indicated as * for $P < 0.05$ according to Kruskal-Wallis t-test, with Dunn's multiple comparisons post-test. NC = Negative Control.

Figure 3. Histology of the brain of AD-like model fly treated and not treated with bacterial secretomes. Representative 3-µm paraffin sections at approximately midbrain of flies 15-days after hatching. **A.** Control: untreated *elav-Gal* (40x magnification), indicating the areas of the brain where the images were captured for analysis. **B.** Untreated *elav-Gal,* 100x. AD-like flies treated with: **C.** Water, negative control, 100x; **D.** Vehicle, 100x; **E.** S1,100x; **F.** S9, 100x; **G.** S27, 100x; **H.** S54, 100x.

Figure 4. Three-dimensional analysis of the HLINLFFDSGTIK and PLLTAGFFSK peptides and their interaction with BACE1 and β-amyloid target sites. A. 3D Image of the interaction between HLINLFFDSGTIK with BACE1. **B.** Zoom of the image A, showing 3D molecular interactions of HLINLFFDSGTIK with BACE1. **C.** 3D Image (Cartoon type) of the interaction between PLLTAGFFSK and β-amyloid plaque. **D.** 3D Image (Surface type) of the interaction between PLLTAGFFSK and β-amyloid plaque.

Figure 5. Genomic organization of the *nuo* operon in the *P. mirabilis* IsAbel.Pmir genome visualized in Artemis program.

Figure S1. Venn diagram representing the proteins identified in the S1 secretome, secreted for Enterococcus feacalis (blue circle) and Proteus mirabilis (yellow circle), according to the peptides found.

Tables:

Table 1.

Stingless bee larval food	
Bacteria (colony)	**Culture medium used for isolation**
1	ISP-2
9	MRS
27	Oatmeal
54	Nutrient

Table 2.

Features Annotated	***Proteus mirabilis***		***Enterococcus faecalis***	
	Reference NC_010554.1	**IsAbel.Pmir**	**Reference NC_004668.1**	**IsAbel.Efae**
Genome size	4,063,606	4,063,606	3,218,031	2,734,422
CDS	3,682	3,789	3,244	2,581
tRNA	83	83	67	33
GC percentage	38.9	40.2	37.4	37.5

Table 3. List of peptides identified in secretome S1 and the respective proteins that are derived.

Protein	Organism	Sequence	Spectrum Intensity	Database Accession
ABC transporter permease	*Enterococcus faecalis, Proteus mirabilis*	MEMIPK	3.54e+006	A0A3N3Z273
MobC domain-containing protein	*Enterococcus faecalis, Proteus mirabilis*	LTEEEK	7.10e+004	R3JUE4
Methionine import ATP-binding protein MetN	*Enterococcus faecalis, Proteus mirabilis*	ENILTFSKK	5.43e+006	C7D2D7
D-2-hydroxyacid dehydrogenase	*Enterococcus faecalis, Proteus mirabilis*	GGIVDTDALIAALAQGR	4.91e+004	A0A4U3NN88
DNA-binding protein	*Enterococcus faecalis, Proteus mirabilis*	GTKIGGQWR	2.24e+005	A0A431H3R4
Sugar ABC transporter substrate-binding protein	*Enterococcus faecalis, Proteus mirabilis*	EGAQMDFGTAK	8.62e+005	A0A3N3Z427
Aldehyde-alcohol dehydrogenase	*Enterococcus faecalis, Proteus mirabilis*	HAMFPK	3.29e+005	A0A059MZJ4
Replication-associated protein RepA	*Enterococcus faecalis, Proteus mirabilis*	GSEITLHNWVENK	1.59e+005	A0A0M2ANR2
Uncharacterized protein	*Enterococcus faecalis, Proteus mirabilis*	IDMYTER	6.55e+004	A0A249XUN9
Holliday junction resolvase RecU	*Enterococcus faecalis, Proteus mirabilis*	ESAIEFGNRGMR	1.49e+005	I6TD06
Glycosyltransferase, group 2 family protein	*Enterococcus faecalis, Proteus mirabilis*	ITLTKFDK	3.13e+006	A0A059MWM1
Uncharacterized protein	*Enterococcus faecalis, Proteus mirabilis*	ISPQGAVRITDAQGN	8.02e+004	S4G069
Uncharacterized protein	*Enterococcus faecalis, Proteus mirabilis*	MFPPK	2.56e+005	A0A6I5JCC5
DUF4393 domain-containing protein	*Enterococcus faecalis, Proteus mirabilis*	RKSFPLPVDK	2.12e+005	A0A6I4Y203
Uncharacterized protein	*Enterococcus faecalis, Proteus mirabilis*	DINQKAHTGTNKNK	9.62e+004	A0A4U4EBD7
Uncharacterized protein	*Enterococcus faecalis, Proteus mirabilis*	AIESFIQSEK	6.75e+005	S4CMY2
Mannitol dehydrogenase family protein	*Enterococcus faecalis, Proteus mirabilis*	EVEIPHFDRASLR	9.62e+004	A0A3N3Z5E8
ABC transporter substrate-binding protein	*Enterococcus faecalis, Proteus mirabilis*	VAPVEKNGDK	2.53e+005	A0A6I5JBA0
Sigma-54 interaction domain protein	*Enterococcus faecalis, Proteus mirabilis*	NIYIRYEALK	5.94e+004	S4CFA9
DNA-binding protein	*Enterococcus faecalis, Proteus mirabilis*	QLDINTNTLR	1.18e+005	A0A0J7JJQ7
Restriction endonuclease subunit S	*Enterococcus faecalis*	LDQSITLYK	7.74e+005	A0A6L7I7P6
YopX domain-containing protein	*Enterococcus faecalis*	MNKMIPK	1.06e+006	E0HA84
MobC	*Enterococcus faecalis*	HLINLFFDSGTIK	1.33e+006	Q8GFD8
GTP 3',8-cyclase	*Proteus mirabilis*	NLPDFLHWIK; QFHAITGQDK	5.23e+004; 2.71e+003	A0A1Z1SX52

Uncharacterized protein	*Proteus mirabilis*	IYTSGGSDK	7.25e+004	A0A5J6T7M9
RNA-splicing ligase	*Proteus mirabilis*	KEVTLESFK	2.48e+005	A0A7G5CG86
Uncharacterized protein	*Proteus mirabilis*	MFPNKPK	1.01e+006	A0A3G8F187
Acetyl-coenzyme A carboxylase carboxyl transferase subunit alpha	*Proteus mirabilis*	LMELAER	1.06e+006	A0A2A5Q6B3
IncFII family plasmid replication initiator RepA	*Proteus mirabilis*	FDFAIHVAHARSR	1.65e+005	A0A7D6ADS9
NADH:ubiquinone reductase (H(+)-translocating) (Fragment)	*Proteus mirabilis*	PLLTAGFFSK	7.74e+005	A0A6N4LVT9
Tyrosine recombinase XerD	*Proteus mirabilis*	VLHQQHHPR	6.26e+005	A0A1Z1SSS8
DNA topoisomerase 4 subunit B	*Proteus mirabilis*	ETTLDPNTR	8.79e+003	A0A1Z1SSP8
Isocitrate dehydrogenase kinase/phosphatase	*Proteus mirabilis*	DKFAPQKTITAER	1.33e+006	A0A2J9L743
3-isopropylmalate dehydrogenase	*Proteus mirabilis*	RFSLNITTK	5.00e+006	A0A1Z1SSM8
Outer membrane beta-barrel protein	*Proteus mirabilis*	ADEELINDK	8.79e+003	A0A6L6M9I3

Table 4.

Peptide	Rank	Docking (Kcal/mol)			
		β-secretase (BACE)		β-amyloid	
		Global energy	ACE	Global energy	ACE
NLPDFLHWIK	0.85	-42.18	-3.16	-70.15	-17.61
ESAIEFGNRGMR	0.63	-25.14	-1.71	-53.93	-11.24
PLLTAGFFSK	0.48	-28.13	-7.94	**-97.41**	**-25.63**
FDFAIHVAHARSR	0.47	-27.65	-6.84	-74.86	-16.98
EGAQMDFGTAK	0.42	-35.50	-7.79	-49.63	-11.58
HLINLFFDSGTIK	0.42	**-42.47**	**-9.02**	-67.13	-12.52

* ACE = contribution of the atomic contact energy.

Table 5:

Peptide Sequence	Toxicity	Net charge at pH 7	pI	Water solubility	Molecular weight (g/mol)
PLLTAGFFSK	Non-Toxic	1.00	9.11	Low	1080.43
HLINLFFDSGTIK	Non-Toxic	0.10	7.09	Low	1504.95

* pI = isoelectric point.

Figures:

Figure 1.

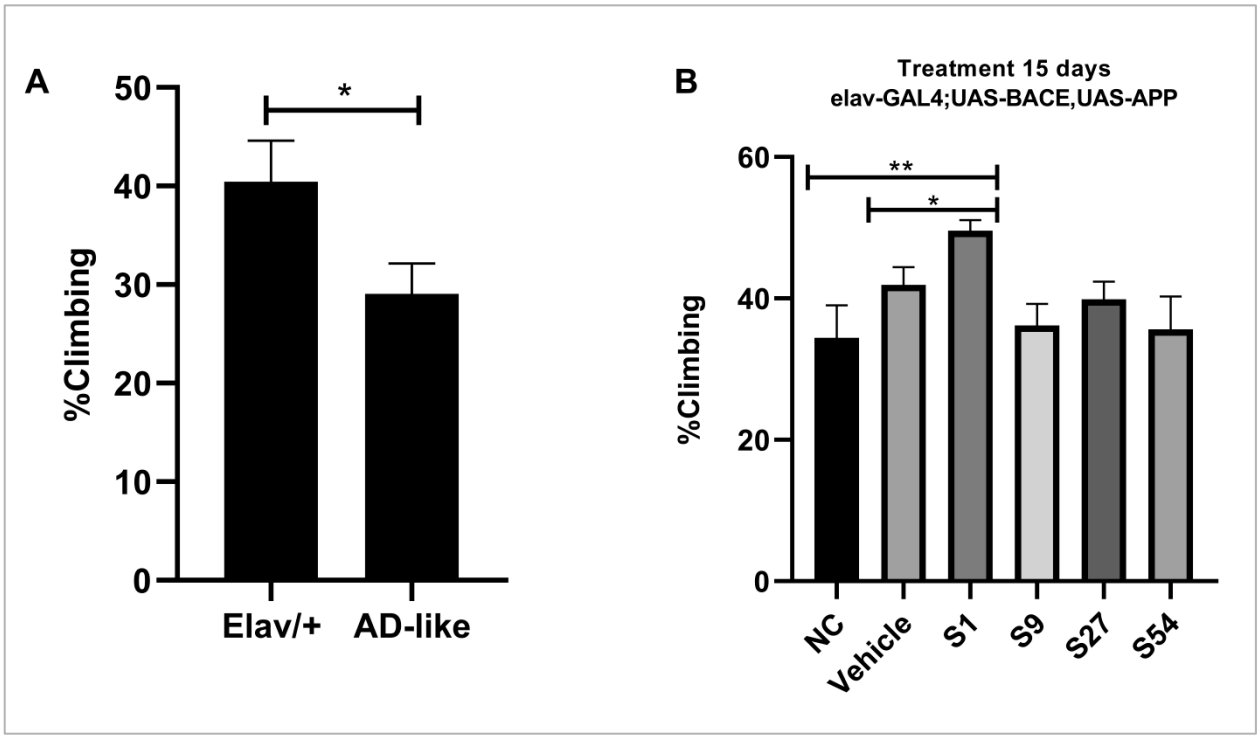

Figure 2.

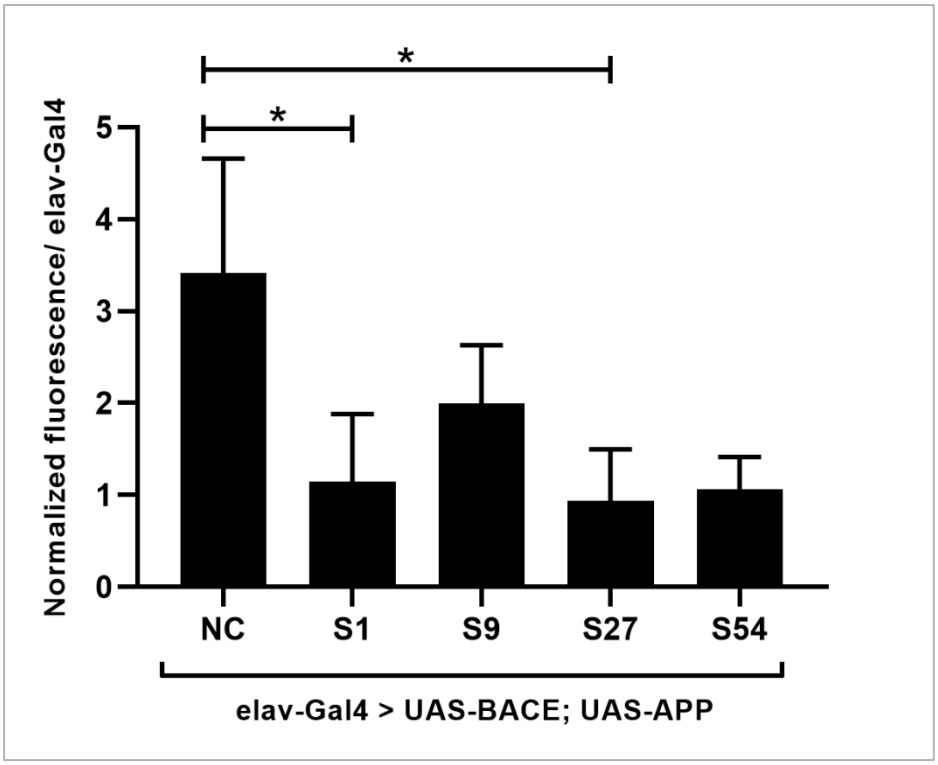

Figure 3.

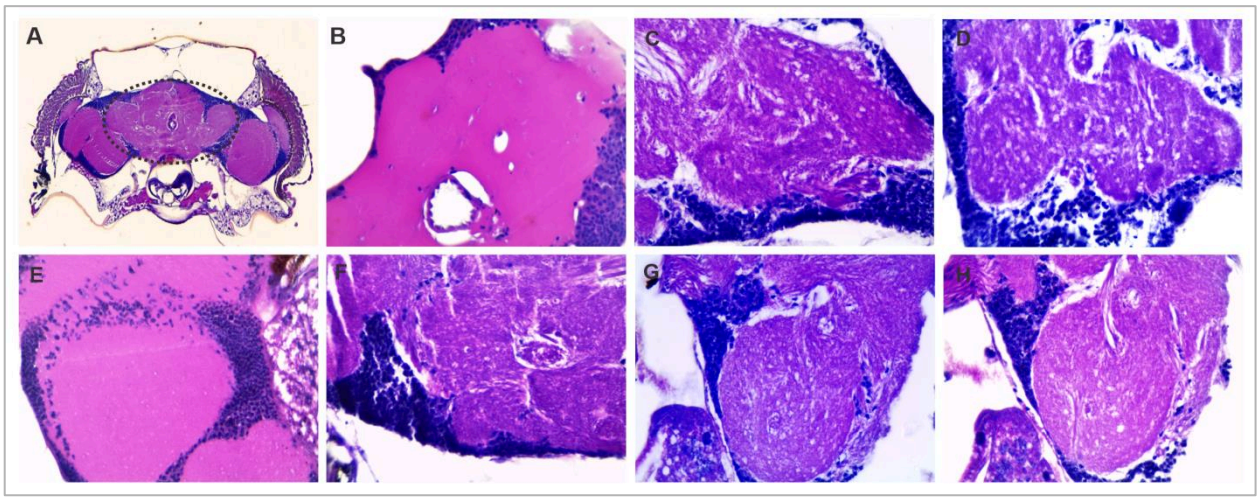

Figure 4.

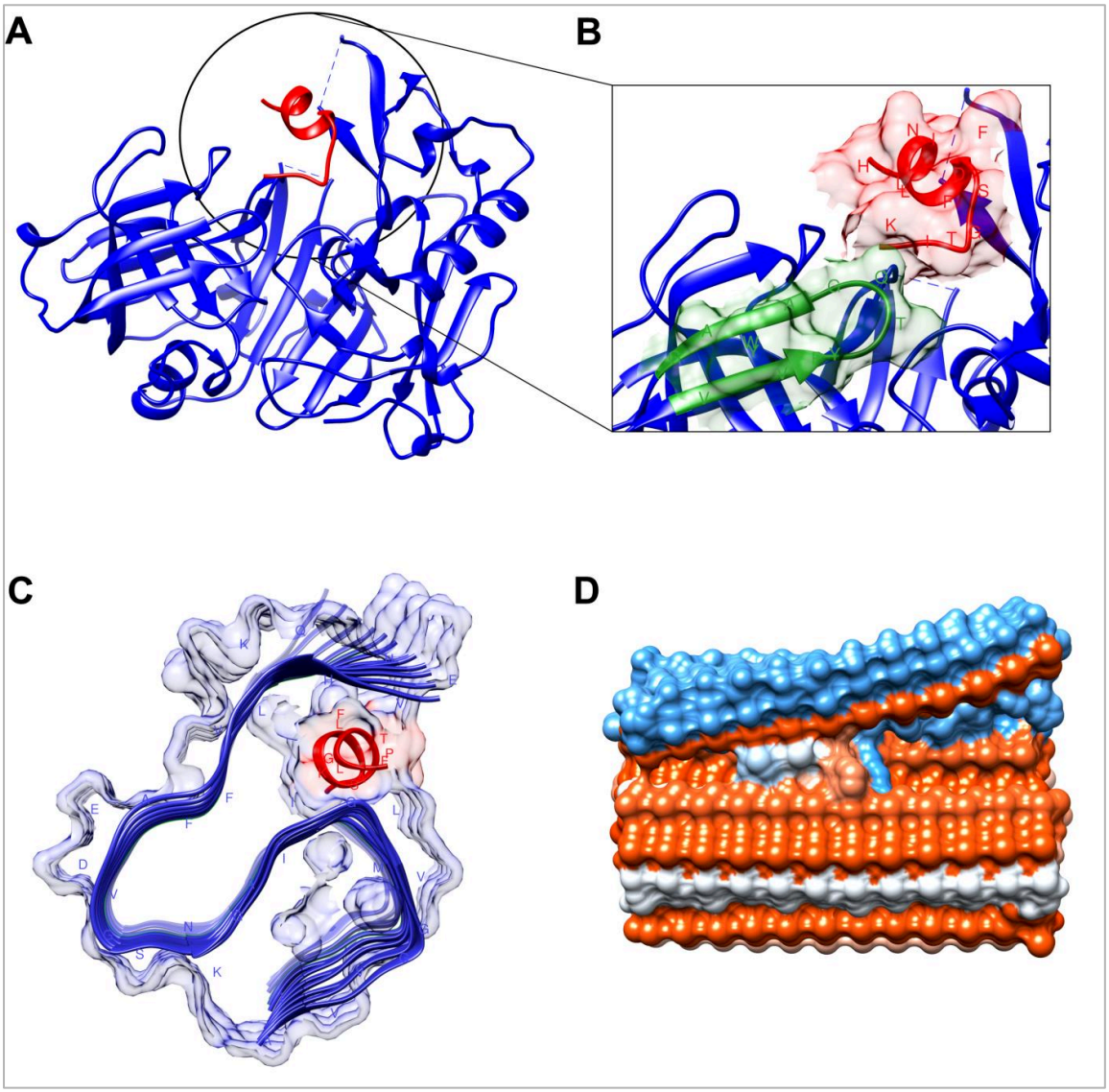

Figure 5.

Figure S1.